48

Control and optimization of a multiple-effect evaporator

A Thesis

Submitted to the Faculty of

The University of Cape Town

by

Patrick D. Smith

In Fulfillment of the

Requirements for the Degree

of

Master of Science

in Chemical Engineering

Supervisors:

Assoc. Professor C.L.E. Swartz

Assoc. Professor S.T.L. Harrison

30 September, 2000

Acknowledgements

The author would like to thank Triangle Limited for their generous support and financial assistance for all aspects of this project. Particular thanks are extended to the Technical Director, Mr Clive Wenman, the Engineering Manager, Mr Ashwin Rana, the Process Engineer, Mr Elisha Mutasa, and the Instrumentation and Control Engineer, Mr Steve Paver. In addition the author would like to thank the process and laboratory staff for their contributions and cooperation, throughout the project.

The author would also like to thank Professor CLE Swartz and Professor STL Harrison for their support and supervision of this project.

Finally, the author would like to thank his family and fiancée, for their support and encouragement.

Table of Contents

List of Figures

List of Tables

Abstract

Falling commodity prices have reduced the profit margins of Southern African sugar producers. Although these price falls have been severe, they reflect a long-term trend of reducing margins for basic commodity producers during the 20th Century. This trend has forced producers to closely examine their processes and to look for areas in which improvements in productivity, yield and efficiency can be achieved. Evaporation is the most energy intensive unit operation in the sugar factory, and it is responsible for the removal of most of the water from sugar solution, or juice, which is extracted from the sugar cane. There is also a large potential to lose sucrose at the evaporators due to the high temperatures and long residence times employed there. The smooth control of the evaporators is thus vital to consistent factory operation, and the evaporators are commonly a sugar factory bottleneck.

This study developed a control strategy for the particular evaporator configuration found at Triangle Sugar Mill in south eastern Zimbabwe. There are currently several evaporator control strategies being used in the sugar industry. Most of these are an assembly of single loop Proportional Integral Derivative (PID) controllers, which cannot optimally account for the interactions encountered in most evaporator stations. Ideally, any evaporator control system should be able to handle the multiple input multiple output problem while anticipating and handling constraints on inputs and outputs. Several multivariable approaches have been tried, but these usually require a great deal of expensive instrumentation.

After a review of the multivariable control literature and testing of several alternative control systems, Dynamic Matrix Control (DMC) was chosen as the best-suited control algorithm for the Triangle control problem. A dynamic model of the Triangle evaporator station was developed to formulate and test the DMC and other controllers. The model was based on a set of differential equations involving mass and energy balances through the evaporators. Real plant data were collected from the SCADA system and the model was tested against this data. After validation the model was used to record step responses of the process to key input variables.

The control system had nine (9) measurable inputs, and three (3) controlled outputs. The objective of the control system was to deliver the maximum amount of consistently high quality syrup, within plant constraints. This was formulated in an objective function which

seeks to minimize a weighted sum of the errors of syrup concentration from a setpoint, and the fluctuations in juice flowrates. Two alternative formulations were developed, and tested on the plant model.

In addition, two level controllers were devised, based on Linear Quadratic Gaussian (LQG) and Model Predictive Control (MPC) approaches. These were then tested on a model of the buffer tanks upstream of the evaporators. The level controllers were found to be useful in different circumstances, and an arrangement has been found which outperforms the existing buffer tank control strategy. The LQG level control strategy has been installed and commissioned at Triangle.

The proposed DMC based controllers were tested in a series of simulations involving step disturbances and real plant data. Both formulations were found to outperform the existing PID control strategy. The second formulation, a combined controller, which managed the control of the entire evaporator station and also controlled the level of an upstream buffer tank, was found to be the most flexible arrangement. This controller was able to accept noisy input signals, and constraints on both inputs and outputs were handled smoothly. It was recommended that this controller be tested in a real plant situation.

Chapter 1 INTRODUCTION

The global fall in commodity prices between 1998 and 2000 has adversely affected profit margins of Southern African sugar producers, who usually export sugar on regional and world markets. Although these price falls have been more severe than usual, they are part of a long-term trend of reducing margins for basic commodity producers. This trend can only be offset by improved productivity, either in terms of yield, efficiency, or other technological enhancement. These effects are forcing producers to examine their processes closely to look for innovative solutions which could outperform conventional technologies. A great deal of effort has been focused on the automatic control of several parts of the sugar factory, such as the extraction plants, the pan boiling, and centrifugal operations. This work was aimed at either reducing the required operating staff, or achieving more accurate automatic control of a previously manually controlled process. This study developed a control strategy for the particular evaporator configuration found at Triangle Sugar Mill in South Eastern Zimbabwe. It is expected that these results could be more widely applied, due to the similarity of the designs used throughout the cane sugar industry. In addition, similar evaporator arrangements are used in the pulp and paper industry (for concentration of weak black liquor in the Kraft process) and the beet sugar industry (for concentration of the sucrose solution extracted from sugar beets).

Multiple effect evaporation has been used in industry since the 1890s. The basic principle is that a liquor, or solution, enters the first evaporator and is heated by steam which condenses in a calandria. This heating causes the solution to boil. The liquor which leaves the vessel is thus more concentrated than the fresh feed, and this liquor is taken to be fed into the next effect evaporator. Meanwhile, the vapour evolved from the first boiling is channeled to be used as heating steam in the calandria of the next effect evaporator. This vapour will however be of a lower temperature than that in the first effect, and so in order to maintain a boiling regime, each subsequent effect must be maintained at successively lower pressures.

In the sugar factory evaporators are typically fed from the extraction plant with a solution containing predominantly sucrose at a concentration of around 12% dissolved solids. This solution must then be concentrated to syrup of around 67% dissolved solids, which is fed to the crystallisers, where the final product is formed. Evaporation constitutes removal of the majority of the water present in the juice, and is the unit operation which consumes the most energy in the factory.

1.1 Problem Statement

Due to changing process conditions such as fluctuations in the juice flowrate, the operation of the evaporators is sometimes erratic. This causes fluctuations in the concentration of the syrup delivered to the crystallising pans. Uneven syrup concentration places an unwanted burden on this downstream equipment. If the syrup is too dilute the crystalliser will require extra heat and time in order to concentrate the syrup before crystallisation can begin.

Unsteady operation can also be blamed for deposition of scale in the evaporator tubes. Uneven flowrates through the evaporators can also lead to long time lags in some of the vessels, causing inversion of the sucrose. Inversion causes a loss estimated at between 1% and 2 % of incoming sugar.

1.2 Aims and Objectives

The main aim of this project was to develop a control system for the Triangle evaporator station. This system should then be compared with other alternatives as well as the existing system. In order to do this a dynamic model of the evaporator station was developed. This model was validated by direct comparison with actual plant data. A secondary objective was to improve the quality and availability of measurements to provide online values for quantifying evaporator performance.

The main objective of the control system at the evaporator station would be to ensure a constant syrup concentration, and to maintain as smooth an operation as possible. This is usually done by manipulating the feed flowrate, interstage juice flowrates or various vapour stream flowrates. This study was aimed at investigating the various possibilities and developing an overall optimization and control scheme that could run the station in a supervisory manner.

1.3 Hypothesis and Motivation

In order to assess the potential areas for improved control, it was first necessary to analyse the main areas in which a benefit could be achieved. The potential benefits from this sort of control can be calculated in three main areas:

- Increasing the productive capacity of the plant, from the same capital base, by increasing the throughput of the plant.
- Increasing sugar production, by reducing losses.
- Reducing operating costs

The overall objective function to be optimized is then a combination of these economic factors. The notes below are preliminary estimates for each factor. The predicted benefits in any area must be compared on a similar basis. This will be done based on an annual sugar production of 300 000 tonnes, and using costs and figures from the 1998 and 1999 seasons.

a) Increasing capacity

There is a significant potential for increasing the capacity of the crystallisers. Crystallisers are commonly the bottle-neck in a sugar factory, and Triangle is no exception. If the proposed control system could ensure a more consistent syrup concentration, then the set-point for this concentration could be raised closer to the maximum desired concentration, of about 72° Brix (°Bx), or 72 % dissolved solids, above which spontaneous nucleation occurs. The benefits could be calculated as follows:

The average Brix, or concentration, of syrup delivered to the crystallisers in 1998 was 64.1°Bx, and the syrup concentration fluctuated widely around this value, and was usually found between 60°Bx and 70°Bx. Tighter control would allow the station to run at a higher concentration set point without the risk of large deviations into the zone of super-saturation of the syrup solution. While it is difficult to predict how tightly the proposed control system could operate, an indication can be derived from various studies which have been done. Rousset *et al.* (1989) reported that an advanced control system improved the range of syrup concentrations from 15% dissolved solids, down to a range of less than 5% dissolved solids. Montocchio and Scott, (1985) used a fairly simple PID based control scheme to reduce fluctuations in syrup concentration from 12°Bx down to less than 2°Bx at Amatikulu mill in

South Africa. Elhaq *et al.* (1999) were able to similarly tighten the control of syrup Brix from +/- 5°Bx to +/- 2°Bx from setpoint, by using a Generalised Predictive Control (GPC) Scheme. Based on these results, it would not be unreasonable to expect a range of 2°Bx.

With this quality of control, it would be quite safe to raise the syrup Brix setpoint to 68°Bx. The delivery of a consistently more concentrated syrup would increase the capacity of the downstream equipment. By increasing the average syrup concentration by 4 units, this would reduce the time required for syrup concentration in the evaporative crystallisers, although it would not affect the time of sugar boiling. This would result in a 2% increase in the productive capacity of this station. Table 1.1 shows estimates of the capacities of various plant items.

Table 1.1 Capacities of essential unit operations at Triangle mill

Unit Operation	Capacity	Equivalent cane capacity
Cane preparation	700 t. c. / hr	700 t. c. / hr
Extraction plants	510 t. c. / hr	510 t. c. / hr
Juice handling	900 t. MJ. / hr	750 t. c. / hr
Evaporators	660 t. CJ. / hr	550 t. c. / hr
Evaporative crystallisers	150 t. syr. / hr	500 t. c. / hr
Cooling crystallisers	200 t. MC. / hr	600 t. c. / hr
Centrifuges	233 MC hr	915 t. c. / hr
Dryers	92. t. sug / hr	736 t. c. / hr

The increase in capacity would allow a further 6000 tonnes of sugar to be produced from the same capital base – assuming the availability of extra cane.

Increased turnover = 300,000 t sug/yr * 2% incr. * US$ 205 /t
= US$ 1 230 000 per year

However, due to the division of proceeds from the sale of sugar, between the growers of the sugar cane and the factories, which produce the sugar, this would result in a smaller profit for the factory. Note : for the 2000 milling season, the blend price of sugar was US$ 205 per tonne and the division of proceeds was 26.5% to the millers and 73.5% to the growers.

Increased revenue to factory = US$ 1 230 000 per year * 26.5 %
= US$ 326 000 per year

b) Reducing sugar losses

In the 1998 season, undetermined sugar losses accounted for about 2.2 % of total production. A large portion of these losses were believed be attributable to the evaporator station. The evaporators involve the highest temperature boiling of any unit operation in the sugar factory. This leads to the possibility of thermal degradation of the incoming sucrose to glucose and fructose by inversion, along with subsequent destruction of these monosaccharides. Unsmooth operation in the evaporators causes rapid changes in the level of juice boiling in the evaporators, and this leads to scaling of the evaporator, and possibly entrainment of the juice with the vapour. Scaling and inversion are both worsened by rapid fluctuations in throughput. These fluctuations can cause the juice to be boiled at unusually high temperatures, leaving areas of the heating tubes dry and thus easily scaled should the flow drop suddenly. A smoother control system should be able to reduce these losses to the industrially accepted figure of around 1% (SMRI final report, 1999). This would result in an extra 3600 tonnes of sugar from the same amount of cane and from the same capital base.

Increased turnover = 300,000 t sug/yr * 1.2% incr. * US$ 205 /t
= US$ 738 000 per year

Again, due to the division of proceeds, this would result in the following increased factory revenue.

Increased revenue to factory = US$ 738 000 per year * 26.5 %
= US$ 196 000 per year

c) Reducing operating costs

Operating costs could be reduced by reducing the amount of steam used, and by reducing the costs of cleaning the evaporators. The boilers at Triangle Limited use waste product bagasse (or cane fibre) for fuel, therefore the economic benefits of an incremental drop in steam consumption are unlikely to be significant. Rousset *et al.* (1989) reported that a smoother operation, which was achieved under automatic control, resulted in reduced energy costs.

However, the authors also note that the economic benefits were difficult to identify. Elhaq *et al.* (1999) estimate an energy saving of 7% due to the implementation of a GPC scheme at SUCRAFOR sugar factory in Morocco. The current cost of steam at Triangle has been calculated as US$ 1.43 per tonne. A similar improvement at Triangle would result in the following benefits:

Reduced costs = 590,000 t.steam/year * 7% saving * US$ 1.43 / t.steam
= US$ 59 059 per year

Currently, Triangle Ltd. spends almost US$ 300,000 per annum on mechanical and chemical cleaning for the evaporators. As explained above, a constraint handling control system involving level control as well as Brix control should iron out the rapid fluctuations, which accelerate scaling. At Triangle, the evaporators are currently cleaned every two weeks. Operating staff at several other mills in Southern Africa, have been able to increase the time between evaporator cleaning from two weeks to three weeks, a reduction of one third of the cleaning cost. This would realise a direct capital saving of US$ 100,000, in addition to a lower requirement for casual labour, and increased time efficiencies due to less frequent cleaning. A long term benefit would be a longer life for the evaporator tubes, due to less erosion from the cleaning equipment.

Reduced costs = US$ 300,000 costs/yr * 1/3 reduction in cleaning frequency
= US$ 100,000 per year

From the brief analysis above, it is clear that the areas which present the greatest opportunity for improvement are maintaining a smoother operation, particularly in reducing scaling, and the delivery of a consistently more concentrated syrup - not in improving the steam economy of either the evaporator or crystalliser stations. This conclusion is vital in formulating a correctly balanced objective function for the control system, and in focusing the direction of this project.

Choice of Controller

The primary control objective should be to deliver syrup of the maximum possible concentration, without allowing spontaneous nucleation to occur, as this produces severe blockage problems at the evaporators. The model of the plant indicates that there are several

measurable input disturbances which affect the syrup concentration, but which are not used by the existing control system. Any of these disturbances could potentially cause a constraint violation.

A second observation was that the throttling of the V2 valve is often insufficient to deal with extreme operating conditions. This valve becomes saturated, and the syrup concentration is no longer brought under control. It was thus necessary to find another variable which could be manipulated in order to improve the flexibility of the system. From these two observations, it was decided that some sort of predictive control should be used, and that the controller should be able to anticipate and handle constraints. In addition, the controller would need to achieve a compromise between several objectives. Due to the interaction of the process, it would be difficult to pair the available input variables in an optimal manner.

For these reasons, a DMC controller was chosen. This is one of the simplest MPC control algorithms. In this controller, a matrix is used to predict the future response of the plant based on the measurement of current disturbances. The matrix takes the form of a convolution model of the plant.

Other Benefits and Objectives :

A) Improved level control

As will be shown later, one of the most frequent disturbances in a sugar factory is a fluctuation in the juice flowrate, due to the erratic supply of sugar cane to the mill. It will also be shown that a fluctuation in juice flowrate has a serious effect on evaporator operation. A surge in juice flowrate could result in entrainment of juice droplets, while a sudden decrease in juice flowrate would result in a collapse of the boiling regime within the tubes, causing the tube surface to dry out, and promoting deposition of scale on the tube walls with the corresponding drop in heat transfer capability. Any change in juice flowrate would also affect the residence time of that juice, and either result in slack syrup, or promote the degradation of the sucrose in the juice by prolonged exposure to high temperatures.

The existing PID controllers do not make the best possible use of the available buffer tanks, and thus it was proposed that a new strategy be devised and implemented. It was decided to

use both the LQG buffer tank control strategy of Love (1999), and the MPC level controller of Campo and Morari (1989).

B) Flow splitting

Previous studies have indicated that the heat transfer coefficient of a multiple effect evaporator can vary by as much as 50% between routine cleaning, (Walthew *et al.*, 1996). By using this result in computer simulations, it will be shown that the distribution of the total clear juice flowrate between the three first effect vessels can substantially affect the resultant syrup Brix. For this reason, it was decided that some measure of the heat transfer capacity of the evaporators was required on line, in order to get an idea of the changing capacity of each individual vessel. An algorithm was also required, which would be able to determine, on line, the optimum distribution of juice to the three first effects.

1.4 Outline of Thesis

Chapter 2 Process Description and Literature Review

Chapter two, which follows, contains a review of the theory behind evaporation, and a brief explanation of some of the more common control philosophies. The evaporator station at Triangle is described, along with the control systems which are currently being used. Several authors have attempted to use alternative control schemes at other installations, and these are also reviewed.

Chapter 3 Model Formulation

In chapter three, a model of the Triangle evaporator station is developed. This model was used to simulate the dynamic behaviour of the multiple effect evaporators. The model was necessary in order to formulate and test the proposed control system. In this chapter, some of the details of evaporator operation are also discussed. These are then incorporated into the model, which is based on a set of differential equations. The accurate estimation of the physical properties of various streams in the model is critical to the value of the model. For this reason, the equations behind these properties are outlined.

Chapter 4 Controller Design

Chapter four begins with an overview of some advanced control strategies; particularly in the relatively new field of model based controllers. The design of the various controllers used in this study is then explained. Two alternative formulations have been used for the primary control layer, which controls the Brix of syrup leaving the evaporators. In addition, two other types of controller have been formulated. First, a controller for the level of juice in buffer tanks upstream of the evaporators. Second, a supervisory, optimization layer, which was used to determine the optimal distribution of juice into the evaporators.

Chapter 5 Results and Discussion

These controllers were then tested using the model of the evaporators. A series of simulations were run, in which the response from each controller was monitored and compared with responses from the existing system. The results of these simulations are presented in Chapter 5. These results are then discussed, and the various controllers are contrasted against one another.

Chapter 6 Conclusions

In Chapter 6, final conclusions are drawn about the work which has been done, and the possible application of this work to the plant. Directions for future work in this area are also discussed.

Chapter 2 PROCESS DESCRIPTION AND LITERATURE REVIEW

2.1 Process Description

Position of Evaporators in the Process

At Triangle Limited approximately 300 000 tonnes of crystalline sugar are produced every year from about 2.5 million tonnes of sugar cane. The sugar cane is delivered to the plant and may be processed on either of two extraction lines. The cane is delivered in bundles of whole stalk cane and is first billeted, and then shredded, before being passed through either the diffuser or the milling tandem (the two extraction lines), as shown in Figure 2.1. The aim of these two lines is to extract as much sucrose as possible from the incoming cane, and to deliver this in a solution called juice to the factory. The remainder of the cane is mainly fibre, and this is burnt in the boilers.

The juice obtained from each line is called draught juice. After the juice from both lines is combined it is termed mixed juice, containing about 12%-dissolved substances along with about 0.5% suspended solids. The solutes in mixed juice are predominantly sucrose (the final product of sugar manufacture) together with a mixture of monosaccharides, such as glucose and fructose, other organic material, and some inorganic salts, usually as phosphates and sulphates. The proportion of dissolved solids in juice which are made up of sucrose is referred to as the juice purity, thus:

$$Purity = \frac{Dissolved\ sucrose}{Total\ dissolved\ substances} = \frac{Pol}{Brix} \qquad (2.1)$$

where Pol and Brix are sugar industry terms which refer to the method of analysis, but very nearly correlate with % sucrose and % dissolved substance, respectively:

Pol = % dissolved sucrose

Brix = % total dissolved substances

Depending on which extraction line was involved, the juice could be at any temperature between the factory ambient temperature of approximately 30°C, and 85°C. This is because the juice is heated in the diffuser, but not in the milling tandem. Juice from each line is weighed into a buffer tank, the mixed juice tank, which has an operating capacity of 180 m^3. From here, two centrifugal pumps take the juice through a series of shell and tube heaters. The juice is heated to 105°C, i.e. above its boiling point, and then flashed to remove any entrained air bubbles. After the flash tank, lime and flocculent are dosed into the stream in order to control the pH of the juice and to enhance clarification in the following stage.

This treated juice then passes into one of three clarifiers. These modified Rapidorr clarifiers separate the mixed juice into mud, which is delivered to the filter station, and a supernatant portion called clear juice, which is sent to the clear juice tank. The clear juice tank is another buffer tank with an operating capacity of 116 m^3. From here, the juice is pumped through two more shell and tube heaters, and on through the evaporator station.

The purpose of the evaporators is to remove the majority of the water present in the clear juice. Multiple effect evaporators should increase this juice concentration to about 65-70% dissolved solids, or Brix. The syrup delivered by the evaporator station is used to feed the evaporative crystallisers, where the sugar crystals are actually formed. These crystals are then grown and separated by centrifugation, before being washed and dried for sale. The evaporators are the unit operation that consumes the most energy in the factory.

The steam that is supplied to the evaporator station is usually exhaust steam from the turbo alternators (T/As). As is the case at many sugar mills the fibrous portion of the sugar cane, called bagasse, is burnt in boilers to produce steam. The steam, termed HP steam, is supplied at about 3 MPa and is then let down through the T/As, producing electricity for the estate. The steam which leaves the turbines is called exhaust steam, and is usually at 180-220 kPa abs.

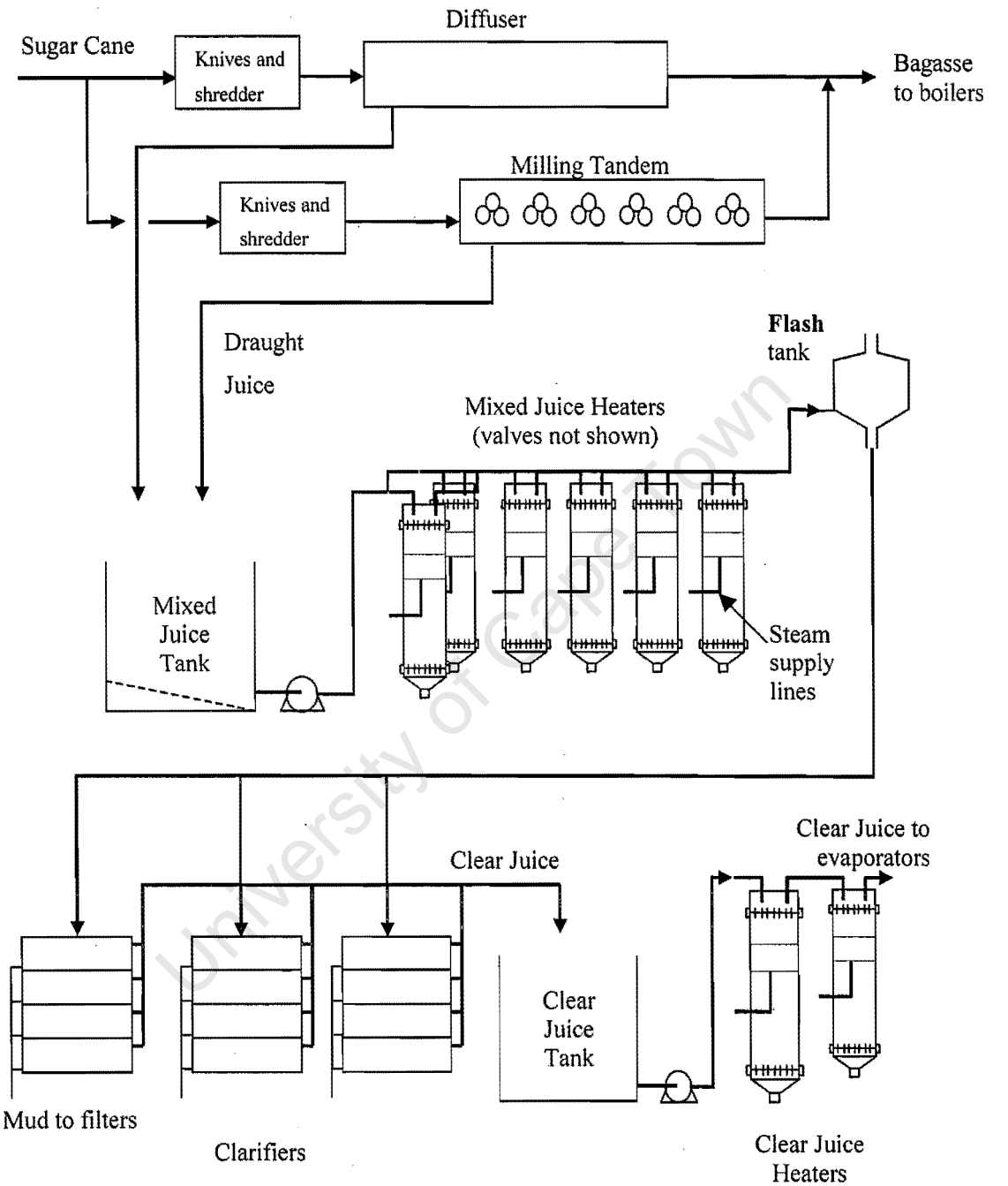

Figure 2.1 Diagram of the extraction and juice handling operations at Triangle mill.

Evaporator theory

Each evaporator consists of two sections. The first is a heating section in which steam is fed into a calandria, or steam chest, where it condenses on the outer walls of tubes through which juice is passing. Juice is usually fed into the evaporator below the bottom tube plate and rises in the tubes either as a result of boiling phenomena, or by forced circulation. Above the upper tube plate there is a disengagement space, in which juice and vapour are allowed to separate. The juice is then channeled to a down take, which may be central or annular, and the vapour is channeled to feed the calandria of the next effect. The most common evaporator design is the Robert type vessel, depicted below.

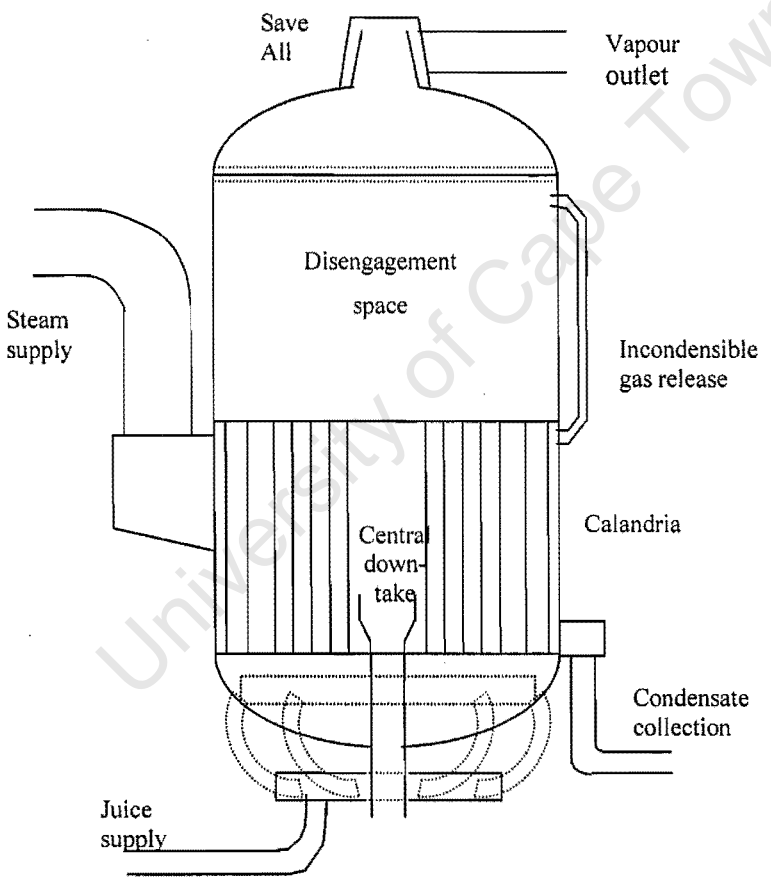

Figure 2.2 Simplified diagram of a Robert evaporator

A common variation on this concept is the long tube, rising film, Kestner type evaporator. The operation is essentially the same as the Robert although Kestner evaporators have two

sections. A vertical calandria, from which juice and vapour are channeled, and the second section a discrete separator, which serves as the disengagement space. There is no downtake, although there may be a recycle of part of the liquid stream from the separator back to join the incoming feed stream. The first and second effects at Triangle are Kestner type evaporators, as shown in Figure 2.3 below:

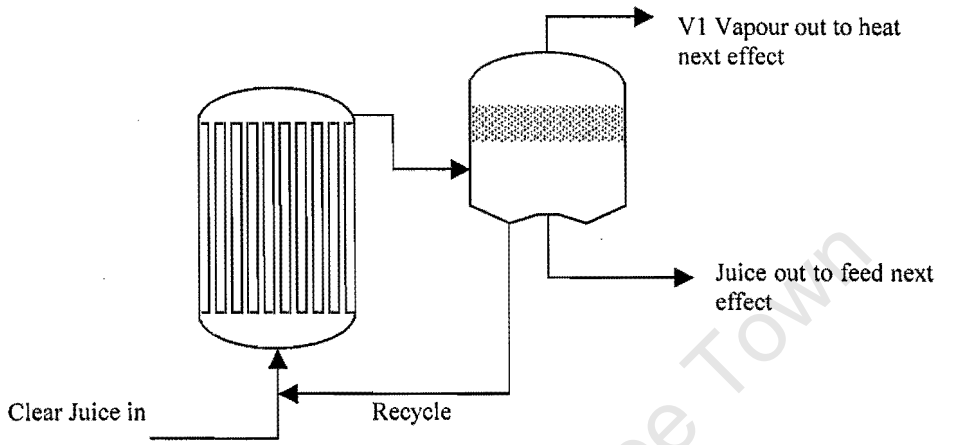

Figure 2.3 Schematic of a Kestner evaporator

Multiple effects

In order to use the heat supplied as efficiently as possible, evaporators are usually designed in a series of between 3 and 6 effects. Steam must only be supplied to the first effect. The boiling juice in this effect produces some vapour which is used to head the calandria of the next effect. The first effect is often supplied with exhaust steam from the Turbo Alternators. The pressure of this steam may be made up by the addition of direct steam from the boiler via a drag valve. The vapour evolved from juice in any effect will, however, be cooler than the steam supplied to that effect. Thus, in order to maintain a suitable temperature gradient across the tube walls, the juice in each subsequent effect must be made to boil at a lower temperature. This is done by operating each subsequent effect at a lower pressure. Due to heating losses, and the need to allow a sufficient driving force for rapid heat transfer, the number of effects in series is usually limited to 5 or 6.

Another consideration, when designing a multiple effect evaporator system is that the juice will deteriorate if kept at elevated temperatures for too long. This process is known as

inversion, and involves the conversion of sucrose to glucose, along with a corresponding loss of glucose to other products. Work by several authors, including Vukov (1965), and Hugot (1983), has indicated that inversion is accelerated by three main factors:

- The operating temperature (the higher the temperature, the faster the rate of inversion, especially when boiling above 90 °C)
- The pH of the juice (the lower the pH, the faster the inversion will occur, especially when operating below pH 6.0)
- The concentration of reducing sugars.

This process is much more serious in cane sugar manufacture, where the purity of the juice is lower than beet sugar manufacture (Chen and Chou, 1993). Purity refers to the percentage of total dissolved substances accounted for as sucrose. The higher this purity is the lower the concentration of reducing sugars, such as glucose and fructose. This means that in a beet sugar factory, where these reducing sugars are present in low concentrations, the evaporators can be operated at higher temperatures than their cane sugar factory counterparts, where the reducing sugars form a larger proportion of total dissolved substances.

In order to take maximum advantage of the steam sent to the evaporators, some of the vapour which is evolved during evaporation in the first few effects is bled to be used in other parts of the factory. Some authors refer to this as "juice steam" (Elhaq *et al.*, 1999). Due to the higher temperatures used in a beet sugar factory, the vapour from several effects, (usually the first four effects) can be used elsewhere (Rousset *et al.*, 1989). In a cane sugar factory, such as that found at Triangle, only the vapour from the first two effects is at sufficiently high temperatures to be useful elsewhere. These two vapours are termed V1 and V2, i.e. the vapours arising from the first and second effects respectively. Depending on the requirements of the rest of the factory, the first two effects must be sized carefully, so as to provide the correct proportions of each vapour, and to avoid wasting any heat.

Multiple effect evaporation at Triangle Ltd.

At Triangle Limited, there are two parallel multiple effect evaporator trains, the A and B sets. This arrangement allows a greater degree of flexibility than a single train, in that either set can be used while the other is being cleaned, or when maintenance work is carried out. Each train then comprises 5 evaporators in series, 1A to 5A, and 1B to 5B. As the throughput of the plant has been increased over the years, additional vessels have been added to the evaporator

station. In order to match the performance of the two trains as closely as possible, vessel 5B is actually made up of two smaller vessels, 5B1 and 5B2. In addition to this, an extra first effect vessel was installed, in 1996, in order to further increase the capacity of the station. The general layout is shown below in Figure 2.4.

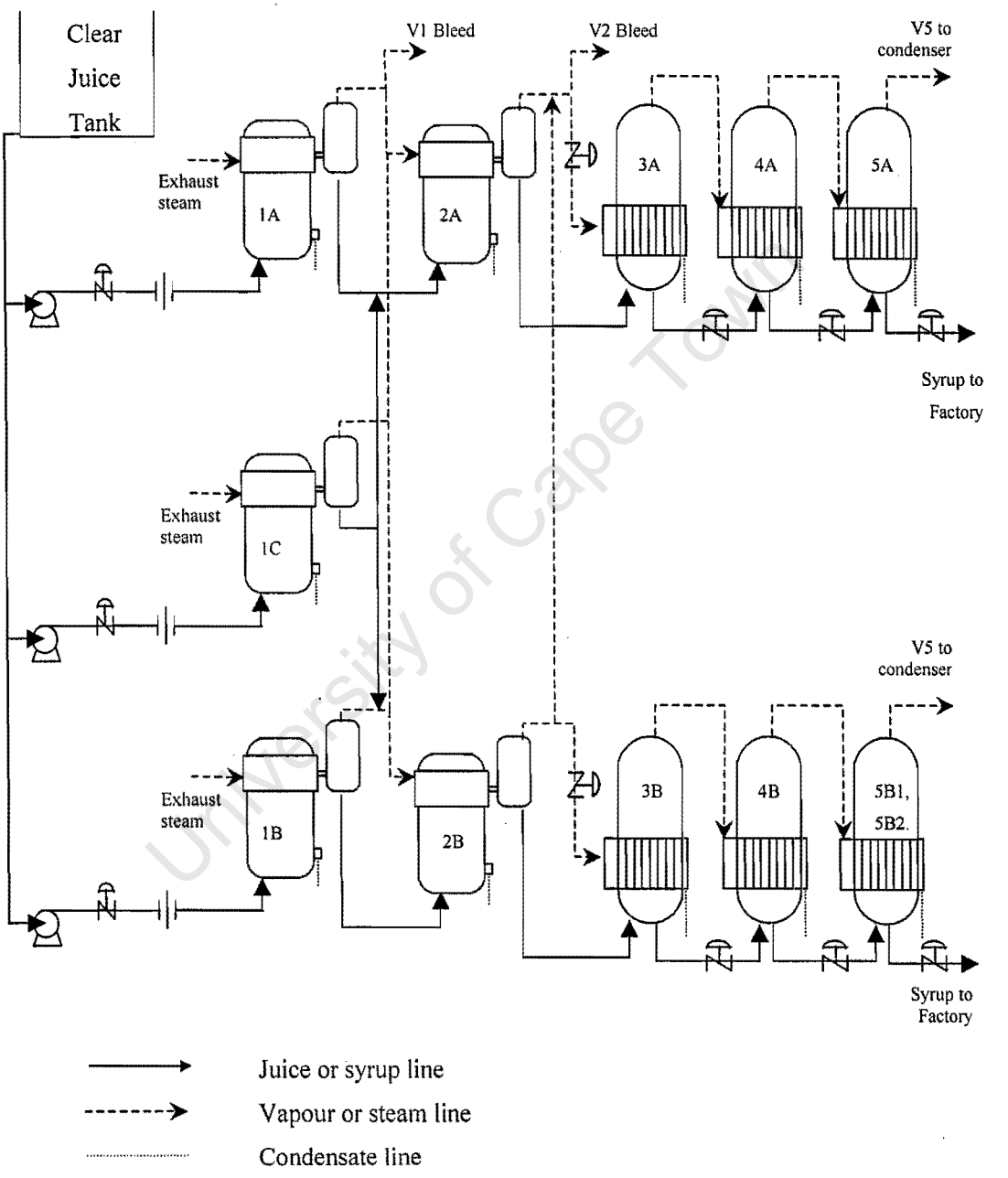

Figure 2.4 Schematic of the evaporator station at Triangle Ltd.

The 1C vessel is similar to the other first effects, 1A and 1B, and receives clear juice and exhaust steam in the same manner. The juice leaving vessel 1C is split evenly to evaporators 2A and 2B, while the vapour from this vessel joins the common V1 line, which feeds both second effect evaporators (2A and 2B) and the bleed line to the rest of the factory.

Another special feature of the Triangle arrangement, which is not common in other sugar mills in Southern Africa, is the nature and scale of the integration of the mill with the agricultural operations. In addition to being one of the largest mills in Africa, roughly 65% of cane processed by Triangle is actually grown on Triangle estate. This is an unusually high percentage. Due to the climate in South Eastern Zimbabwe, this sugar cane requires irrigation throughout much of the year, amounting to roughly 15 megalitres (Ml) per hectare, or about 200000 Ml per annum for the whole estate.

These factors combine to provide a situation which requires a great deal of electricity. Thus the turbo-alternators at Triangle need to be sized for an unusually high capacity, and thus require almost all of the high pressure steam that is generated by the boilers. The net result of this situation is that the steam which the evaporators receive is predominantly exhaust steam, and there is relatively little control over the quality and pressure of this steam, which may hence vary considerably.

2.2 Control of Industrial Evaporator Systems

Conventional control

The problem of evaporator control has long plagued plant engineers. The most common arrangements to be found in Southern African Sugar mills can be grouped as follows:

- Brix control
- Throughput control.

The first of these systems controls the Brix of the exiting syrup, but may allow large variations in the throughput of the station, whereas the alternative, throughput control, maintains as steady as possible a throughput, while allowing minor fluctuations in Syrup Brix. The system currently used at Triangle is a variation on throughput control. The available variables may be listed as follows:

Manipulated variables:

i. the valve position on the feed juice line to each first effect evaporator
ii. the valve opening on juice lines leaving each of the Robert vessels, effects 3, 4 and 5
iii. the valve setting for the vapour supplied to the calandria of effect 3
iv. the valve setting on the cooling water line to the condenser above the final effect

Controlled variables:

i. the level of juice in each Robert vessel
ii. the final syrup Brix
iii. the absolute pressure in the final effect vapour space
iv. the juice throughput into each first effect

For a PID based control system, each of these variables must be paired, using a single loop. For both conventional systems, the final effect pressure is controlled by manipulating the cooling water flowrate, although cooling water exit temperature may be used as the controlled variable, depending on operator preference.

Figures 2.5 and 2.6 give an outline of the control loop setup for each of the conventional systems – so called Brix control, and Throughput control.

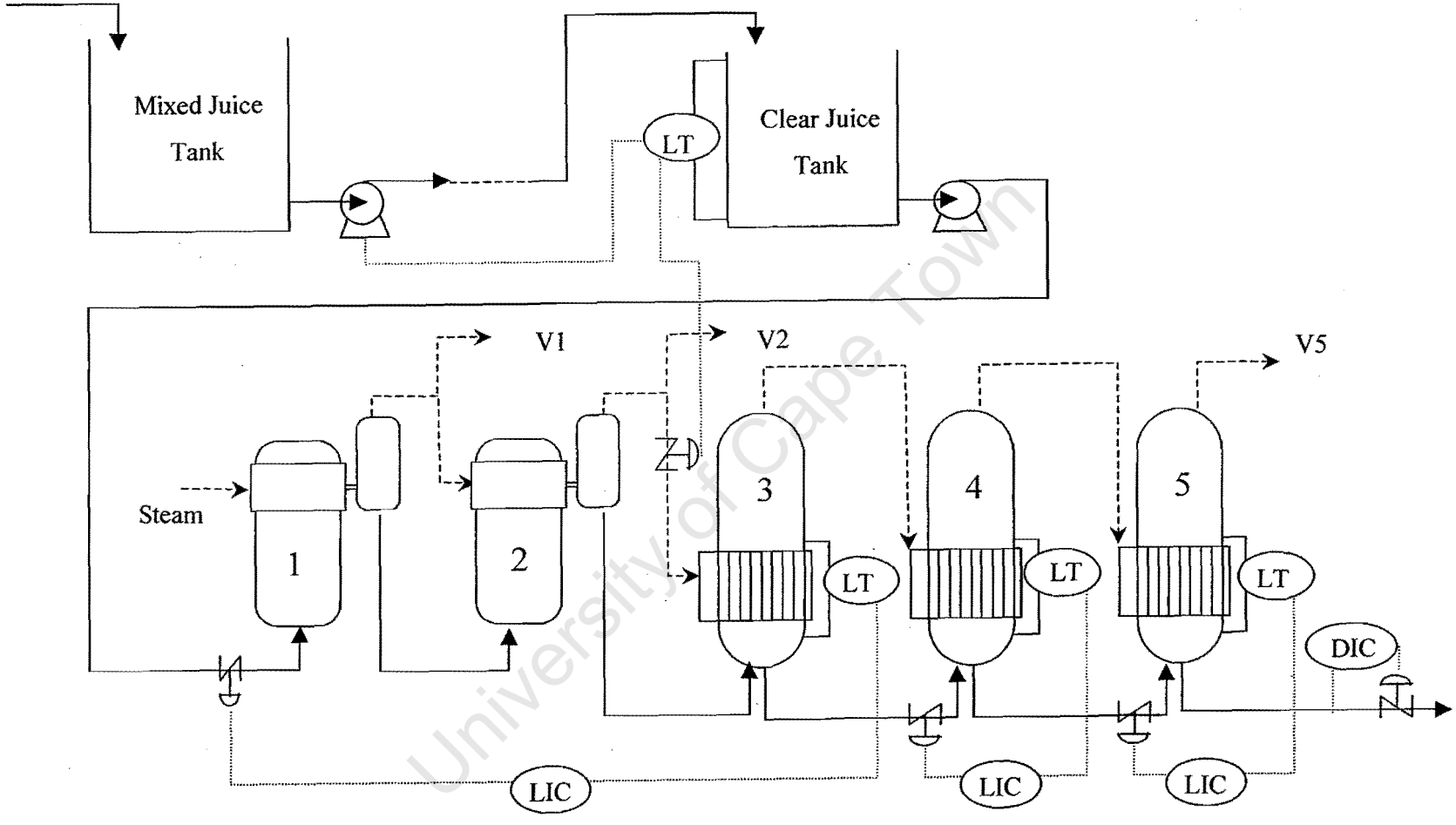

Figure 2.5 *Schematic diagram of the Brix control system*

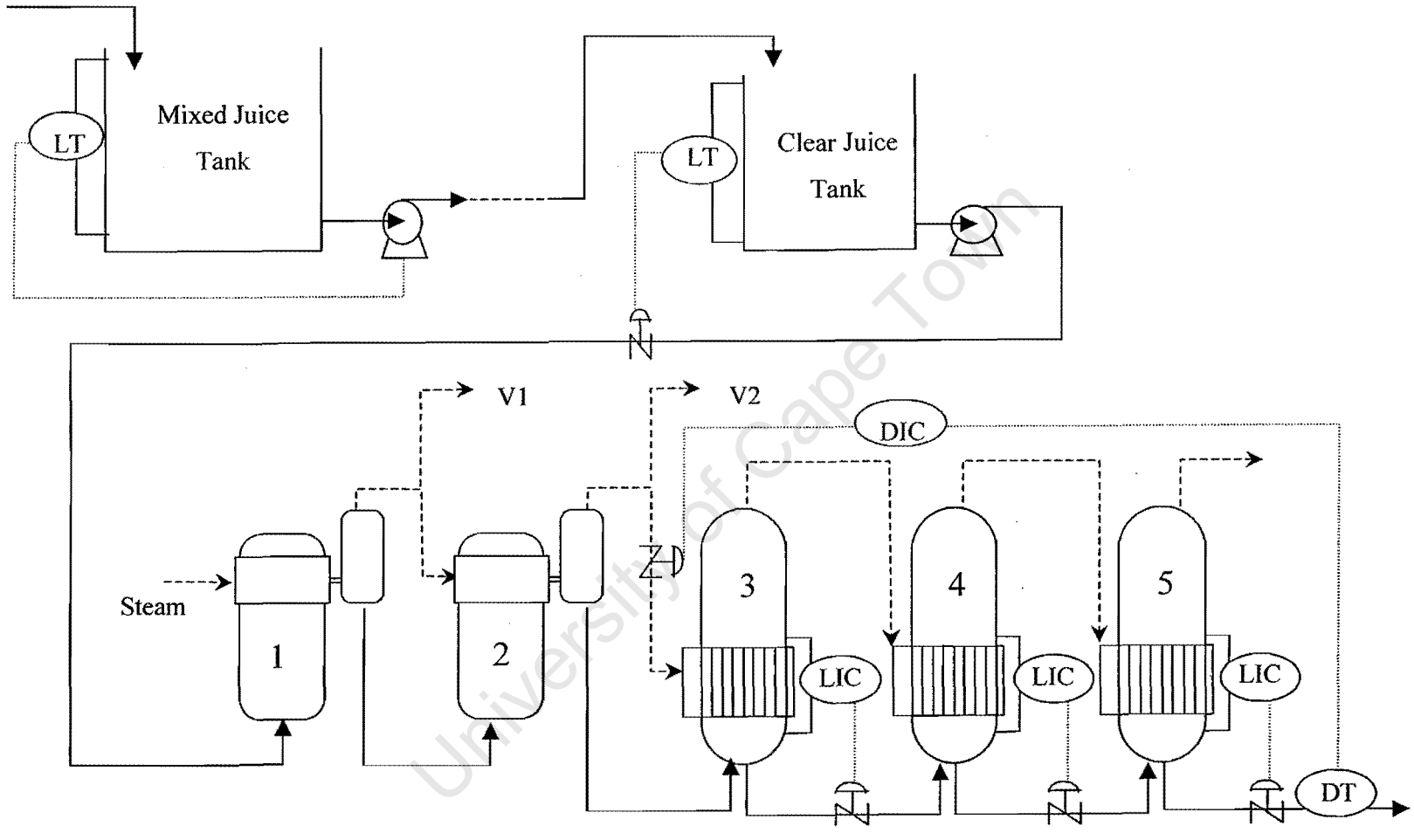

Figure 2.6 *Schematic diagram of the throughput control system*

These two control systems are differentiated based on the primary control objective – if the main concern is that throughput is kept at a maximum, then the system is termed "Throughput Control"; if the primary concern is that the syrup Brix is kept steady, while possibly constraining the total throughput through the station, then the system is "Brix Control".

The "Brix control" system usually involves the following pairings:

- Level in each vessel is controlled by manipulating the juice valve on the *supply* side of the evaporator.
- Final syrup Brix is controlled by manipulating the valve on the discharge side of the final effect – it is this action which has the potential to constraint throughput.
- The total throughput to each set is manipulated according to the level in the first effect.
- The level of juice in the clear juice tank serves as a signal by which to control the throttle valve on the V2 line to the third effect.

The "Throughput control" system usually involves the following pairings:

- Level in each vessel is controlled by manipulating the juice valve on the *discharge* side of the evaporator.
- Final syrup Brix is controlled by manipulating the throttle valve on V2 line to the third effect – this is often a very slow acting form of control, and may not provide very accurate Brix control.
- The total throughput to each set is simply controlled according to the clear juice tank level. The mixed juice flowrate is controlled based on the mixed juice tank level.

The system currently used at Triangle is a mixture of these two conventional systems. The levels of vessels 3, 4 and 5 are controlled as in the throughput control system – by manipulating the flowrate of juice leaving that vessel. Also, as for throughput control, the V2 throttling valve is manipulated based on density measurements on the syrup stream. However, the control of mixed and clear tank levels, is more similar to the Brix control system. At Triangle, the clear juice tank level is controlled by manipulating the mixed juice flowrate, and the clear juice flowrates into each train are controlled according to operator supplied setpoints, as shown below in Figure 2.7.

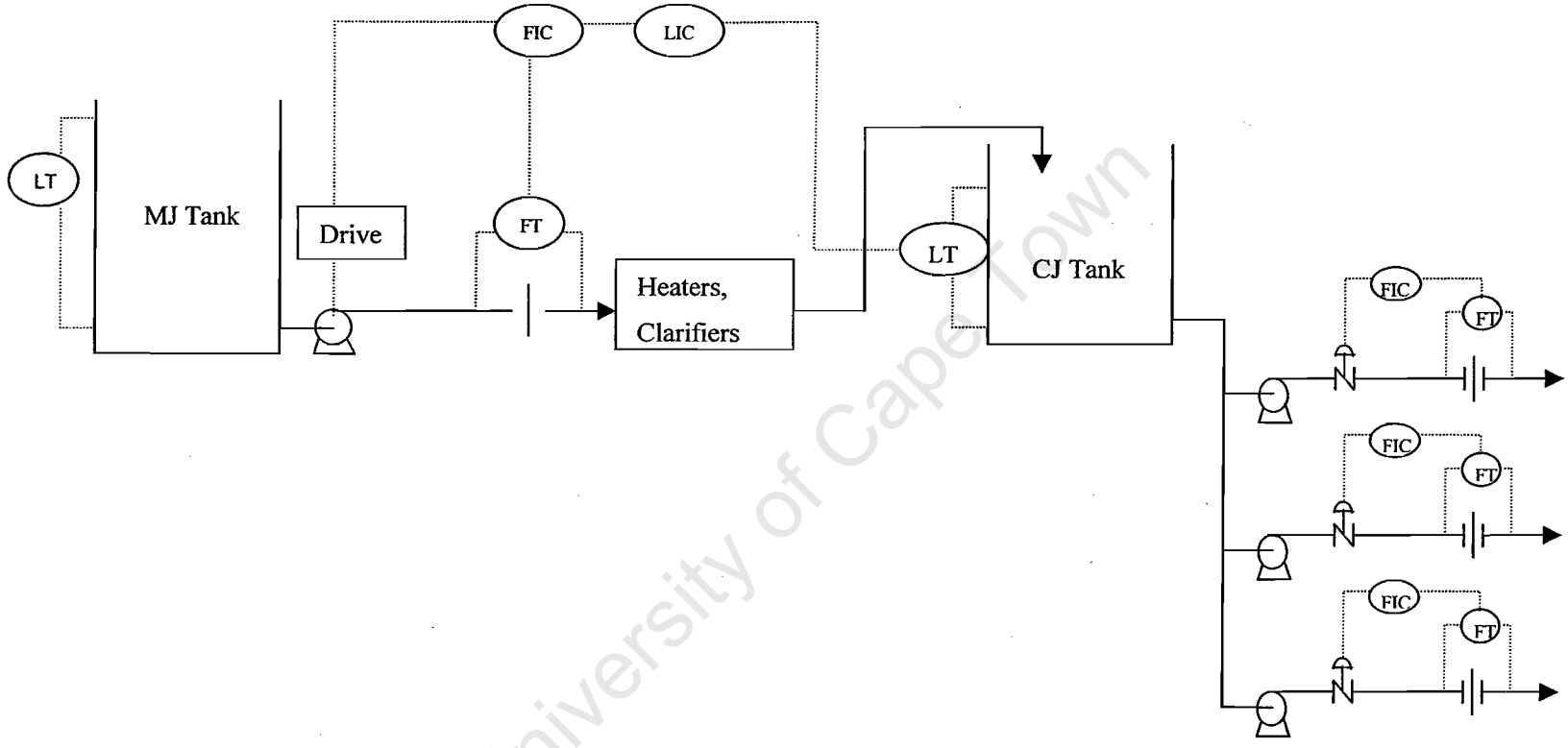

Figure 2.7 *Schematic flow diagram of the tank level control strategy at Triangle Ltd.*

Except for very well designed plants, which are able to operate at the limits of the available equipment, these solutions are not optimal, as will be shown by a brief review of the literature. With Brix control, the throughput of the station is often compromised, whereas with throughput control, the consistency of the syrup Brix is often sacrificed. Lee and Newell, (1989) developed a model of just a single effect and stated that control loop pairing was difficult due to the high degree of interactions observed. It is believed that by eliminating the need for directly pairing these variables an optimal solution can be found, which will best satisfy the overall objective.

Another consideration is the inherent propagation of errors which occurs with either system of level control. Invariably the control move which alters the level in any one vessel will cause a fluctuation in an adjacent vessel, the upstream level in the case of Brix control, or the downstream level in the case of throughput control. A novel algorithm has been developed for the control of levels in floatation cells by Mintek, using the combined upstream inventory as process variable, and this warrants further investigation (Hulbert, 1996).

Alternative evaporator control schemes

Several systems have been proposed by authors using a wide range of techniques to solve this problem.

Montocchio and Scott (1985) reported very good results when they switched their evaporator control system at Amatikulu sugar mill in Natal from throughput control to the Brix control system described above. This conversion was done while only utilizing the distributed single loop Proportional plus Integral (PI) controllers that were already fitted on the plant. The important fact about this work was that the system that was previously used was inherently unstable, and by changing the control variable pairing, a more robust arrangement was found. However, it was also noted that the good results obtained were partly due to a very well sized station, where most vessels were operated continuously at their full capacity, and the throttling steam supply valve to the third effect was almost always fully open. In addition the authors comment that "A prerequisite for this form of control is very steady mixed juice flow control", thus eliminating one of the major disturbance variables from the process. This cannot be assured in all plants where delays due to lack of cane are not uncommon.

Lee and Newell (1989) developed a non-linear control system for a simulated single effect evaporator, (Bequette, 1991). However, this study was only based on model simulation results as opposed to any real plant data, (Elhaq *et al.*, 1999). The control scheme which the authors propose is Generic Model Control (GMC) (Lee and Sullivan, 1988). This is also a model based approach, but differs from other forms of Model Predictive Control (MPC) in that constraints are not handled directly. The control system is based on ensuring a positive rate of change of state variables towards their desired states. Lee and Sullivan (1988) present GMC as superior to a number of alternatives including Dynamic Matrix Control (DMC) and PI control. However, in a later paper Harris and McLellan (1990) lower the significance of this result by exposing the various simplifications made to the models involved in the alternative schemes. Another disadvantage of the proposed GMC technique for practical applications is that only one future move is predicted. Thus it would be difficult to anticipate constraint violations and to plan for them.

Hsiao and Chen (1995) also reported promising results using an improved PID (proportional plus integral plus derivative) controller. Their algorithm includes a form of gap action control augmentation whereby the simple PID output is modified in the face of excessive variations or unusual operating conditions, thus:

$$MV = F(f, g, h) \tag{2.2}$$

Where F = algorithm of the integrated control move

f = function of simple PID loop

g = function of control variable abnormality, (e.g. very high syrup Brix, very low mixed juice tank level)

h = function of milling abnormality (i.e. high or low crushing rate)

This algorithm also allows for rapid response by both the upstream and downstream juice valves in the case of a juice level deviation, which greatly enhanced performance of this control loop. In addition, the control of syrup Brix was accelerated by allowing a variable recycle back to the last effect. Other than those exceptions, the control system retained a single loop structure.

The recirculation of syrup would constrain the final effect capacity, and is thus not an optimal economic solution to syrup Brix control. The use of an integrated control system is also

process specific, and any extreme action taken in the face of unusual process conditions is bound to require specific tuning for each subsequent application. Such a system is not capable of handling hard constraints on inputs and states. This may become particularly difficult if there is a sustained disturbance which also qualifies as an extreme operating condition – e.g. a prolonged milling stop. This may have prompted a quick reduction in the evaporation rate, which might not be optimal when considering a longer period of time.

Rousset *et al.* (1989) developed a control scheme for two beet sugar factories in France. First, a system of equations was developed to compute the optimum static operating point under any given set of process conditions. Then these static set points were followed by single loop controllers. Each loop contained both a predictive element, using a simplified First Order Plus Dead Time model for the juice system, based on tracer test, and a feedback PID controller. Typically one loop of the control system would receive several signals in order to determine the optimum action on one manipulated variable.

However, according to the authors, such a system would not be possible without the high level of instrumentation found at these two plants. Both plants were fitted with flowmeters on all of the bleed vapour lines, as well as on-line Brix measurement at three different points, after the 1st, 3rd, and 5th effects. Unfortunately, very few plants can justify that number of instruments, and therefore such a system would be impractical. In addition to this, constraints were not dealt with directly, but added later in an ad hoc manner to suit each process individually. Ideally, one would like to be able to investigate the effects of various constraints prior to implementation and to include them in the problem formulation so as to make a more widely applicable controller.

These papers highlight the problems encountered with evaporator control – mainly the long process delays or dead times involved, and the large number of process disturbances. While some of these can be measured easily, such as vapour bleed requirements and changes in exhaust steam pressure, others are either expensive or impossible to measure directly, e.g. fouling resistance or a drift in the Brix of clear juice.

Finally, Elhaq *et al.* (1999) present some very promising results from a beet sugar factory in Morocco. The evaporators in this factory were modelled using fundamental relationships and a First Order Plus Dead Time approximation of the dynamics of both the juice and vapour systems between each vessel. The next step was to identify a usable control model of the

evaporator system. This was done using step response tests and a controlled auto-regressive integrated moving average (CARIMA) model structure. The model structure was developed with several intuitive relations in mind, and was primarily tested against these. Once a suitable model had been developed and verified, a multivariable generalized predictive control approach was used, based on Mohtadi *et al.* (1987). The objective function used there was based on the total operating cost. The implemented system produced a uniform syrup Brix and, importantly, minimized steam usage which was one of the main objectives there.

It is important to note here the different objectives for the Beet and Cane sugar manufacturing industries. Some of the main differences are listed below.

- First, due to the higher purity of beet juice, there is a reduced risk of inversion, and so higher evaporator temperatures are used.
- Due to these higher temperatures, vapour is often bled from all of the effects, as opposed to cane sugar manufacture, where usually only the first juice vapours are bled.
- The higher fibre content of sugar cane means that plants will usually not be constrained as tightly by steam supply, because burning the fibre in boilers will usually provide more than enough steam for the factory.
- The higher level of impurities in cane juice results in an increased risk of scaling, and thus smooth operation of the station is imperative.
- Both operations are carried out continuously, although due to the nature of the two crops, beet factories may experience fewer stops on the extraction lines. In the USA, beets are actually stockpiled in huge sheds before manufacture. Cane, which deteriorates quickly must be cut every day, and this pressure may result in a less steady juice flowrate.

Chapter 3 MODEL FORMULATION

3.1 Dynamic Model

In order to test any proposed controller, it was necessary to first develop a model of the evaporator station at Triangle. This model would then mimic the behaviour of the actual station, and thus allow many tests to be performed without actually disrupting the station at all. Several existing evaporator models have been based on a steady state situation, and used largely for design purposes, such as the PEST program written at Tongaat Hulett, TMD, (Hoekstra, 1980). However, in order to be able to observe the transient behaviour of the evaporators and the nature of the interactions between the various parameters, a dynamic model was required. Previous dynamic multiple effect evaporator models have usually made use of the following simplifying assumptions:

1) Vapour pressures in each vessel are fixed.
2) Vapour bleed rates have been fixed.

This model was constructed without these assumptions, so that a more accurate plant representation could be generated. In addition to this, these variables could be later added in as input disturbances to the plant. This was done by supplying the vapour pressures of the two first effect evaporators as inputs from the plant's Supervisory Control And Data Acquisition (SCADA) system. As will be shown later, this then allows the calculation of vapour bleed.

The dynamic model was based on mass and energy balances about each evaporator effect. The following diagram shows the various parameters associated with each vessel.

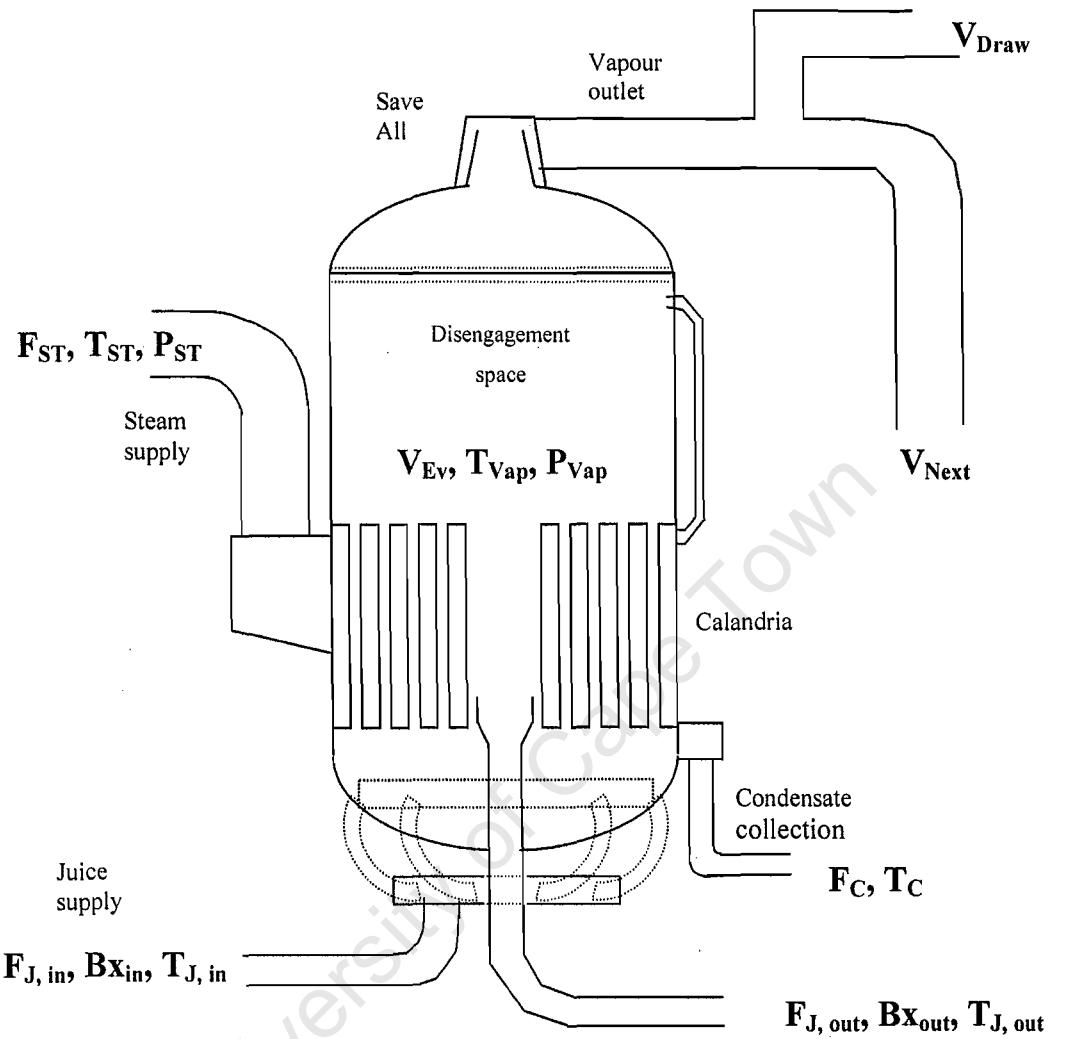

Figure 3.1 Schematic of an evaporator effect, showing the variables used in the model

In this diagram, the following definitions were used:

$F_{J, in}$	-	Mass flowrate of juice entering the evaporator (INPUT)	t / hr
Bx_{in}	-	Brix of Juice entering the evaporator (INPUT)	%
$T_{J, in}$	-	Temperature of juice entering the evaporator (INPUT)	°C
F_{ST}	-	Flowrate of heating steam supplied to the evaporator calandria	t / hr
T_{ST}	-	Temperature of heating steam	°C

P_{ST}	-	Pressure of heating steam (INPUT)	kPa abs
$F_{J,\,out}$	-	Flowrate of juice leaving the evaporator	t / hr
Bx_{out}	-	Brix of juice leaving the evaporator	%
$T_{J,\,out}$	-	Temperature of juice leaving the evaporator	°C
V_{Ev}	-	Flowrate of Vapour evolved from boiling juice	t / hr
T_{Vap}	-	Temperature of Vapour evolved from boiling juice	°C
P_{Vap}	-	Pressure of Vapour evolved from boiling juice	kPa abs
V_{Next}	-	Vapour drawn by the calandria of the next effect (INPUT)	t / hr
V_{Draw}	-	Vapour drawn by equipment elsewhere in the factory (only for first and second effects) (INPUT)	t / hr

Assuming that the conditions of the juice leaving the evaporator are equivalent to the average conditions within the evaporator, we have the following :

By energy balance :

$$M_J C_p \frac{dT}{dt} = F_{J,in}\hat{H}_{J,in} - F_{J,out}\hat{H}_{J,out} - V_{Ev}\hat{H}_{V,Ev} + Q \tag{3.1}$$

where :

M_J	=	mass of liquid in the evaporator (assumed fixed)
C_p	=	specific heat capacity of the juice, a function of Bx_{out} and $T_{J,\,out}$. (Section 3.2)
$\hat{H}_J$	=	specific enthalpy of the juice, a function of Bx and T_J (Section 3.2)
Q	=	heat transferred by the condensing steam
$\hat{H}_{V,Ev}$	=	specific heat capacity of the vapour stream, a function of P_{Vap} and T_{Vap} (Section 3.2)

Assuming saturated steam in the vapour phase:

$$T_{ST} = fn(P_{ST}) \tag{3.2}$$

$$Q = UA(T_{ST} - T_{J,out}) \tag{3.3}$$

$$T_{Vap} = T_{J,out} - B.P.E. \tag{3.4}$$

where :

B.P.E. = (Boiling Point Elevation) is a function of Bx_{out}, $T_{J,\,out}$, and vessel dimensions. (Section 3.2)

$$P_{Vap} = fn(T_{Vap}) \tag{3.5}$$

$$\frac{Vol}{RT}\frac{dP}{dt} = V_{Ev} - V_{Draw} - V_{Next} \tag{3.6}$$

where:

Vol = the volume of the vapour space in the evaporator (assume fixed)

By mass balance :

$$\frac{dM_J}{dt} = F_{J,in} - V_{Ev} - F_{J,out} \tag{3.7}$$

$$M_J \frac{dBx}{dt} = F_{J,in}Bx_{in} - F_{J,out}Bx_{out} \tag{3.8}$$

In the above equations, there are four key output variables, $T_{J,\,out}$, Bx_{out}, V_{Ev}, and P_{Vap}. In addition, the following four variables are solved for, T_{Vap}, Q, T_{ST}, and $F_{J,\,out}$, which accounts for the 8 equations required, equations (3.1) to (3.8), giving a properly determined system. In order to complete the solution for each of the variables shown in Figure 3.1 above, the following relationships would be required :

$$T_C = T_{ST} \tag{3.9}$$

$$F_{ST} = \frac{Q}{\Delta H_{Vap,ST}} \tag{3.10}$$

$$F_C = F_{ST} \tag{3.11}$$

where :

$\Delta H_{Vap,\,ST}$ = heat of vapourisation (condensation) of the steam, is a function of the input P_{ST} (Section 3.2)

Thus in total there are 6 inputs:

$F_{J,\,in}$ $T_{J,\,in}$ Bx_{in} P_{ST} V_{Draw} V_{Next}

and 11 outputs:

$F_{J,\,out}$ $T_{J,\,out}$ Bx_{out} T_{ST} F_{ST} V_{Ev} P_{Vap} T_{Vap} Q T_C F_C

Which would require the 11 equations shown above.

This analysis allows a similar set of equations to be used for each vessel, in that the vapour required by the following effect is used as an input to solve for the variables in the effect under consideration. Similarly, the steam requirement of the current effect is a solved output from the preceding effect. The final effect is unique, in that the vapour evolved from boiling juice in this effect is simply condensed in a condenser. The additional input required is the temperature of the final vapour, which can either be obtained on-line, or calculated based on the condenser cooling water flowrate and the tailpipe temperature.

The model has several features in common with past attempts to model evaporators. However, where the original models kept the vapour pressures in each evaporator fixed (a reasonable assumption except in the case of fluctuating juice flowrates, or fluctuations in the vapour drawn by the factory) the new model frees up both the temperature and the concentration in each effect, and allows them to reach their own equilibrium. There is now a set of two differential equations (in the two states of concentration and juice temperature) governing the boiling of juice in each evaporator effect. A third differential equation, in the state of vapour pressure accounts for vapour evolved and drawn by either the next effect calandria, or other downstream factory equipment.

3.2 Model Features

An important requirement of the model is that the physical properties are estimated accurately. This is done at every iteration step using a subroutine, or f-file in the Matlab environment. This function returns physical properties based on the temperature and Brix of the stream under consideration. The equations used here are all found in an excellent review by Peacock (1995). The function file PhysPropEst.m (Appendix B) returns the physical properties required for the model equations (3.1) to (3.11), as well as those required for the estimation of the heat transfer coefficients, equation (3.20).

Boiling Point Elevation, °C

$$B.P.E. = 6.064*10^{-5}*\left(\frac{(273+T)^2*Bx^2}{(374.3-T)^2}*5.84*10^{-7}(Bx-40)^2+0.00072\right) \quad (3.12)$$

Density, kg / m^3

$$\rho = 1000*\left(1+Bx*\frac{(Bx+200)}{54000}\right)*\left(1-0.036*\frac{(T-20)}{(160-T)}\right) \quad (3.13)$$

Specific Enthalpy, kJ/kg

$$\hat{H} = 2.326*\left(\left(\frac{Bx}{10}\right)*\frac{(100+Bx)}{(900-8Bx)}+1.8T*\left(1-\frac{Bx}{100}\right)*(0.6-0.0009T)\right) \quad (3.14)$$

Specific Heat Capacity, kJ/kg.K

$$C_p = 4.1253-0.02804*Bx+6.7*10^{-5}Bx*T+1.8691*10^{3}T-9.271*10^{-6}T^2 \quad (3.15)$$

Thermal Conductivity, W/m.K

$$k = 1.162222*10^{-3}*(486+1.55T-0.005T^2)*(1-0.0054Bx) \quad (3.16)$$

Viscosity, Pa.s

$$\mu = \left(\frac{1}{1000}\right) * 10\text{^}\left(22.46N - 0.114 + \left(1.1 + 43.1N^{1.25}\right) * \left(\frac{30-T}{91+T}\right)\right) \tag{3.17}$$

where:

$$N = \frac{Bx}{1900 - 18Bx}$$

Heat of Vapourisation, kJ/kg

$$\Delta H_{vap} = 2889 * (1 - Tr)\text{^}\left(0.3199 - 0.212Tr + 0.25795Tr^2\right) \tag{3.18}$$

where

$$Tr = \frac{T + 273.15}{647.13}$$

Enthalpy of Saturated Steam, kJ/kg

$$H_{ST} = \frac{2500}{P^{0.0195}} - 0.26P + 4.187T \tag{3.19}$$

where, assuming saturated steam :

$$P = 10\text{^}\left(7.8656 - \frac{2188.8}{T + 273.15}\right)$$

and throughout equations (3.12) to (3.19),

T = Temperature (°C)

Bx = Brix (%, or °Brix)

Considering the overall station, the data which were input to the model from the SCADA system were the condition of the incoming juice stream to the first effect (temperature, concentration and flowrate), the condition of the incoming exhaust steam from the turbines (temperature and pressure), the amount of vapour drawn off of the first and second effects, and the temperature of the final vapour. The temperature and pressure of the exhaust steam were monitored using data gathered by the SCADA system in order to determine the steam

quality. Having done this over a period of a week, the quality was assumed constant and used, together with the on line pressure reading, as a single input into the system.

The model was programmed in the Matlab/Simulink environment, as a set of discrete ordinary differential equations (ODEs), which were solved using the ODE15s solver, available in Matlab, for the solution of stiff differential equations. The temperature, dissolved solids concentration, and vapour pressure in each effect were taken as the state variables. Thus there are 33 state variables which were solved for at each time step.

The temperature and flowrate of the incoming juice stream is continuously monitored, and would be available to an on line controller. However, the concentration would be difficult and expensive to measure accurately, and so, instead, an average figure would either be assumed for the entire season, as was done for the model, or an analytical result could be routinely supplied to the controller by the laboratory.

The condition of the steam supplied to the evaporator station (exhaust steam from the turbines) is also monitored, and may be controlled to a certain degree, by the addition of direct HP steam from the boilers. However, due to the power plant arrangement at Triangle, it is reasonable to assume that this steam will be of a constant quality, and thus only the pressure reading was used as a controller input.

Vapour draw : As has already been mentioned in Chapter 2, there is a significant quantity of vapour (V1 and V2) drawn by the factory for use in the crystallising pans and juice heaters. Any model will be sensitive to the values chosen for these bleed streams and any fluctuations. Several studies of evaporator control, (Elhaq *et al.*, 1999), (Rousset *et al.*, 1991) have been done in factories where these steam bleed rates are measured accurately and on line, using magnetic flowmeters. This is a very expensive solution and is not viable at Triangle.

In this model, the vapour bleeds were initially assumed to be a linear function of incoming juice flowrate, in order to mimic the average behaviour of the existing factory layout. This assumption was valid over a period of several hours, as will be shown in Section 3.3. However, there are also short-term fluctuations in V1 drawn by the factory, which are largely due to the batchwise operation of some of the evaporative crystallising pans. These could not be accounted for accurately until the V1 and V2 pressures were used as further inputs to estimate vapour draw. In this case there must still be 11 equations, but equation (3.6) must

now be considered from the point of view that P_{Vap} is now an input, and V_{Draw} is an output. P_{Vap}, i.e. the vapour pressures V1 and V2 are available on-line from the SCADA system.

V2 valve dynamics : Vessel 3 calandria pressure is always lower than the vapour space pressure in vessel 2, due to the throttling valve on the connecting line between these two areas. For this vessel, effect 3, there is an additional input, i.e. the throttling valve position, and thus an additional equation must be found to relate the pressure drop across the valve to it's position. The dynamics of the V2 throttling valve are highly nonlinear. This valve is used to control the flow (pressure) of steam to the third effect calandria, and in so doing, to control the amount of evaporation which takes place in the final three vessels. By using data gathered by the SCADA system, a plot of the relationship between the ratio of upstream and downstream pressures and the valve position was obtained.

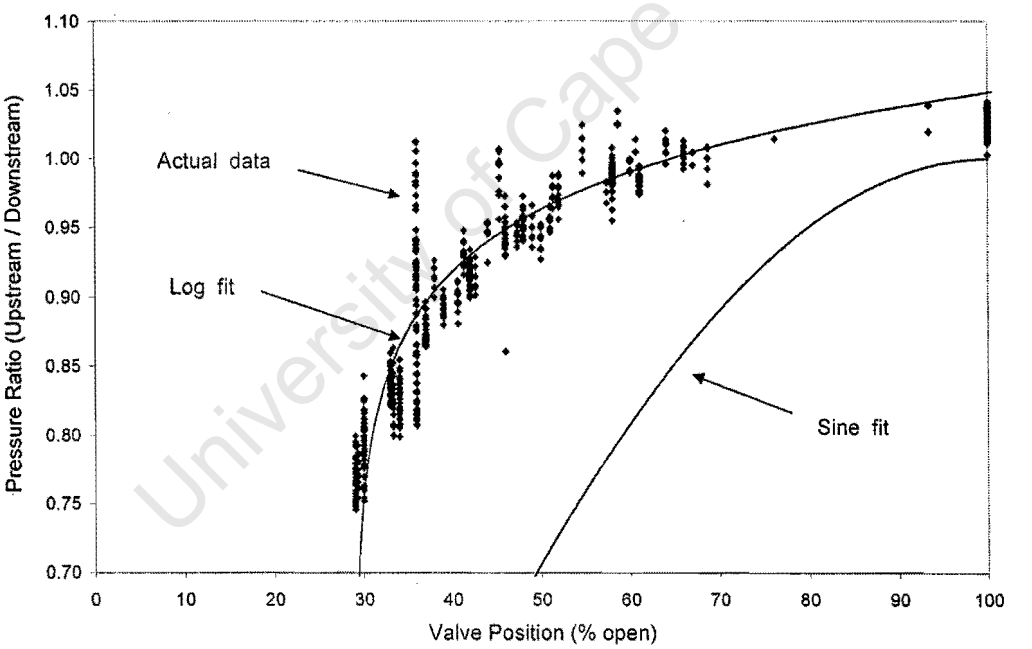

Figure 3.2 Graph to show the relationship between valve position and pressure drop.

Theoretically this relationship should take the form of a sine curve, based on the cross sectional pathway available for flow, although from Figure 3.2 a logarithmic curve appears to fit the data more closely for the range of interest, i.e. 20% to 100% open.

Heat transfer coefficient : Previous evaporator studies have reported great difficulty in obtaining accurate estimations of the heat transfer coefficients. These problems have been attributed to the highly complex nature of juice boiling, as well as the lack of accurate data. In the final implementation of this control system, it was proposed that this may be overcome by accurate on line measurement of the condensate flowrate, which will in turn give a measure of the amount of steam being used for heating in each vessel. This measurement would then be filtered to achieve the necessary stability.

An accurate heat transfer coefficient is crucial (Khan *et al.*, 1998), in order for there to be good agreement between the model and real life. Having reviewed the literature on this subject, there seemed to be two main approaches. Several authors (Hussey, 1974), (Elhaq *et al.*, 1999), were content to fit correlations to existing data and then use these in future work and their models, while Mulholland, (1991) designed a Kalman filter to observe the heat transfer coefficients on line based on plant measurements of flowrates and temperature. Other authors (Khan *et al.*, 1998), (Peacock and Starzak, 1996) have attempted a first principles approach, in which differential equations of heat and momentum transfer are used to arrive at a rigorous model. Khan *et al.*, (1998) incorporated the theory of multiple boiling zones with the most reliable empirical correlations, in order to come up with a dynamic solution. To simplify matters, it was assumed that the boiling regime be split into two zones - a sensible heating zone, in which the juice is brought up to boiling point; and a two phase zone, in which the juice and evolved vapour both rise up the tube as a mixture. This approach has been tried, and it was found that the most important variable in determining the HTC was the juice flowrate.

Both the first principles approach and the use of correlations have their advantages and disadvantages – too rigorous a model may not be able to take into account the particular conditions encountered with the plant under consideration, whereas a model based purely on correlations may provide an infeasible solution if the data are extrapolated beyond their range of applicability. In this model, both approaches have been used. Firstly, the heat transfer coefficients for each vessel in the Triangle station were calculated based on SCADA measurements and lab analyses over a period of two months during the 1999 crushing season. This gave a solution for the operating conditions at the average or steady state. Next, this solution was generalized by using the method of Dittus and Boelter, i.e. by scaling relative to the Reynolds and Prandtl numbers raised to the following powers.

$$U = U_0 \frac{N_{Re}^{0.8} N_{Pr}^{0.4}}{N_{Re,0}^{0.8} N_{Pr,0}^{0.4}} \tag{3.20}$$

where :

Reynolds Number = $N_{Re} = \frac{Dv\rho}{\mu}$

D = tube diameters (m)

V = velocity of juice in tubes (m/s)

ρ = the density of the juice (kg/m^3)

μ = the viscosity of the juice (Pa.s)

Prandtl Number = $N_{Pr} = \frac{C_p \mu}{k}$

C_p = the specific heat capacity of the juice (kJ/kg.K)

k = the thermal conductivity of the juice (W/m.K)

and the subscript $_0$ refers to steady state operation.

This relationship was originally intended for turbulent two phase flow, which is the case for the majority of the tube length in an evaporator, due to the flashing which usually occurs as the juice enters at the base of the vessel. Although there is also a significant amount of film boiling, and even annular flow, the Dittus-Boelter equation is simple to use in practice, and proved to be a fairly accurate representation of what was observed on the station.

Time lags and juice levels : The existing model makes the assumption of constant liquid volume hold-up for the each of the evaporator effects. Originally the levels in the final three effects were modelled dynamically using the existing PID controller settings. However, this made the model more complicated, and did not add any significant accuracy. An alternative was to use the level signals from the SCADA as inputs into the model, although was also found to be unnecessary for the accuracy of model which was required. The following graph, Figure 3.3, shows the behaviour of liquid levels on the last three vessels of the A set after the startup of the station at about 18:30 hrs. It is important to note how quickly the levels are brought under control, even after a massive disturbance such as a startup. This is why it was decided to assume constant values for the liquid levels in each evaporator.

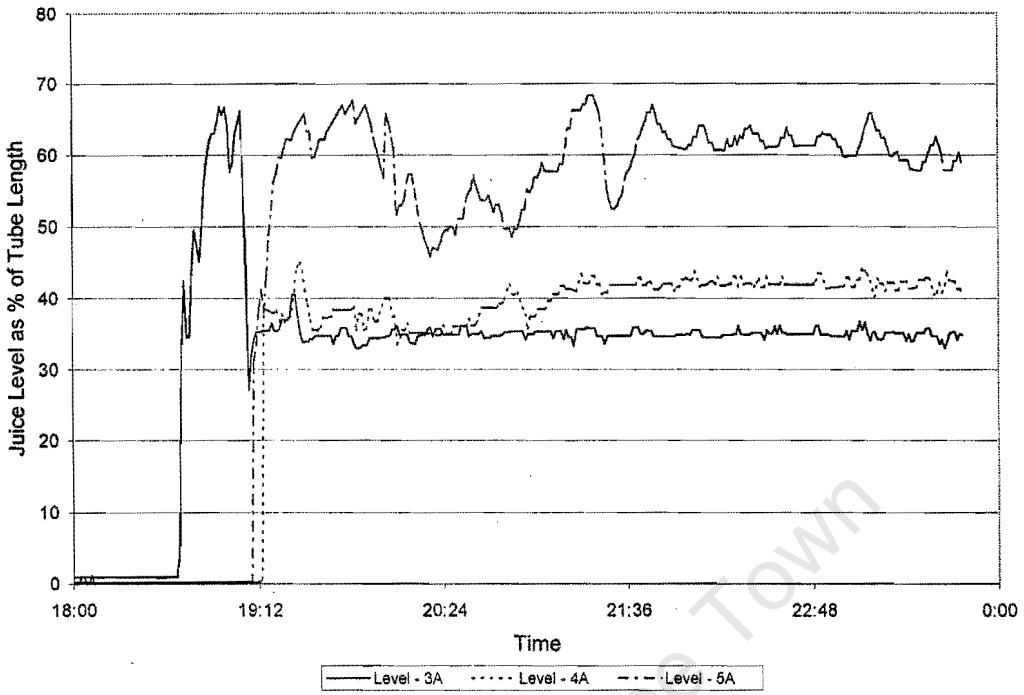

Figure 3.3 The behaviour of liquid levels in vessels 3A, 4A and 5A, after plant startup.

On the real plant, the pipes that transport juice from the outlet of one vessel into the inlet of the next are relatively long and cause a significant time lag between the effects. Table 3.1 gives an approximation of these delays:

Table 3.1 Time Lags in the Juice System

Stage	Juice Flowrate (tph)	Pipe Length (m)	Pipe ID (mm)	Time Lags (s)
1-2	358	40	250	60.4
2-3	277	30	200	26.2
3-4	226	10	200	10.1
4-5	172	15	200	20.0

In order to account for this, two methods had been proposed for this model, and these were both coded into the Matlab environment and then compared. First a model using one script file to calculate all of the state derivatives was used, i.e. the differential equations for all for

the vessels. This was found to be computationally modest and to provide a good approximation to the real plant data. As no discrete time lags could be included in this system, the section of pipe between each vessel must be approximated by a number of CSTRs in series.

Second a similar model was constructed, which included separate scripts for each effect with the associated transport delays, or time lags, incorporated explicitly between each effect. This second structure proved to be a fairly cumbersome model to solve and with the existing solvers was very sensitive to slight input deviations (or "stiff"), and would become unstable easily.

When the results of the two models were compared with real plant data there was found to be no significant improvement with the second model, and so the first was adopted.

3.3 Results of Modelling

Once the model had been completed it was tested by supplying some input data from the SCADA system. Figure 3.4 shows the inputs which were collected on the 28th of November 1999 from the Triangle evaporator station. These inputs were, clear juice flowrate, clear juice temperature, exhaust steam pressure, final effect pressure for each train (vessels 5A and 5B), and vapour 2 throttling valve position for each third effect (3A and 3B).

Other inputs were required for the model and these had to be supplied either from historical data or from the laboratory. The Brix of the incoming clear juice is measured by the laboratory on an hourly basis, and this was also supplied to the model. In this simulation the vapour drawn (vapour 1 and vapour 2) by the rest of the factory was assumed to be a linear function of throughput. By doing this, the pressures of these two vapour streams could be solved for, and used to compare the model against actual plant data. As was mentioned in Section 3.2, the model is also capable of accepting vapour 1 and vapour 2 pressures (available on-line from the SCADA) and then solving for the two vapour draws.

Figure 3.5 shows the outputs of the model, compared with the real plant data, collected from the SCADA and the laboratory. The variables which are compared are the vapour 1 and vapour 2 pressures, and the final syrup Brix for each evaporator train (A set and B set). The laboratory only analyses the syrup Brix every hour, and this sample represents a composite of the preceding hour. The results from the model, however, are continuously updated every minute.

There is a good agreement between the vapour pressures obtained from the model, and the general trends observed in the plant record. Any disagreement was possibly due to random variations in the amount of vapour drawn by the rest of the factory. The model prediction of syrup Brix was also fairly accurate, as shown in the lower trace of Figure 3.5. The model trace does however show several fluctuations which are not evident in the laboratory analyses. This was due to the fact that these analyses are hourly averaged, and so most of the peaks and troughs are eliminated.

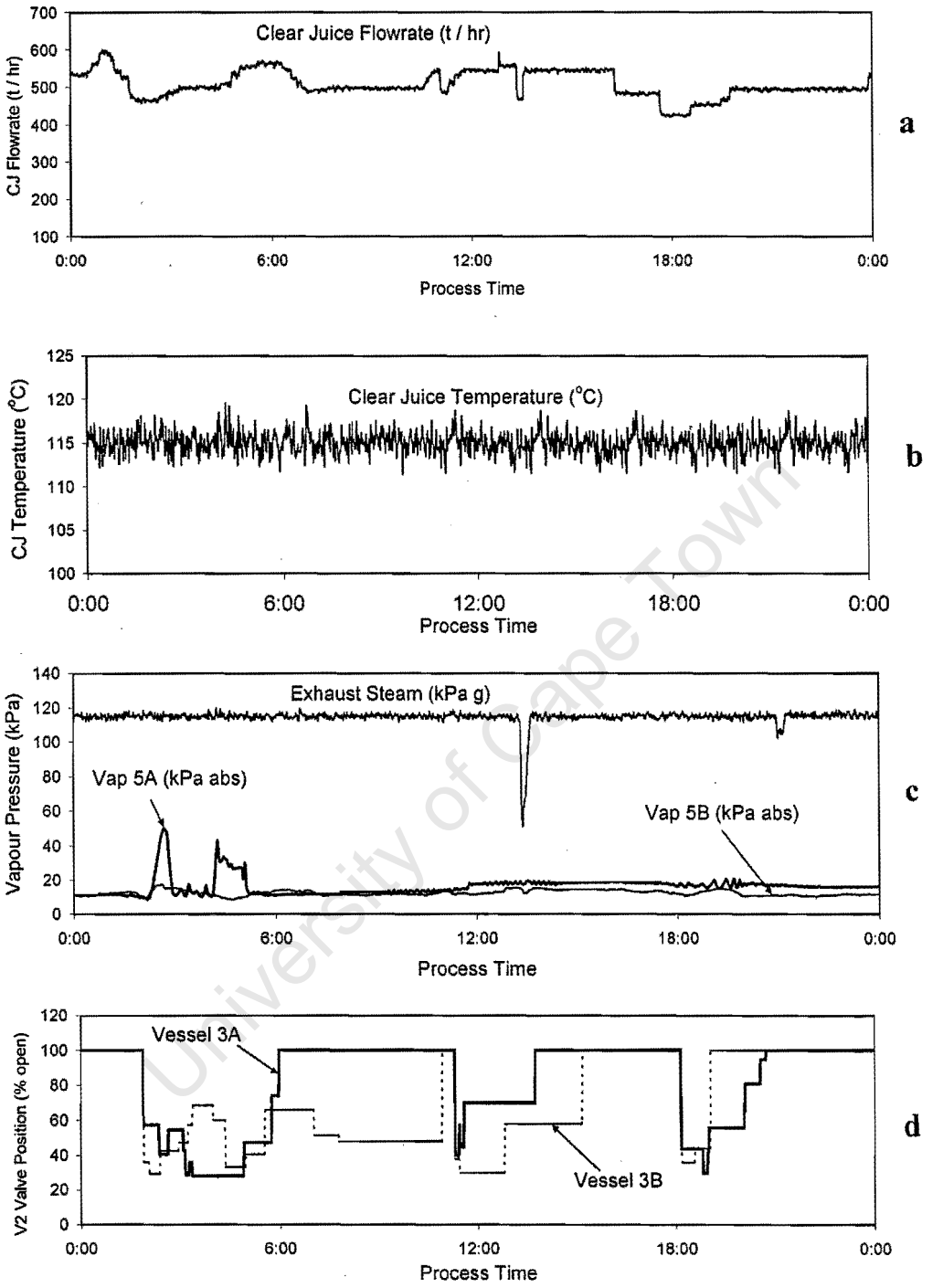

Figure 3.4 *Graphs of the data which were collected and used as inputs to the model where (a) shows clear juice flowrate, (b) shows clear juice temperature, (c) shows vapour pressures, and (d) shows V2 throttling valve positions.*

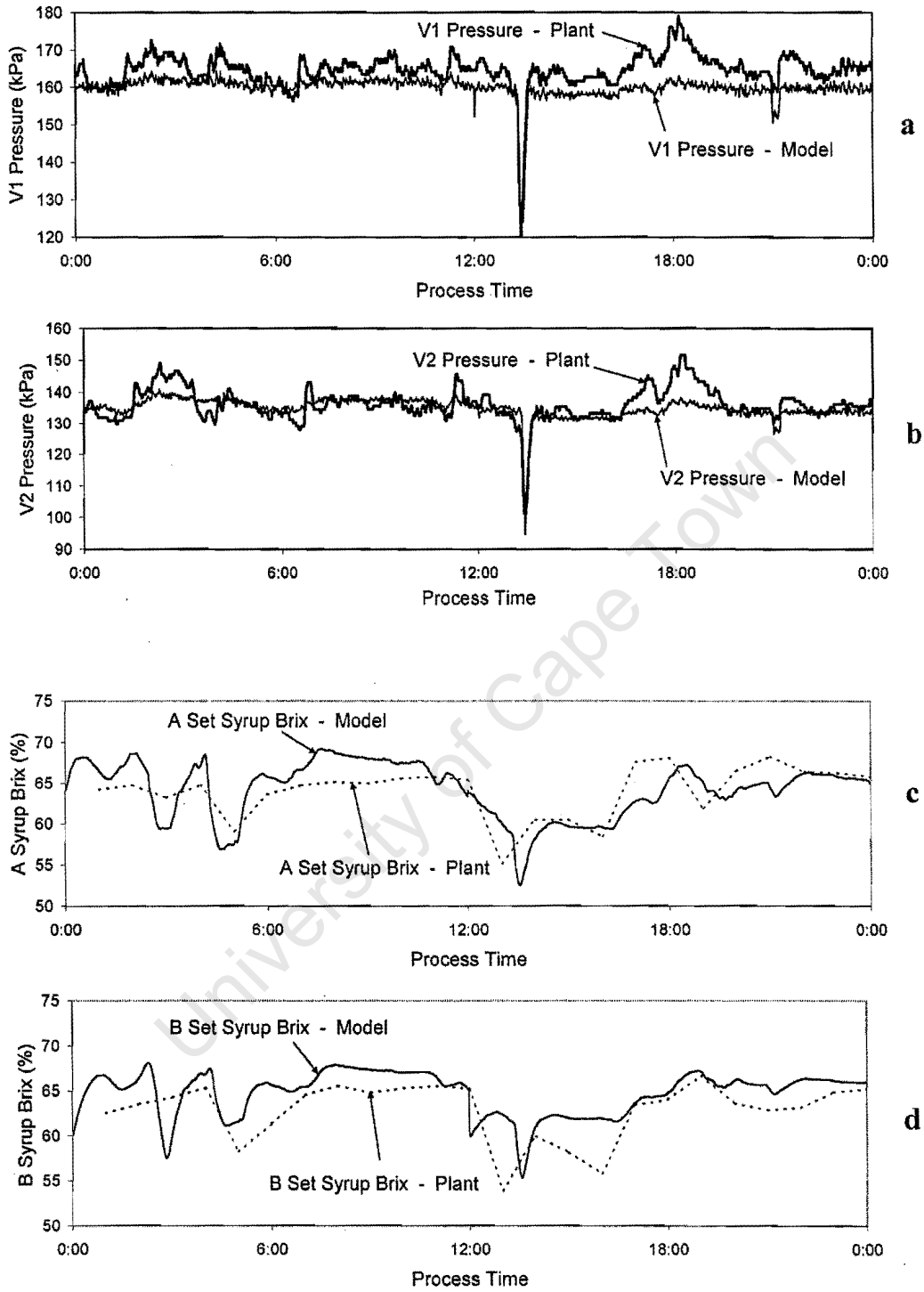

Figure 3.5 *Graphs of the outputs from the model in comparison to the real plant data where (a) shows the V1 vapour pressure, (b) shows the V2 vapour pressure, (c) shows the A set syrup Brix, and (d) shows the B set syrup Brix.*

Chapter 4 CONTROLLER DESIGN

4.1 Advanced Control System Theory

Advanced model predictive control

Since about the 1960s there has been a great deal of attention focused on so called advanced control systems. The major impetus behind this attention was undoubtedly a frustration with the limitations encountered with conventional (PID based) control (Bequette, 1991), (Garcia and Morari, 1982). With increasing global competition, industries are forced to operate more efficiently and to produce more consistent products which will satisfy stringent quality control criteria (Qin and Badgewell, 1996).

These factors have motivated most plants to be operated at the very limit of their physical capabilities – that is at an intersection of constraints under which the system must run (Prett and Gilette, 1979). In order to do this an efficient and stable control system must be implemented which will allow tight control for economic reasons, while providing a realistic answer for practical reasons. In a practical plant situation any control system should also be sufficiently transparent to the operator in order to ensure that the system gains acceptance (Garcia, Prett and Morari, 1989).

Any control system should exhibit the following behaviour and may be judged by these criteria (Garcia and Morari, 1982) :

1. Regulatory behaviour – the system must maintain the process as close as possible to the required setpoint, even under the effect of disturbances.

2. Setpoint tracking – the controller must be able to move the process from one set point to another, swiftly and smoothly.

3. Robustness – the system must be stable, and excessive control action should be avoided, even when the operating conditions change.

4. Constraint handling – the controller must be able to deal with constraints on the manipulated inputs and the states of the process.

However, in order to justify the expenditure required to develop an advanced technique, or even a novel application of an existing technique, the overall system must be able to optimize the process as well as maintain a steady state of operation. Optimization could be with regard to economics, compliance with safety and environmental regulations, or product distribution and quality given a certain mix of raw materials (Garcia, Prett and Morari, 1989). It has been noted (Garcia and Morari, 1982), that the major economic return from expenditure in advanced process control systems is from the optimization of process conditions, rather than good regulatory behaviour (Lee and Weekman, 1976).

The most common objectives are a combination of economics and logistics, and it is a widely reported fact that the optimal operating point of a plant, from an economic point of view, will be at the intersection of constraints (Arkun and Stephanopoulos, 1980), (Prett and Gillette, 1979). For this reason it is essential that any new control system be able to anticipate constraints on both input variables and states, while not allowing violations, to maintain the states as close as possible to the constraints. Finally, given the high expense of developing a new control strategy, it should ideally be adaptable to as wide a range of situations as possible (Garcia, Prett and Morari, 1989).

Several advanced techniques have been developed to meet these criteria. Amongst the first advanced multivariable controllers were Linear Quadratic Regulators. These were aimed at controlling a multiple input multiple output process by minimizing a quadratic objective function. This was done using a linear state space model of the process, such as :

$$x_{k+1} = Ax_k + Bu_k \tag{4.1}$$

$$y_k = Cx_k \tag{4.2}$$

where x = a vector of states
u = a vector of manipulated inputs
y = a vector of outputs, and
A, B and C are constant matrices.

By defining all variables as deviations from a steady state value of zero, one can then arrive at an objective function which penalizes the weighted squares of both state errors, and manipulated variable moves.

The objective function used is commonly notated, J:

$$J = \sum_{l=1}^{\infty} \left(\left\| x_{k+l} \right\|_Q^2 + \left\| u_{k+l} \right\|_R^2 \right) \tag{4.3}$$

where l = the time step
$\left\| x_{k+l} \right\|_Q^2$ = the 2 – norm, defined as follows :

$$\left\| x \right\|_Q^2 = x^T Q x \tag{4.4}$$

and Q and R are the weighting matrices for the state error, and manipulated variable move suppression, respectively.

This objective function then serves the dual purpose of forcing the process closer towards the desired state, and preventing excessive control action, thereby improving the system's robustness. The infinite time horizon over which the control is computed ensures good stability for any reasonable plant, that is one which is stabilizable and detectable (Qin and Badgewell, 1996).

Several variations on this method have been used, including the Linear Quadratic Gaussian controller, as well as other optimal quadratic control systems. However, none of these methods were able to directly handle constraints. This minimized the practical applications of this technique. So it was not surprising that the impetus behind the first Model Predictive Control schemes was from industry. Cutler and Ramaker, two engineers from Shell, outlined

Dynamic Matrix Control, or DMC, in 1979, and Richalet *et al.* described Model Predictive Heuristic Control in 1978 (Garcia, Prett and Morari, 1989). While the ideas encountered here were not entirely new, these papers first showed successful practical applications of this technique. There are several important differences between these methods and the previously mentioned optimal control (Qin and Badgewell, 1996), mainly :

- The use of a finite receding prediction horizon, as opposed to an infinite horizon
- An explicit process model is used by the controller to predict future plant dynamics
- Input and output constraints are included as part of the problem, and thus allow prediction of future constraint violations.

DMC, MAC and IMC

The DMC problem formulation is most easily demonstrated using a state space model, although any suitable mathematical model may be used. Most commonly, the internal model used by the controller takes the form of a step response matrix. This matrix is developed by stepping each of the input variables by 10—20%, in both directions, while maintaining all other inputs at their nominal or steady state values, and then monitoring the resultant effects on each of the outputs. This may be done either on the real plant, or else in simulations on a model of the plant. For each possible pair of one input and output, a matrix can be generated to represent the effect on that output (i) of a step change in that input (j). This matrix is commonly notated A_{ij}. Figure 4.1 shows how this matrix would be developed. The values of the change in each output (a_i) are recorded at discrete measuring intervals, t = 1, 2, 3,..., following the input disturbance (a step change from 5 to 6, here).

Two major assumptions are made in the DMC formulation,

- linearity; i.e. changes in more than one input, would result in a simple addition of the responses from changes in each input individually, and a change in any input would cause a change in an output which is directly proportional to the magnitude of the change in the input, and
- time invariance, i.e. the effects of each input on each output are similarly independent of when those changes occurred.

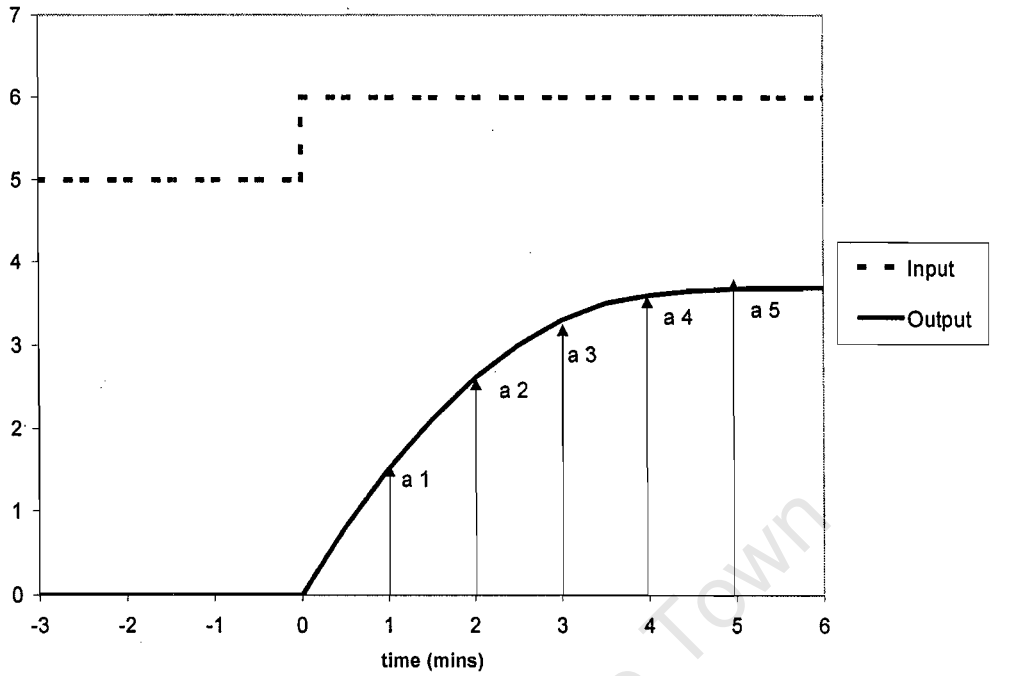

Figure 4.1 *Graph showing step response coefficients*

Matrices for each input and output pair are then combined, to form an overall dynamic matrix, notated A.

$$A_{ij} = \begin{bmatrix} a_1 & 0 & \cdots & 0 \\ a_2 & a_1 & \ddots & \vdots \\ \vdots & a_2 & \ddots & 0 \\ a_M & \vdots & \ddots & a_1 \\ \vdots & & & a_2 \\ a_N & & & \vdots \\ \vdots & & & \vdots \\ a_N & a_N & \cdots & a_N \end{bmatrix} \tag{4.5}$$

$$A = \begin{bmatrix} A_{11} & A_{12} & \cdots & A_{1T} \\ A_{21} & A_{22} & & \vdots \\ \vdots & & & \vdots \\ A_{S1} & & & A_{ST} \end{bmatrix} \tag{4.6}$$

where M = the number of future manipulated moves

N = the number of timesteps to steady state
S = the number of outputs, and
T = the number of inputs.

The prediction of outputs, $\tilde{y}$, is done by considering past and present inputs, and measured disturbances :

$$\tilde{y} = A\Delta u + y^* + d \tag{4.7}$$

where $\tilde{y}$ = a vector of the predicted outputs
A = the Dynamic Matrix
Δu = the future control moves
y^* = the predicted impact of past control moves on the output, and
d = the measured disturbances to the system, which are assumed constant in this case.

The impact of past control moves, y^*, is predicted thus :

$$y^* = B\Delta u_{past} \tag{4.8}$$

where :

$$B_{ij} = \begin{bmatrix} a_2 & a_3 & \cdots & a_n \\ a_3 & a_4 & & \vdots \\ \vdots & \vdots & \ddots & \vdots \\ a_{N-1} & a_N & & a_N \\ a_N & \vdots & & \vdots \\ \vdots & & & \vdots \\ a_N & a_N & a_N & a_N \end{bmatrix} \tag{4.9}$$

$$B = \begin{bmatrix} B_{11} & B_{12} & \cdots & B_{1T} \\ B_{21} & B_{22} & & \vdots \\ \vdots & & & \vdots \\ B_{S1} & & & B_{ST} \end{bmatrix} \tag{4.10}$$

and the disturbance vector, d, is the vector of predicted disturbances at times t = $k+l$, where $0 \le l \le P$, which is calculated thus :

$$d(k+l|k) = d(k|k) \tag{4.11}$$

and

$$d(k|k) = y_m(k) - \{y^*(k-1) + A\Delta u(k-1)\} \tag{4.12}$$

where $y_m(k)$ = the vector of measured outputs

In this manner the future disturbances are predicted as constant at the value of the current disturbances. Importantly, this disturbance vector takes into account both model (prediction) error as well as unmeasured process disturbances (Garcia, Prett and Morari, 1989).

Using the notation as above, the objective function is usually a similar weighted quadratic objective, J, which penalizes both output errors from setpoint, and manipulated variable moves :

$$J = (y_{set} - \tilde{y})^T .Q.(y_{set} - \tilde{y}) + \Delta u^T .R.\Delta u \tag{4.13}$$

where y_{set} = the vector of output setpoints.

When considering discrete measurements, the objective may be written :

$$\min_{\Delta u(k),\Delta u(k+1),\cdots\Delta u(k+M-1)} J = \sum_{l=1}^{P} \left(\|y_{set}(k+l) - \tilde{y}(k+l)\|_Q^2 + \|\Delta u(k+l)\|_R^2 \right) \tag{4.14}$$

where P = the prediction horizon, given as a number of discrete time steps

M = the number of allowed control moves

$y_{set}(k+l)$ = the vector of desired outputs at time $(k+l)$

$\Delta u(k+l)$ = the vector of changes in the manipulated variables at time $(k+l)$, and

$\tilde{y}(k+l)$ = the vector of predicted outputs at time $(k+l)$ based on information and measurements available at time k.

Constraints are dealt with directly by including an inequality in the problem :

$$y_{\min} \le \tilde{y}(k+l) \le y_{\max} \tag{4.15}$$

$$u_{\min} \le u(k+l) \le u_{\max} \tag{4.16}$$

$$\Delta u_{\min} \le \Delta u(k+l) \le \Delta u_{\max} \tag{4.17}$$

The other early model predictive scheme, Model Algorithmic Control, or MAC, was derived along similar lines, with some important distinctions :

- The model uses an impulse response model, as opposed to a step response model.
- The number of input moves is set to the prediction horizon, $M = P$.
- The disturbance estimate is filtered to give a less sensitive estimate.

Internal Model Control, IMC, was developed to combine the advantages of the different unconstrained MPC schemes and to facilitate the tuning of the resultant controller, (Garcia, Prett and Morari, 1989). This scheme has a similar structure to that used for the previous two techniques, whereby an internal model is used to predict the future behaviour of the plant. The design procedure of the actual controller is slightly different, however. Figure 4.2 presents a simplified IMC structure (Garcia and Morari, 1982) :

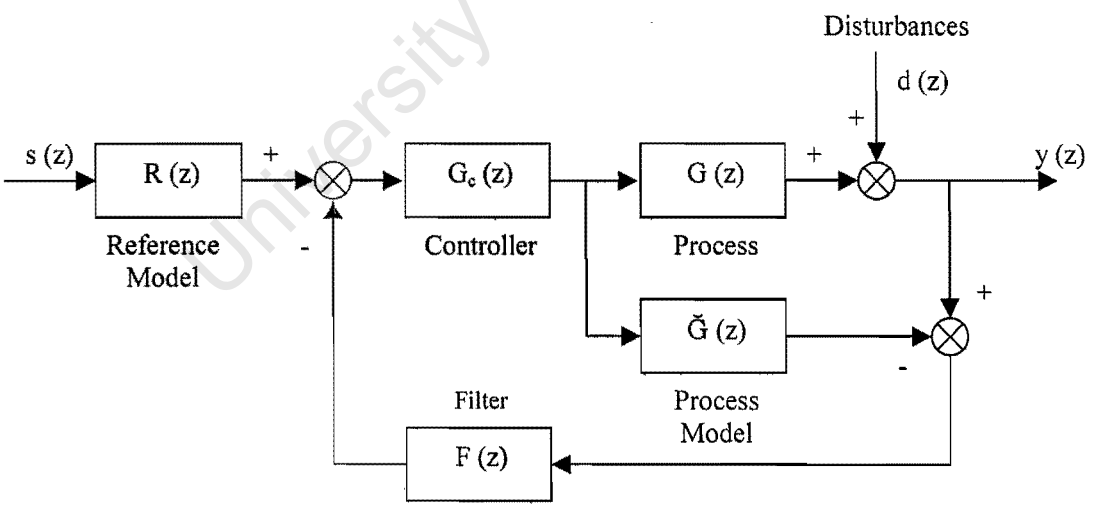

Figure 4.2 Schematic control diagram of an IMC controller

Briefly, the controller consists of two parts. First, a "perfect" controller is designed that will allow perfect regulatory and servo behaviour. The output from this controller is then detuned

by a low pass filter which reduces the manipulated variable moves and improves the system robustness. Overall this reduces the number of adjustable parameters from the DMC and MAC cases, while retaining their positive properties of ensured system stability for a stable controller (Garcia, Prett and Morari, 1989), (Garcia and Morari, 1982).

Nonlinear model predictive control

Since these first MPC techniques were developed there has been a lot of work done, especially towards the extension of these ideas to nonlinear systems. Henson (1998) reviews the progress in this field, and points out the most common methods of dealing with this problem.

Linear control cannot provide an adequate solution when either the process is highly non-linear, or it is only moderately non-linear but has a wide operating regime (Henson, 1998). In this case it may be necessary to use a nonlinear controller. Di Marco *et al.* (1997) compare three potential controllers for the control of a highly nonlinear process, a teropolymerization reactor. First, the nonlinear model of the process was linearized over the whole range of operation about some steady state. Second, a number of linearizations are performed, and then a weighted average of these models was used in the predictive controller. Finally, a fully nonlinear model was used which was linearized for solution at each time step. This paper compared the relative effort required and potential benefits to be gained by the three approaches.

If it is decided that a nonlinear controller will be necessary, then first a model must be developed, and tested. The most common nonlinear models used are fundamental sets of ODEs and algebraic constitutive equations, which physically describe the system. However, if the process is very complex, or there is insufficient knowledge about the system characteristics, then an empirical model may be used. Usually a NARMAX, or non-linear auto-regressive moving average with exogenous inputs, type of algorithm is used, with Hammerstein, Wiener, Volterra, ARMAX, and artificial neural networks all having been reported, (Henson, 1998) (these are subsets of the NARMAX structure). An attractive alternative would be to use a hybrid model, which is based partly on fundamentals, but incorporates an empirical element to approximate poorly understood parameters, such as the heat transfer coefficient.

The nonlinear control problem is usually formulated very similarly to the linear case, thus with a system described by the following state space relationships (Henson, 1998) :

$$x' = f(x,u) \tag{4.18}$$

$$0 = g(x,u) \tag{4.19}$$

$$y = h(x,u) \tag{4.20}$$

where x = a vector of states
u = a vector of manipulated inputs
y = a vector of outputs, and
$f, g, h,$ = (possibly) non-linear functions of their arguments

The objective function may then be to minimize the objective function, J :

$$\min_{\Delta u(k),\Delta u(k+1),\cdots\Delta u(k+M-1)} J = \Phi\left[\tilde{y}(k+l|k)\right] + \sum_{l=1}^{P-1} L\left[\tilde{y}(k+l|k), u(k+l|k), \Delta u(k+l|k)\right] \tag{4.21}$$

where ϕ and L are functions chosen by the control system designer, but are usually of quadratic form, with constant weighting factors for the penalized parameters.

This is subject to constraints, which may vary with time :

$$y_{\min} \le \tilde{y}(k+l|k) \le y_{\max} \tag{4.22}$$

$$u_{\min} \le u(k+l|k) \le u_{\max} \tag{4.23}$$

$$\Delta u_{\min} \le \Delta u(k+l|k) \le \Delta u_{\max} \tag{4.24}$$

The objective function may have several different forms, and in particular, may not include a separate penalty for the final output at the prediction horizon, the first term above (Elhaq *et al.*, 1999), (Bequette, 1991), (DiMarco *et al.*, 1997).

By inspection, this is a fairly simple extension of the linear MPC controllers discussed earlier. However, the solution of such a problem is far more involved for the nonlinear case. The control engineer has several methods at his/her disposal, with successive linearization of the

system about a chosen operating point, and sequential model solution and optimization being the most common (Henson, 1998). There have also been proposals to simultaneously solve and optimize the system of equations, after discretization of the relevant differential equations (Rawlings *et al.*, 1994).

In conclusion, MPC technology can be seen as a range of related techniques which offer the control engineer some important advantages – mainly direct constraint handling and the inclusion of dead time and interaction effects through the embedded process model, together with simple tuning guidelines and good stability properties. Importantly too, there have been several stability results in the literature, (Garcia and Morari, 1982), (Qin and Badgewell, 1997), (Garcia, Prett and Morari, 1989), which allow the stability of MPC to be analysed. It is believed that a model predictive controller will best suit the current problem, due to the large number of constraints on the system (mainly physical equipment constraints), and the dead times associated with the juice flow through the station.

In the following section (section 4.2), the design of the DMC controllers is presented, and this is followed by the two additional control layers – level controllers (section 4.3) and a steady state optimizer (section 4.4).

4.2 DMC Design

It was decided that the most efficient method for tackling this control problem would be through the formulation of a DMC model predictive controller. There are several advantages in using an MPC approach. The most important of these here would be the ability of the system to anticipate and handle constraints, and its ability to deal with multiple inputs, and multiple outputs. Two control systems were devised, and their performance was then compared; these will be presented below.

Control of evaporators

Chapter 1 dealt with the motivation behind the three control objectives which have been decided upon. These will now be described in detail, along with the possibilities for combining them. The major part of this project was concerned with the design of the control system for the delivery of syrup of a smooth Brix from the evaporator station. It has been noted that many of the difficulties that arise in multiple effect evaporator control, are due to process fluctuations. In a sugar factory, the most important of these is a fluctuation in the flowrate of the clear juice which is delivered to the station. Therefore, two types of tank level controller have also been designed and tested on a model of the plant. These will be described later. The final consideration was to determine the best split of the total clear juice flowrate between the three first effect vessels, based on their condition (i.e. their evaporative potential on a given day). The first two objectives (Brix control and level control) must be dealt with continuously on line and will thus be dealt with first, whereas the steady state optimization is only required periodically and will be dealt with later.

Brix - level control system

The Brix – level control system was based on the DMC algorithm first presented by Cutler and Ramaker, (1979). The objective of this controller is to deliver the maximum amount of consistently high quality syrup to the evaporative crystallisers, within the constraints of juice availability and evaporator station capacities.

The existing controllers have already been described, and the first step was to determine which of these controllers would be retained, and which would be incorporated into the proposed control system. The existing level controllers for the final three effects of each train

were retained, along with the absolute pressure controllers on each final effect, vessels 5A and 5B. The remaining adjustable inputs for the station are the throttling valve on the vapour supply line to each third effect calandria, and the juice flow controllers on each of the three first effect vessels. It is important to consider the advantages of various controller designs, especially as regards the Triangle evaporator station. Due to the fact that the two trains are cleaned on alternate weeks, they are usually able to achieve different performances at any given time. For this reason, it was decided that the inputs (V2 valve position and clear juice flowrate) for each evaporator train should be controlled independently. However, a further problem was encountered at Triangle, where there is an additional first effect vessel, the 1C Kestner, which delivers juice equally to vessels 2A and 2B.

The SCADA system provides online readings of the most significant three disturbances, i.e. clear juice temperature, exhaust steam pressure and final effect pressure. The effects of these disturbances are efficiently included in the DMC formulation. Inputs were chosen as the two adjustable variables, (1,2), and the three disturbance variables (3,4,5). Taking into account all the vessels in the actual station, this amounts to 9 process inputs.

1. Clear juice flowrate (x3) – these can be directly manipulated via the throttling valves on each inlet line
2. V2 valve throttling position (x2) – these can be directly manipulated.
3. Clear juice temperature (1) – any variation in this variable must be due to random process disturbances, as the set point is constantly set at 115 °C, and a single loop PID controller actuates a steam valve on the steam line feeding the juice heaters.
4. Exhaust steam pressure (1) – this is difficult to vary due to the arrangement with the turbo-generators. As the electrical load of the estate changes, the operating configuration of the power plant will change and this will alter the exhaust steam pressure. There is a degree of control in that a drag or let down valve will inject high pressure (3.0 MPa) steam into the line, if the pressure drops below setpoint. However, this control is not very accurate, and therefore, steam pressure will be treated as a disturbance.
5. Final effect pressure (x2) – this is also controlled about a constant setpoint, and so any fluctuations could be counted as a disturbance. The control of final effect pressure actually involves two measurement signals, those of the deviations of temperature and absolute pressure from their setpoints. These two signals are then multiplied together and used to manipulate the cooling water flowrate to the condenser.

DMC control hinges on the ability of the controller to predict future behaviour of the plant based on current disturbance measurements. Once the dynamic model had been completed, several step tests were done to determine the response of the model to a 10% step in the key input variables. In order to test the sensitivity of the model, step tests were also performed on the vapour bleed rates. In this way, the effect of a step in each input variable on each output variable was measured. A sampling time of 1 minute was used, as this was a convenient interval for analysis, and has proven adequate for obtaining all of the process dynamics from this system. The overall juice residence time in the multiple effect evaporator is about 45 minutes, and so the settling time to steady state was safely set at two hours. 10% steps were made as both increases and decreases in the key input variables after an initial settling period of two hours, and this was followed by another two hours of data gathering. The results of the step tests showed that for each of the observed disturbances, 120 minutes were sufficient to allow the system to settle to a new steady state.

From the step tests, the assumptions inherent in DMC of linearity and time invariance allowed the computation of a mean step coefficient for each input (increase step response – decrease step response) / 2, and hence the construction of the Dynamic Matrix. The predicted future outputs may then be computed by the equation:

$$\tilde{y} = A\Delta u + y^* + d \tag{4.25}$$

here, $\tilde{y} \in \Re^{2P}$ = the predicted outputs (for two outputs, e.g. syrup Brix; clear juice flowrate)

$A \in \Re^{2P \times 5M}$ = the Dynamic Matrix, (for two outputs and five inputs) which was determined in simulations, made up of sub-matrices for each input-output pair, $A_{ij} \in \Re^{P \times M}$

$\Delta u \in \Re^{5M}$ = the future control moves (clear juice flowrate; V2 valve position), as well as measured but uncontrollable inputs (clear juice temperature, exhaust pressure, final effect pressure) – a total of five inputs

$y^* \in \Re^{2P}$ = the predicted impact of past control moves on the outputs, and

$d \in \Re^{2P}$ = the impact of measured disturbances on the outputs, including the effects of any plant model mismatch.

In order for the Brix control level to fit in with the other control systems on the station, it is necessary to consider any overlapping or interacting variables. It has already been stated that the two variables available for Brix control are the V2 throttling valve and the clear juice flowrate. However, it is also necessary to control the clear juice flowrate so that the clear juice tank neither overflows, nor runs dry. Furthermore, it is necessary to distribute the clear juice flowrate in an optimal manner between the three first effect vessels.

The main consideration was how to combine the first two control objectives (assuming a clean plant, with each train performing equally) – smooth control of Brix, and level control of the clear juice tank:

i The first alternative was to cast two separate controllers, which would operate in cascade – a level controller which passes a flowrate setpoint to the Brix controller.

ii The second alternative would be to formulate the controller as a single larger DMC controller which would have to deal with both the level objective and the Brix objective.

Alternative 1 - cascade formulation

In this system there are two separate Brix controllers, one for each set, which receive a cascaded flowrate setpoint from a separate level controller (section 4.3). The level controller receives signals of the actual flowrate of clear juice and the actual tank level in the clear juice tank. This actual clear juice flowrate is the sum total from the three flow measurement devices which are fitted on the three juice supply lines (one to each first effect evaporator). From these measurements the juice level controller (LIC) decides on the optimal juice flowrate, and sends this as a set point to the distribution controller (section 4.4), as shown in Figure 4.3.

The distribution controller (Eco / Opt Splitter in Figure 4.3) has inputs of the optimal total clear juice flowrate (from the juice level controller), the three actual juice flowrates (into each first effect), and the estimated heat transfer coefficients from the 5 Kestner evaporators. These heat transfer coefficients will be the basis of the flow splitting. The outputs from the

distribution controller will be three juice flowrate setpoints, one for each first effect evaporator.

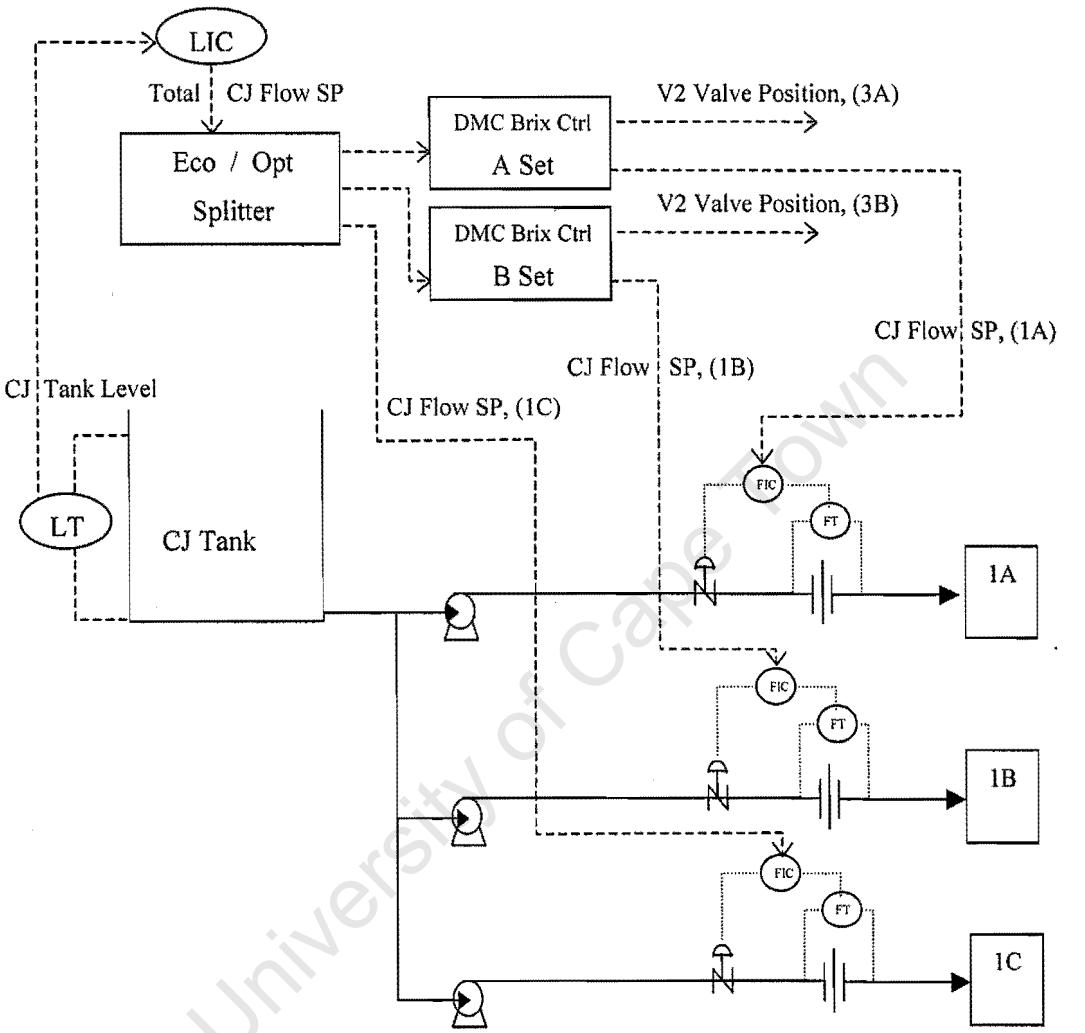

Figure 4.3 *Arrangement of three controllers for Alternative 1 (cascade formulation) showing the level controller, the economic optimization layer, and the two DMC Brix controllers, one for each set.*

The setpoint for clear juice flowrate into vessel 1A will be sent to the Brix controller for the A set, and the setpoint for clear juice flowrate into vessel 1B will be sent to the Brix controller for the B set. The last output from the distribution controller, the setpoint for clear juice flow to the 1C evaporator, will be sent directly to the FIC controller which actuates the control valve on that line.

Each Brix controller also receives a Brix setpoint from the operator (usually 68-72°Bx), along with measurements of the disturbances to that set, and these are used in the calculation of the relevant clear juice flowrate and V2 valve position. The clear juice flowrate determined by the DMC Brix controller is then fed as a set point to the appropriate PID flow controller, which also receives the actual flowrate, and which manipulates the clear juice flow control valve position. The structure of the control system is shown in Figure 4.3.

For each DMC Brix controller there are two outputs per line, and six inputs, and so the dynamic matrix would appear thus:

$$A\Delta u = \begin{bmatrix} A_{11} & A_{12} \\ A_{21} & A_{22} \end{bmatrix} \cdot \begin{bmatrix} \Delta u_1 \\ \Delta u_2 \end{bmatrix} + \begin{bmatrix} A_{13} & A_{14} & A_{15} A_{16} \\ A_{23} & A_{24} & A_{25} A_{26} \end{bmatrix} \cdot \begin{bmatrix} \Delta u_3 \\ \Delta u_4 \\ \Delta u_5 \\ \Delta u_6 \end{bmatrix} \tag{4.26}$$

Where each sub matrix corresponds to output *i* and input *j*.

For the A set, outputs, i, refer to :

1. Syrup Brix (5A)
2. Clear juice flowrate (1A)

and inputs, j, refer to:

Manipulated inputs

1. Clear juice flowrate (1A)
2. V2 valve throttling position (3A)

Disturbance inputs

3. Clear juice temperature
4. Exhaust steam pressure
5. Final effect pressure (5A)
6. Clear juice flowrate, (1C)

The clear juice flowrate is treated here as both an input and an output – the transfer function relating them in the dynamic model is unity. This flowrate could have been fixed and removed from the DMC controller. However, its inclusion allows it to be used as a manipulated variable with a specified bias value at which it will settle. This scheme is common in industry, where there are typically more manipulated variables than controlled variables (Qin and Badgewell, 1996).

The clear juice flowrate (manipulated input) referred to in the DMC formulation is really a setpoint to a cascaded lower level PI flow controller, which is again typical of industrial MPC implementation (Qin and Badgewell, 1996).

The optimization problem would then be to minimize the weighted sum of squares of the setpoint tracking errors and the manipulated variable moves, subject to the system equation (4.25) above and the following constraints :

1) CJ flowrates for each line must be kept between 0 and 300 tph.
2) V2 valve position must be kept between 0 and 100 %.
3) Syrup Brix should be kept between 72 and 55° Brix.

The optimization program was as follows :

$$\min_{\Delta u_1(k),\cdots\Delta u_1(k+M-1),\Delta u_2(k),\cdots\Delta u_2(k+M-1)} J = \left(y_{set} - \tilde{y}\right)^T .Q.\left(y_{set} - \tilde{y}\right) + \Delta u^T .R.\Delta u \qquad (4.27)$$

here, $y_{set} \in \Re^{2P}$

$\Delta u \in \Re^{2M}$

$\tilde{y} \in \Re^{2P}$

$Q \in \Re^{2P\times 2P}$

$R \in \Re^{2M\times 2M}$

This is subject to the following hard constraints, for the whole prediction horizon, i.e. for $P \geq l > 0$:

$$\Delta u_{\min} \leq \Delta u(k+l) \leq \Delta u_{\max} \qquad (4.28)$$

$$u_{\min} \le u(k+l) \le u_{\max} \tag{4.29}$$

and the following constraints for the constraint window, i.e : for $P \ge l > L$, :

$$y_{\min} \le \tilde{y}(k+l) \le y_{\max} \tag{4.30}$$

where, for this constraint, equation (4.30) :

$$\tilde{y}(k+l) \in \Re^{2(P-L)}$$

$$\tilde{y}(k+l) = \begin{bmatrix} \tilde{y}_1(k+L+1) \\ \tilde{y}_1(k+L+2) \\ \vdots \\ \tilde{y}_1(k+P) \\ \tilde{y}_2(k+L+1) \\ \tilde{y}_2(k+L+2) \\ \vdots \\ \tilde{y}_2(k+P) \end{bmatrix} \tag{4.31}$$

and L is the time until the start of the constraint window ($1<L<P$).

A clear distinction has been made between variables that are actually disturbances, and cannot be freely manipulated by the control system, and genuine adjustable inputs. The Input-Output structure of each of the DMC Brix controllers is shown in Figure 4.4 (for the A set):

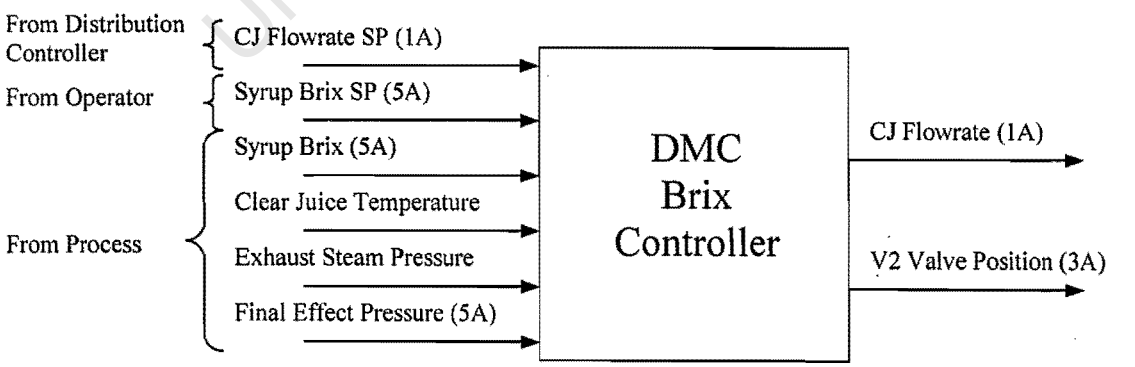

Figure 4.4 Input / Output structure of the DMC Brix controller

Formulation in QP

The DMC controller was then coded into the Matlab Simulink language. The controller itself was incorporated as an s-function with the following basic structure :

⇒ Load Dynamic Matrix

⇒ Initialize states in controller (variable moves over move horizon)

⇒ Receive inputs:

Set Points (for Brix and clear juice flowrate)

Output Measurements (Brix, Clear Juice Flowrates)

Disturbance measurements (Clear juice Temperature, Exhaust Steam Pressure, Final Effect Pressure)

⇒ Calculate disturbance estimate over prediction horizon.

⇒ Compute optimal sequence of input moves using Matlab function fmincon(function, Initial guess)

⇒ Load weighting matrices Q and R

⇒ Set constraints

dU min =	-20
dU max =	20
U min =	[0 ; 0]
U max =	[300 ; 100]
Y min =	[50 ; 0]
Y max =	[80 ; 300]

⇒ Function to be minimized = objective function.

⇒ Constraint matrix = constraints from above.

⇒ Update record of input moves

⇒ Send input moves to actuators

Constraints were included as follows :

$$C\Delta u \leq D \tag{4.32}$$

where matrices C and D will be described in the Appendix.

Alternative 2 - combined Brix / level formulation

In this alternative, the level and Brix controllers are cast within the same DMC algorithm, and their two objectives are combined. The overall controller receives signals of the clear juice tank level, the disturbances to each evaporator vessel, and the actual Brix delivered by each final effect vessel. From these measurements the controller determines the optimal values for 5 manipulated variables. These are three flowrates (into each first effect Kestner) and two vapour throttling valve positions (fitted on the steam lines to the calandrias of evaporators 3A and 3B), as shown in Figure 4.5.

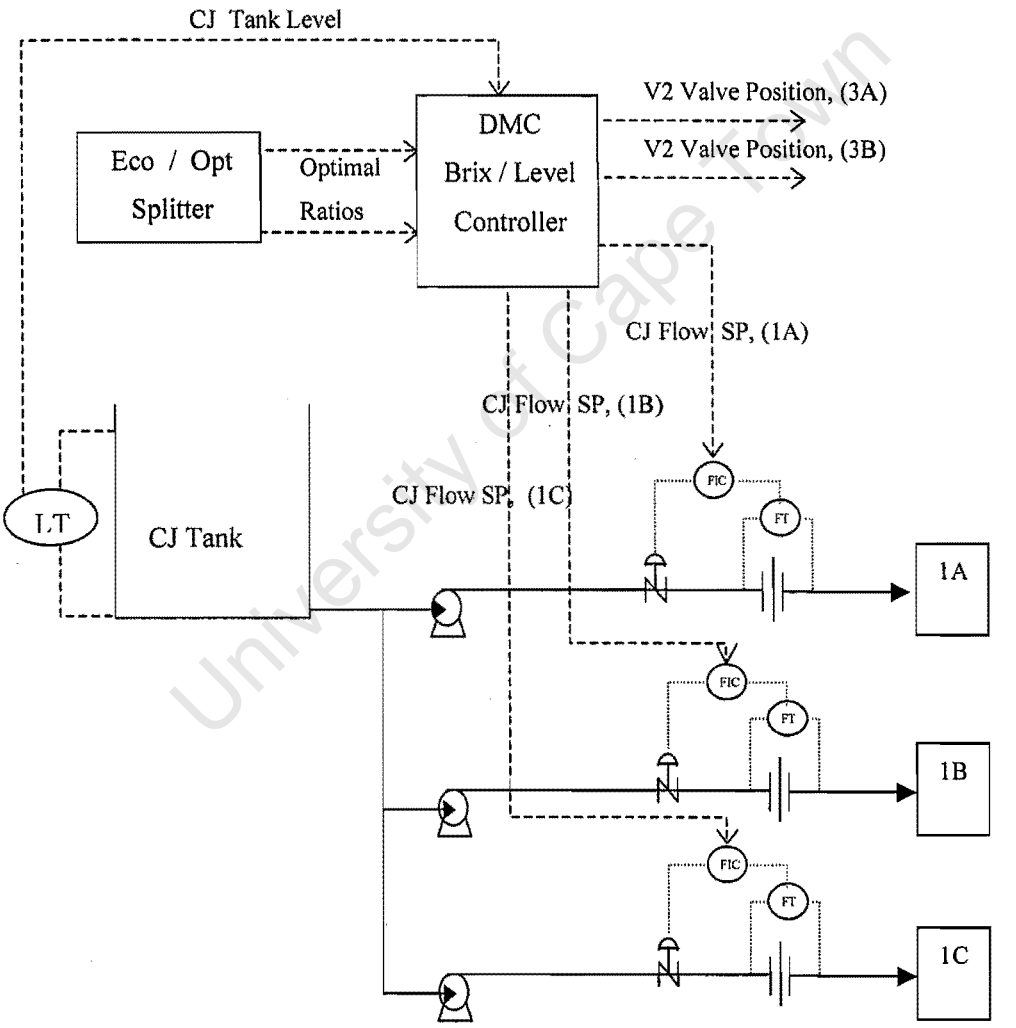

Figure 4.5 *Arrangement of control system for Alternative 2 (combined formulation) showing the economic optimization layer, and the combined DMC Brix / level controller.*

This controller also receives the optimal juice split from the steady state distribution controller (section 4.4), which receives estimated heat transfer coefficients from the 5 Kestner evaporators. However, in this case the flow split is communicated in the form of two ratios – those of the B and C set to the A set flowrate. There is then a quadratic penalty applied to any deviation from these ratios. Alternately, an end-point constraint could be included to force the three clear juice flowrates to achieve these ratios, but this adversely affects the flexibility of the system, as will be shown later.

The overall Brix / level controller also receives a Brix setpoint from the operator (usually 68-72°Bx) for each final effect and these are used in its calculation of the clear juice flowrates and V2 valve positions.

Here, the dynamic matrix has two outputs, with nine inputs, as shown in equation (4.33) :

$$A\Delta u = \begin{bmatrix} A_{11} & A_{12} & A_{13} & A_{14} & A_{15} \\ A_{21} & A_{22} & A_{23} & A_{24} & A_{25} \end{bmatrix} \cdot \begin{bmatrix} \Delta u_1 \\ \Delta u_2 \\ \Delta u_3 \\ \Delta u_4 \\ \Delta u_5 \end{bmatrix} + \begin{bmatrix} A_{16} & A_{17} & A_{18} & A_{19} \\ A_{26} & A_{27} & A_{28} & A_{29} \end{bmatrix} \cdot \begin{bmatrix} \Delta u_6 \\ \Delta u_7 \\ \Delta u_8 \\ \Delta u_9 \end{bmatrix} \quad (4.33)$$

where each sub matrix corresponds to output i and input j.

Outputs, i, refer to:

1. Syrup Brix (5A)
2. Syrup Brix (5B)

and inputs, j, refer to:

Manipulated inputs

1. Clear juice flowrate (1A)
2. Clear juice flowrate (1B)
3. Clear juice flowrate (1C)
4. V2 valve throttling position (3A)
5. V2 valve throttling position (3B)

Disturbance inputs

6. Clear juice temperature
7. Exhaust steam pressure
8. Final effect pressure (5A)
9. Final effect pressure (5B)

The optimization problem would then be to minimize a weighted sum of squares of:

- the setpoint tracking errors of both delivered syrup Brixes,
- manipulated variable (V2 valves) moves,
- the error from the optimal flow distribution ratios, and
- the Maximum Rate of Change of Outlet flow (Campo and Morari, 1989) of any of the three clear juice flowrates, (section 4.3).

The three clear juice flowrates do not have any actual bias values, and as such are not process outputs, in the DMC sense, although there are constraints on the values which these variables must achieve, in that they affect the level of the clear juice tank which must return to setpoint within the prediction horizon. In this sense, the change in clear juice flowrates, or MRCO is a process output. However, the clear juice flowrates are freely available as process inputs, which allows the system the same degrees of freedom for disturbance rejection as in Alternative 1 above.

The optimization is subject to system equation (4.25) above and the following constraints:

1) CJ flowrates for each line must be kept between 0 and 300.
2) V2 Valve positions must be kept between 0 and 100.
3) Clear Juice tank level must never be allowed to go above 100 or below 0.
4) Clear Juice tank level must return to setpoint by the end of the prediction horizon.
5) Syrup Brix should be kept between 72 and 55°Brix.

The Model Predictive Optimal Averaging level controller of Campo and Morari (1986) was formulated so that optimal *flowrates* were chosen to control a tank level. In this case, due to the structure of the dynamic matrix, the *changes in flowrate* were chosen to achieve both good Brix control, and to satisfy the level constraints mentioned above. In addition, the effects of changing all three clear juice flowrates must be considered (into vessels 1A, 1B and 1C), as

opposed to the single flowrate considered in the original formulation. The minimization program was as follows :

$$\min_{\mu,\Delta u_1(k),\cdots\Delta u_{51}(k+M-1)} J = (y_{set} - \tilde{y})^T .Q.(y_{set} - \tilde{y}) + \Delta u^T .R.\Delta u + \left(\frac{Q_B}{Q_A} - Ratio_{B/A}\right)^T \cdot S \cdot \left(\frac{Q_B}{Q_A} - Ratio_{B/A}\right) + \left(\frac{Q_C}{Q_A} - Ratio_{C/A}\right)^T \cdot S \cdot \left(\frac{Q_C}{Q_A} - Ratio_{C/A}\right) + c \cdot \mu \quad (4.34)$$

where c, S, Q, R = weighting matrices;

μ = the MRCO for all clear juice flowrates.

Here, $y_{set} \in \Re^{2P}$

$\tilde{y} \in \Re^{2P}$ such that :

$$\tilde{y} = \begin{bmatrix} \tilde{y}_1(k) \\ \vdots \\ \tilde{y}_1(k+P) \\ \tilde{y}_2(k) \\ \vdots \\ \tilde{y}_2(k+P) \end{bmatrix} \quad (4.35)$$

$Q \in \Re^{2P\times 2P}$

$R \in \Re^{2M\times 2M}$, and

$\Delta u = \Delta u_1 \cdots \Delta u_5 \in \Re^{5M}$ such that :

$$\Delta u_{1\cdots 5} = \begin{bmatrix} \Delta u_1(k) \\ \vdots \\ \Delta u_1(k+M) \\ \Delta u_2(k) \\ \vdots \\ \Delta u_2(k+M) \\ \vdots \\ \vdots \\ \Delta u_5(k+M) \end{bmatrix} \quad (4.36)$$

This was subject to the following hard constraints, over the entire prediction horizon, i.e. for $P \geq l > 0$, :

$$\Delta u_{\min} \leq \Delta u(k+l) \leq \Delta u_{\max} \tag{4.37}$$

$$u_{\min} \leq u(k+l) \leq u_{\max} \tag{4.38}$$

$$1\mu \geq -\Delta u_{1\ldots3}(k+l) \tag{4.39}$$

$$1\mu \geq \Delta u_{1\ldots3}(k+l) \tag{4.40}$$

where

$$\Delta u_{1\ldots3} = \Delta u_1 \cdots \Delta u_3 \quad \text{or,} \quad \Delta u_{1\ldots3} = \begin{bmatrix} \Delta u_1(k) \\ \vdots \\ \Delta u_1(k+M) \\ \Delta u_2(k) \\ \vdots \\ \Delta u_2(k+M) \\ \Delta u_3(k) \\ \vdots \\ \Delta u_3(k+M) \end{bmatrix} \tag{4.41}$$

$$h_{\min} \leq h(k+l) \leq h_{\max} \tag{4.42}$$

where $h(k+l)$ = tank level at time $t = (k+l)$, which, although not explicitly related via the dynamic matrix, is affected by flowrate inputs, as shown in the Appendix.

$$h(k+P) = h_{sp} \tag{4.43}$$

and the following constraints for the constraint window, i.e : for $P \geq l > L$, :

$$y_{\min} \leq \tilde{y}(k+l) \leq y_{\max} \tag{4.44}$$

where for this constraint, equation (4.44) :

$$\tilde{y}(k+l) \in \Re^{2(P-L)}$$

$$\tilde{y}(k+l) = \begin{bmatrix} \tilde{y}_1(k+L+1) \\ \tilde{y}_1(k+L+2) \\ \vdots \\ \tilde{y}_1(k+P) \\ \tilde{y}_2(k+L+1) \\ \tilde{y}_2(k+L+2) \\ \vdots \\ \tilde{y}_2(k+P) \end{bmatrix} \tag{4.45}$$

and L is the time until the start of the constraint window ($1<L<P$). Thus the Input-Output structure of the Brix / Level controller is shown in Figure 4.6 :

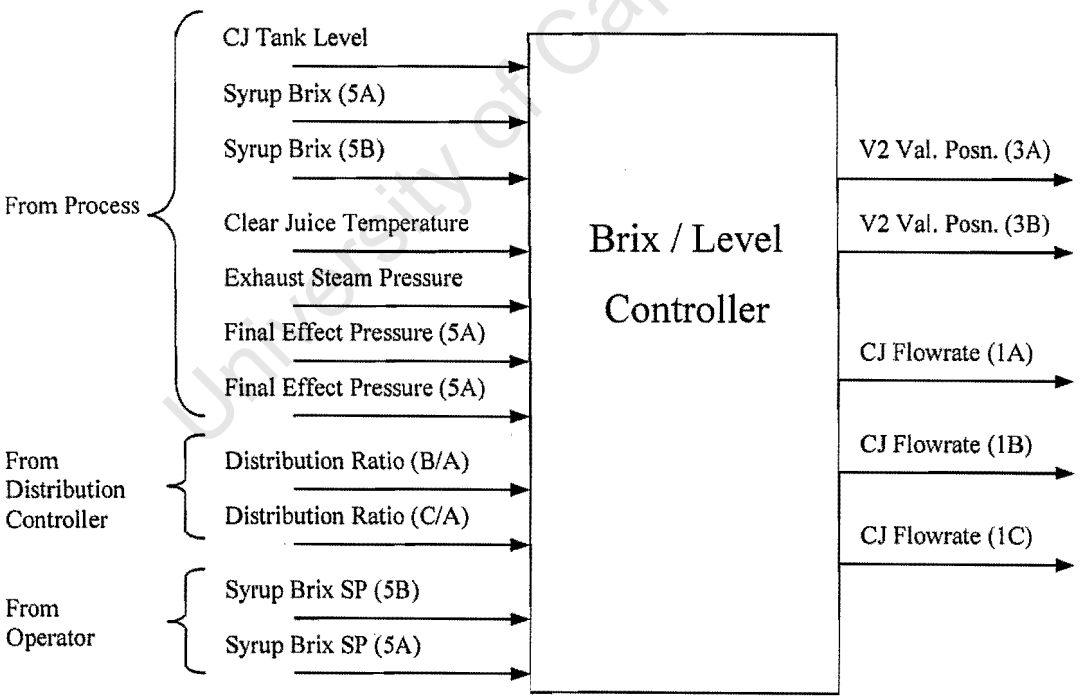

Figure 4.6 Input / Output structure of the DMC Brix / level controller

Formulation in QP

The DMC controller was then coded into the Matlab Simulink language. The controller itself was incorporated as an s-function with the following basic structure:

⇒ Load Dynamic Matrix

⇒ Initialize states in controller (variable moves over move horizon)

⇒ Receive inputs:

Set Points (for Brixes and clear juice tank level)

Optimal clear juice ratios

Output Measurements (Brixes)

Disturbance measurements (clear juice temperature, exhaust steam pressure, final effect pressure)

⇒ Calculate disturbance estimate over prediction horizon.

⇒ Compute optimal sequence of input moves using Matlab function fmincon(function, Initial guess)

⇒ Load weighting matrices Q, R and S.

⇒ Set constraints

dU min =	-20
dU max =	20
U min =	[0, 0, 0, 0; 0]
U max =	[300, 300, 300, 100, 100]
Y min =	[55; 55]
Y max =	[80; 80]

⇒ Function to be minimized = objective function.

⇒ Constraint matrix = constraints from above.

⇒ Update record of input moves

⇒ Send input moves to actuators

Constraints were included as follows

$$C\Delta u \leq D \tag{4.46}$$

where matrices C and D will be explained in the appendix.

Tests done on DMC Brix and level controllers

Once the controllers had been designed, various tests were done to check their operation under a range of operating conditions, most importantly the ability of the controller to handle constraints. These tests were done using the model of the plant, and not the actual plant, in order to safely get an idea of how the controller performed. The first tests consisted of stepping disturbance variables by 10% both as increases and decreases, and observing the system responses.

Fluctuations in the clear juice flowrate create common and highly significant disturbances to the evaporator station. For this reason, the juice supply was abruptly increased in a series of simulations, and the responses of each system were observed. Another common disturbance is a variation in the pressure of steam supplied to the station. This exhaust steam pressure was increased in the next simulations, and the response of each control system could then be compared.

Several step tests were combined to test the constraint handling ability of each formulation. These simulations ensured that the conditions affecting each set (the A set and the B set) were different, which allowed an analysis of the flexibility of each control system.

Finally, real plant data of all of the controller inputs were collected from the SCADA system, over a period of one week during June 2000. These data were then used as the inputs to the control system. This simulation was essential, in that the controllers had to deal with the noisy signals which are commonly received from plant instrumentation. Results of all of these simulations are presented in Chapter 5.

4.3 Level Control

Juice flow / tank level control

In Chapter 1 it was emphasized that good tank level control (or alternately good flow filtering) would greatly improve the potential for evaporator control. Alternative 1, described above, requires that a flowrate setpoint be cascaded from an upstream level controller. The problem of level control has been widely studied, (Campo and Morari, 1989).

Two algorithms have been developed for the problems faced at Triangle. Each of these can either be applied to a single buffer tank, or a series of buffer tanks, although their objectives are slightly different. The first, an LQG controller proposed by David Love, formerly of TMD, Tongaat Hulett, allows an offset after a disturbance and aims to minimize the combined weighted error of tank level from set point, and flowrate from setpoint.

The second controller, based on work by Campo and Morari, (1989), aims to minimize the maximum rate of change of outlet flow, while driving the tank level back to setpoint within a finite prediction time following a disturbance. Each of these algorithms could be separately applied to both the clear juice and mixed juice tanks, and this has been done at Triangle, although focus will be mainly directed towards the clear juice tank in this discussion, due to its direct impact on evaporator control. Both controllers would have a similar structure, as shown in Figure 4.7 :

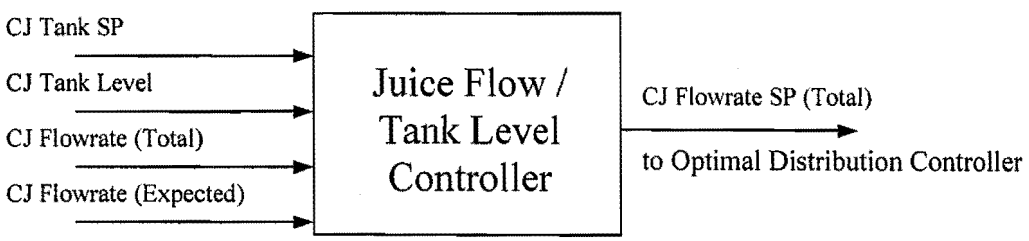

Figure 4.7 Input / Output structure of the juice flow / tank level controllers

LQG level controller

The existing level control system has already been described in Chapter 2, Figure 2.7. At present, only the clear juice tank level is under automatic control. This level is kept near its setpoint by manipulating the flowrate of mixed juice, upstream of the tank. The flowrates of clear juice into each evaporator train, A, B, or C, are controlled based on setpoints given by the operator. Thus it is necessary for the operator to keep on changing the clear juice setpoints to keep the mixed juice tank level within its limits.

The proposed level control system is based on a derivation of Linear Quadratic Gaussian control (see Appendix), although this derivation is only important from stability considerations, as the resultant control equation is a simple linear controller. The control algorithm continually computes the optimal rate of change of outlet flow from the control equation (4.47), below :

$$\frac{dQ}{dt} = -\left(\frac{4W}{A^2}\right)^{1/4}\left(Q - Q_{sp}\right) + W^{1/2}\left(h - h_{sp}\right) \tag{4.47}$$

where Q = outlet flow
Q_{sp} = outlet flow setpoint
h = tank level
h_{sp} = tank level setpoint
W = weighting factor, and
A = cross sectional area of tank.

Equation (4.47) must then be integrated to give the optimal flow setpoint, which is passed to a single loop PID flow controller, which in turn manipulates the flowrate via a variable speed drive or control valve. Importantly, this algorithm is inherently stable (Love, 1999), and fairly simple to implement in the real plant situation.

As can be seen from the above equation, the algorithm makes the essential trade off between the contrasting objectives of tight flow control and tight level control. This is achieved via the weighting factor W, where a high value will result in good level control, and a lower value will result in better flow control. h_e and Q_e must also be set by the operator as the expected

level and flowrate. This may be changed according to the operating regime, depending on the importance of tight flow or level control.

As the system is linear, there is no guarantee that the tank will neither overflow nor run dry, so some modifications were required in order to improve the system.

High and low level handling

In the event of one or both of the extraction lines having to be stopped, the inflow to the mixed juice tank could be greatly reduced, or even shut off completely, not an uncommon occurrence during the season. In this case, should the level in the mixed juice tank fall below 20%, the controller will ramp up the weighting factor, W, to a value of 80 in order to bias the algorithm towards achieving tighter level control. This will very smoothly reduce the outlet flow so that the tank will not run dry. This value was found for this particular system by trial and error of the worst case scenario, i.e. a reduction of inflow from 700 tph to 250 (equivalent to the complete shutdown of the larger extraction line, the diffuser). This weighting factor provides sufficient tank level bias to ensure that the outlet flow would be saturated at its minimum value before the tank runs dry. When the extraction lines return to normal operation, and the level is recovered to at least 40%, the weighting factor would be ramped back to its set value.

A similar provision has been made for a high tank level scenario, i.e., when the tank level rises above 80%, the weighting factor would once again be ramped up to 80, thus biasing the system towards tighter level control, and gradually the outlet flowrate would be increased until the disturbance was eliminated. Once the level had been brought back below 60%, the weighting factor would be ramped back down to its set value.

In this case, the weighting factor necessary to provide output saturation in the face of extreme tank level violations would be lower for the case of high level handling than for the case of low level handling. In order to saturate the flow at maximum (900 tph) it is only necessary to deviate 200 tph above the setpoint, of 700 tph. However, when dealing with low levels, the flow must be saturated at its minimum value of 0 tph, and the deviation from its setpoint is greater (700 tph). Thus any weighting factor which was sufficiently large to saturate the flowrate at a minimum value (for low levels) would also sufficiently bias the controller towards tight level control to saturate the flowrate at a maximum value, (for high levels).

Moving average setpoint

As can be seen from the discussion above, the offset that can occur with this sort of linear control is due to a compromise between error from tank level setpoint and error from juice flowrate setpoint. If the juice setpoint was continuously changed to match the current inflow regime (based on crushing rate, and the number of extraction lines being used) any offset would be eliminated. In order to maintain a robust system, however, this setpoint cannot be changed too rapidly. A good compromise may be found by using a moving average of past inlet flowrates. The time period for this average was set in excess of one hour.

The inclusion of a moving average setpoint preserves the advantages of the offset for short term disturbances – i.e. the controller would allow small level offsets following a short term disturbance, and these offsets would anticipate the return to average conditions. Long term changes, however, would not cause a sustained offset, as this would be eliminated as the moving average setpoint (expected flow target) was updated to meet the current situation. For example if the flowrate into the tank were to increase suddenly the tank level would stabilize at a level slightly higher than setpoint. Then should the flowrate return back to normal, the tank would be carrying extra liquid volume in order to more smoothly deal with the transition.

MPC level controller

The alternative formulation which has been used (Campo and Morari, 1989), is to minimize the MRCO or (Maximum Rate of Change of Outlet flow) of the tank under consideration, with constraints that the level should not violate upper or lower bounds over some prediction horizon. The authors successfully applied a MPC algorithm to this problem, and a derivation is given in the Appendix. Briefly, a simple internal model predicts the future behaviour of the tank level based on the past two level measurements and the previous outlet flow, as outlined in equations (4.48) and (4.49) below :

$$h_{predict}(k+l+1) = h(k) - \frac{\Delta t}{A} \cdot \sum_{i=1}^{l} [Q_o(k+i) - Q_i(k+i)] \tag{4.48}$$

where $h_{predict}$ = the predicted tank level

Δt = the time-step used

$Q_{i,o}$ = the inlet and outlet flowrates

A = cross sectional area of tank, and

$$Q_i(k-1)=\frac{A}{\Delta t}[h(k)-h(k-1)]+Q_o(k-1) \tag{4.49}$$

with Q_i assumed constant over the prediction horizon, i.e. $Q_i(k+l)=Q_i(k-1)$ for $0<l<P$.

The future outlet flowrates are chosen so as to minimize the MRCO objective, while obeying constraints on the permissible tank levels and flowrates. In addition a final constraint is added, that the level must return to set point by the end of the prediction horizon (P). The control algorithm was formulated as shown below in equations (4.50) – (4.54), for any present time $t = k$.

$$\min_{Q_o(k),Q_o(k+1),\ldots Q_o(k+P)}\left[\max_{0<l<P}\left|Q_o(k+l)-Q_o(k+l-1)\right|\right] \tag{4.50}$$

for $0<l<P$, subject to :

$$Q_o(k+l)\le Q_{o,\max} \tag{4.51}$$

$$Q_o(k+l)\ge Q_{o,\min} \tag{4.52}$$

$$h_{\min}\le h(k)+\frac{\Delta t}{A}\cdot(l+1)\cdot Q_i-\frac{\Delta t}{A}\cdot\sum_{i=0}^{l}Q_o(k+i)\le h_{\max} \tag{4.53}$$

$$h(k+P)=h_{sp} \tag{4.54}$$

Only the first outlet flowrate is implemented, and the optimization is repeated at the beginning of the next time-step. A simple derivation of these equations is given in the Appendix.

Both of these level controllers have been coded into the Matlab/Simulink environment, and they were then tested on a simple model of the plant using real data gathered by the SCADA system. Results of these simulations are given in Chapter 5.

4.4 Flow Splitting - Economic Optimization Layer

After an initial assessment had been done, it was decided that any constraint on the overall capacity of the station would reduce the economic objective, which suggests an optimization through the apportioning of the juice flowrate between the first three effects. The solution is restricted by adding a constraint that the total juice flowrate into the three first effects must add up to the clear juice flowrate set point as dictated by the level control system. Because the evaporators are cleaned on a rotation basis they may be operating at different efficiencies at any one time, and the aim of a particular flow distribution should be to optimize their current operational condition. The objective function for this controller would be to maximize the syrup concentration, as predicted by an internal model.

Condensate flowmeter

The distribution controller needs to receive some measure of the condition of the evaporators before optimization can be performed. This can be achieved by measuring the flowrate of condensate leaving each evaporator. However, condensate flow measurement provides particular difficulties because the fluid being measured is at its saturation temperature. Love (1999), proposed that a particular design of linear weir, (Heller, 1980), would effectively address the limitations of conventional flow measurement techniques.

The condensate flowmeter, as illustrated in Figure 4.8, was designed, built and tested on the Triangle station. The flowmeter was designed so that there is a linear relationship between flowrate and head maintained in the outer cylinder, as given below in equation (4.55) :

$$Q = kh \tag{4.55}$$

where Q = the flowrate of condensate (t / hr)
h = the height of liquid in the measurement arm (mm), and
k = a constant (t / hr.mm).

The upper vent of the flowmeter was connected to the incondensable gas withdrawal line. This maintained the downstream side of the flowmeter at sufficient pressure to prevent flashing in the meter, which would have disturbed the reading.

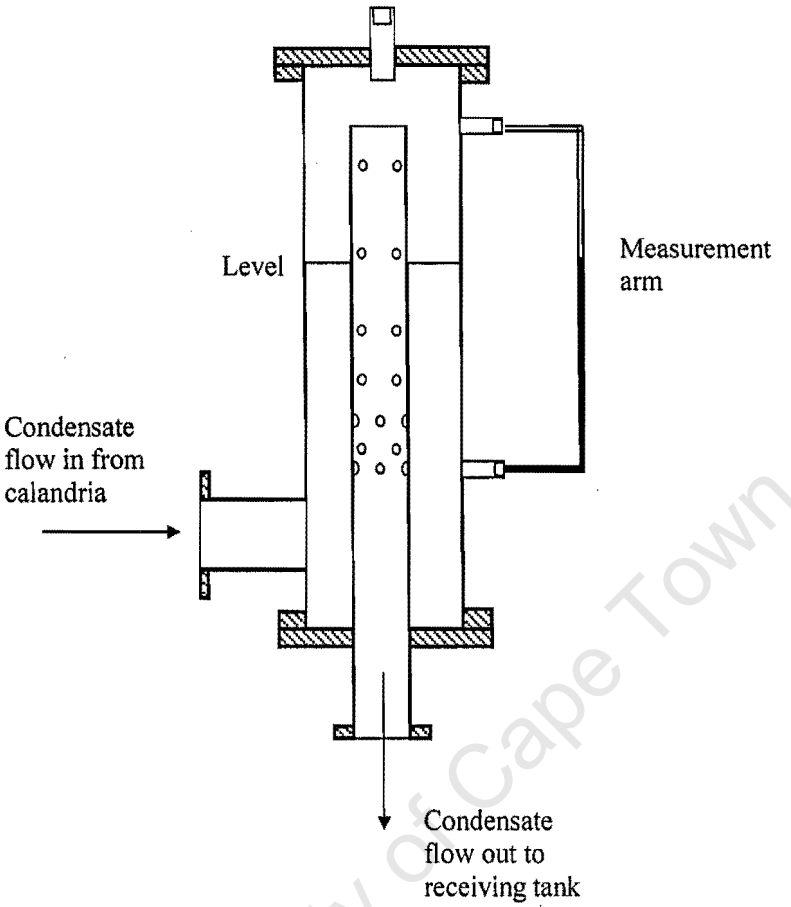

Figure 4.8 Condensate flowmeter, (Love 1999, after Heller 1980)

The design equations for this flowmeter are outlined in the Appendix.

Testing was first done on the unit to ensure that its calibration would be sufficiently accurate to be of practical use. A number of tests were performed using a cooling water return line to relate the height of liquid in the measurement arm and the flowrate of condensate. Of key interest was the orifice discharge coefficient. This was found to be approximately 0.6.

Having been tested, the flowmeter was then installed on the 1C Kestner vessel. This vessel was chosen due to its position on the edge of the station, and thus easy accessibility. Preliminary readings taken towards the end of the 1999 crushing season (April – December) indicated that the flowmeter was operating satisfactorily, and the flowrates measured did correlate to laboratory analyses of evaporator performance.

In the 2000 season two additional meters have been fabricated and installed on the other first effect Kestner vessels, i.e. 1A and 1B. These have proven useful in indicating the degree of cleanliness of each vessel, and the vessels' evaporative potential. It is proposed that the remaining Kestner vessels, 2A and 2B, are similarly fitted with condensate flowmeters. This will be useful in identifying which vessels are under-performing, and thus in arranging cleaning schedules and flow splits.

The Kestner vessels (long tube climbing film as opposed to effects 3, 4 and 5, which are short tube climbing film Robert vessels) are most seriously affected by scaling, and these are the only vessels that require routine chemical and mechanical cleaning. It is undecided whether or not dP cells will be purchased in order to provide an online flow measurement from the flowmeters, but in any case, the existing sight-glasses should be able to give operators some indication of the relative extents of scaling.

The flowmeters, as designed in Figure 4.8, did not provide online measurement of condensate flowrate, because of problems in sourcing the required instrumentation. However, the level of condensate in the sight glass was used to monitor evaporative potential. manually by measuring the height of liquid against a calibrated ruler. This was done hourly. and the results were averaged for each shift. The resultant heat transfer coefficients were then used to determine the optimum split of clear juice between the three first effects.

These measurements can be manipulated to provide heat transfer coefficients for each of the Kestner evaporators, a total of five vessels (1A, 1B, 1C, 2A and 2B), from the available variables for each effect (pressure of heating steam, pressure of the vapour space in the evaporator, condensate and juice flowrates, as shown in the Appendix).

In simulations these averaged heat transfer coefficients were used in an optimization program where the objective was to maximize the amount of water evaporated off the juice. This is done by calculating the weighted Brix of the juice which would leave the second effects, using a simplified version of the evaporator model described in Chapter 3. The input – output structure of the distribution controller is shown in Figure 4.9. Depending on the availability of instrumentation, the practical development of this concept could extend to the use of an online condensate flow measurement. This would then need to be filtered, probably using a Kalman filter, (Mulholland, 1991).

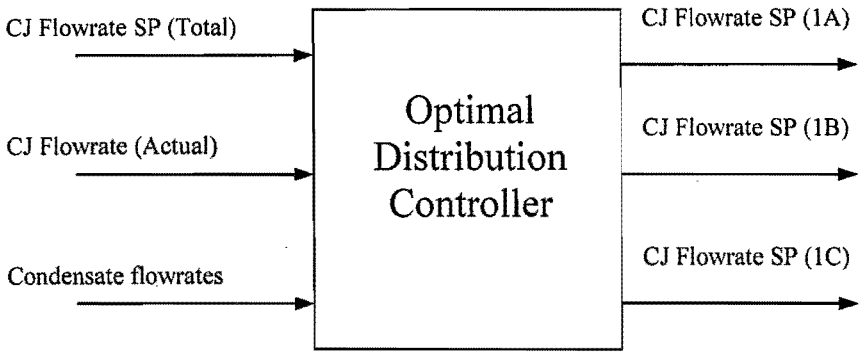

Figure 4.9 Input / Output structure of the optimal distribution controller

The objective function for this optimization routine was to minimize the amount of water present in the juice leaving the second effects :

$$\min_{F_{0,Aset},F_{0,Bset},F_{0,Cset}} J = \left(F_{J,2A}\left(100 - Bx_{2A}\right) + F_{J,2B}\left(100 - Bx_{2B}\right)\right) \tag{4.56}$$

where for any evaporator effect, e :

$$Bx_e = Bx_{e-1}\frac{F_{J,e-1}}{F_{J,e}}$$

$$F_{J,e} = F_{J,e-1} - F_{V,e}$$

$$F_{V,e} = \frac{U_e A_e\left(T_{V,e-1} - T_{J,e}\right)}{\Delta H_{vap,e-1}} \quad \text{, and}$$

$$T_{J,e} = T_{V,e} + B.P.E.$$

Here,

$F_{0,Aset}$	=	the flowrate of clear juice into the A set, i.e. evaporator 1A
Bx_e	=	the Brix of juice leaving effect e
$F_{J,e}$	=	the flowrate of juice leaving effect e
$F_{V,e}$	=	the flowrate of vapour evolved from effect e

U_e = the heat transfer coefficient of effect e, which was calculated from the condensate flowrates (Appendix) and was related to flowrate, via the Dittus-Boelter equation, equation (3.20)

A_e = the heat transfer area available in effect e

$T_{V,e}$ = the temperature of vapour leaving effect e, which is a function of the vapour pressure, $P_{V,e}$, which is available online

$T_{J,e}$ = the temperature of juice leaving effect e

$\Delta H_{vap,e}$ = the heat of vapourisation / condensation in effect e, which is a function of $T_{V,e}$ and $P_{V,e}$, and

$B.P.E.$ = the boiling point elevation of juice in effect e, which is a function of $T_{J,e}$ and Bx_e.

This was subject to the following constraints :

$$F_{0,Aset} + F_{0,Bset} + F_{0,Cset} = F_{0,SP} \tag{4.57}$$

and

$$0 \leq F_{0,Aset} \leq 300$$

$$0 \leq F_{0,Bset} \leq 300$$

$$0 \leq F_{0,Cset} \leq 300 \tag{4.58}$$

This distribution controller was finally tested, based on a range of experimentally observed HTCs. Once again these tests were done within the Matlab environment, whereby the heat transfer coefficients for each of the 5 Kestners were varied, and the response of the controller was observed. Results of these simulations are presented in Chapter 5.

Chapter 5 RESULTS AND DISCUSSION

5.1 LQG vs MPC Level Control

As was discussed in Chapter 4, the first formulation, Alternative 1, requires a flowrate setpoint from an independent level controller. The two proposed level controllers were tested by running simulations on a model of the mixed juice tank using the actual plant parameters given below in Table 5.1.

Table 5.1 Mixed Juice Tank Parameters

Cross sectional area	38.5 m^s
Nominal level (setpoint)	50 %
Maximum level constraint	90 %
Minimum level constraint	10 %
Nominal outlet flow	700 t / hr
Tank height	6.67 m
Outlet flow capacity	0 – 900 t / hr
Sampling time	1 min

The following graphs, Figures 5.1 and 5.2, show the results of the two level control systems under a common situation on the Triangle plant, i.e. a step increase in draught juice (DJ) flowrate - the juice delivered by the extraction lines. For the purposes of these two simulations the tuning parameters were as follows : for the LQG controller the weighting factor, $W = 0.1$; for the MPC controller the prediction horizon, $P = 10$ minutes.

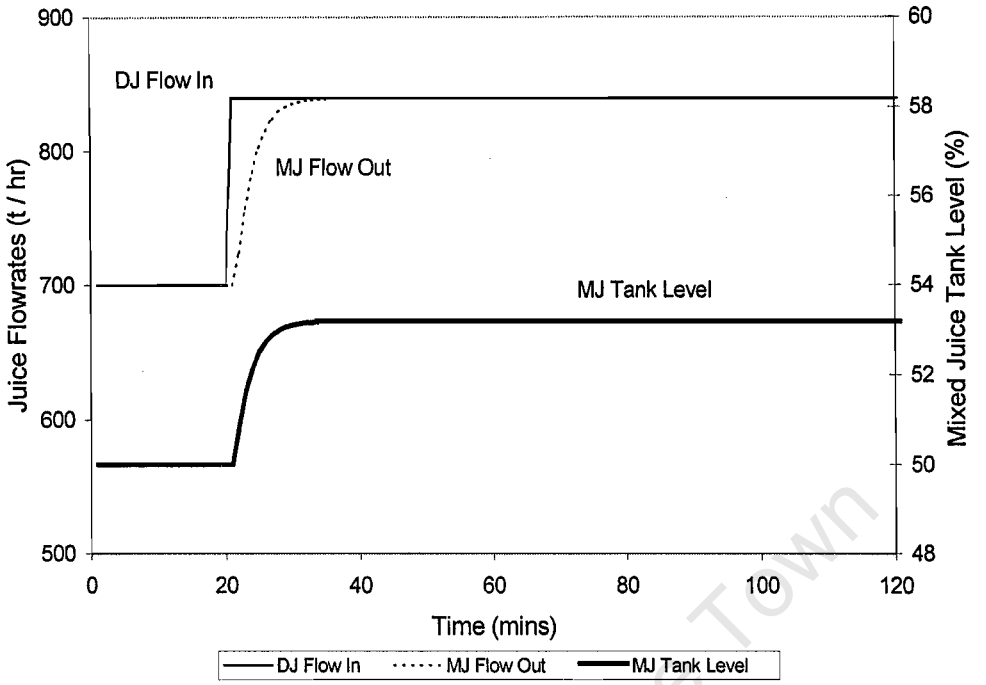

Figure 5.1 *Response of the LQG level controller to a step increase in juice supply*

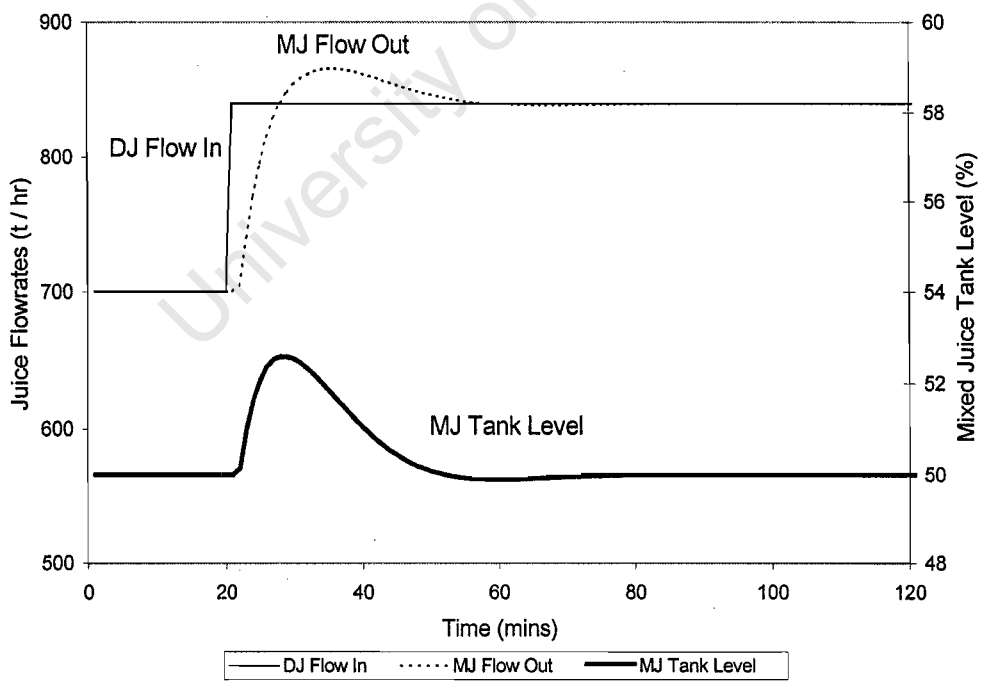

Figure 5.2 *Response of the MPC level controller to a step increase in juice supply*

As can be seen, both methods handle the disturbance smoothly, although the LQG controller will inevitably result in some offset in this test. For example, when the disturbance is an increase in draught juice flowrate a new steady state will be reached when the mixed juice flowrate has been increased to match the new draught juice value. At this value, the weighted error in flowrate (from setpoint) exactly balances the weighted error in tank level (from setpoint). Although this system is useful for the plant situation where disturbances are equally likely to occur which raise or lower the incoming juice flowrate, it is important to remember this offset. Fortunately, the offset is relative to a fixed setpoint, and thus a series of one disturbance type, high or low, will not accumulate offsets as the total offset is only related to the total input flowrate. Table 5.2 shows the steady state offsets that were achieved with various weighting factors after 20% steps in draught juice flowrate.

Table 5.2 Level Offsets After a 20% Step Increase in Flowrate

Weighting factor (W)	Level offset (%)
0.1	56.8
1	31.9
10	17.9
100	10.1
1000	5.7
10000	3.2

By adding a gap action element to the LQG controller a complete shutdown of both mills can also be accommodated, i.e. when the level falls below 5%, the controller is put into manual, and the pumps are stopped, only to be restarted once the level rises above 10%. Importantly, neither of these proposed level control schemes require the measurement of the upstream disturbance flowrate, as this input is inferred by the change in tank level.

The second level controller, the MPC controller of Campo and Morari, (1989), is formulated so that there is no offset after the prediction horizon. This is the tuning parameter in this case, and it can be shown that for any given disturbance there is a critical prediction horizon, i.e. the time at which the tank would overflow with no control action. As the prediction horizon is increased, the MRCO objective is continually improved until this critical horizon is reached. Thereafter, only the settling time is increased, with no further benefit to flow

filtering. For example, for controlling the mixed juice tank level, if a 10% step increase in flow is expected, then the critical horizon length is 226 minutes, for a 20% increase, 113 minutes.

In this example, the prediction horizon was chosen as 10 minutes, which resulted in a settling time of 110 minutes, with an MRCO of 35.7, and a maximum flowrate of 866.3 tph. With a smaller prediction horizon of 5 minutes, the settling time could be reduced to 65 minutes, at the expense of a higher MRCO of 78.4, and a slightly higher maximum flowrate, 867.9 tph.

By comparison, the LQG controller in this case ($W = 0.1$) gave a value for the MRCO of 33.4, and this could be decreased, at the expense of a greater level offset and longer settling time, for any given disturbance. Should the LQG or MPC controller be implemented in the 2000 season, the clear juice tank level would also be controlled by a similar mechanism, except that in this case the total upstream inventory would be used, i.e. the weighted sum of clear juice and mixed juice tank levels. In this way, any disturbances would be most rapidly removed from the system, e.g. if the mixed juice tank level is high, then both mixed juice and clear juice flowrates would be increased simultaneously, rather than just increasing the mixed juice flowrate, which would then propagate the error, and cause a larger disturbance in the clear juice tank level, prompting a larger increase in the clear juice tank level.

The step test is simple and the results are easy to analyse. However, of more practical benefit would be the response of each control system in the face of actual plant disturbances. The following graphs show responses based on 400 minutes of data supplied by the SCADA system from June 26, 2000. These tests were based on controlling the mixed juice tank level and mixed juice flowrate, in the face of disturbances in the draught juice flowrate which was delivered to the mixed juice tank from the extraction lines.

Figures 5.3 and 5.4 show the responses of the LQG system to the plant data, at two weighting factors, $W = 1000$ and $W = 1$. Figure 5.3 shows the responses of the mixed juice flowrate to the disturbance input, at the two weighting factors. Also included in this figure is the response of the existing control system, in which the mixed juice flowrate is manipulated by conventional PID controllers to tightly control the clear juice tank level. Figure 5.4 shows the resultant effects on the mixed juice tank level, under the three control alternatives (existing PID control, LQG at $W = 1$ and LQG at $W = 1000$).

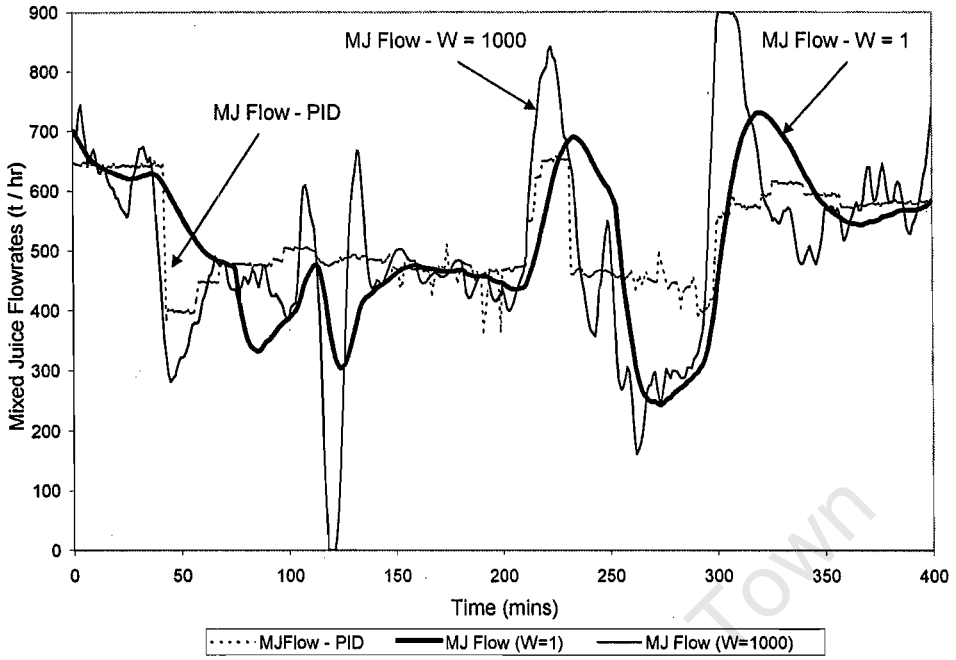

Figure 5.3 *Response of mixed juice flowrates to fluctuations in draught juice flowrate, under existing PID control and LQG level control at two weighting factors.*

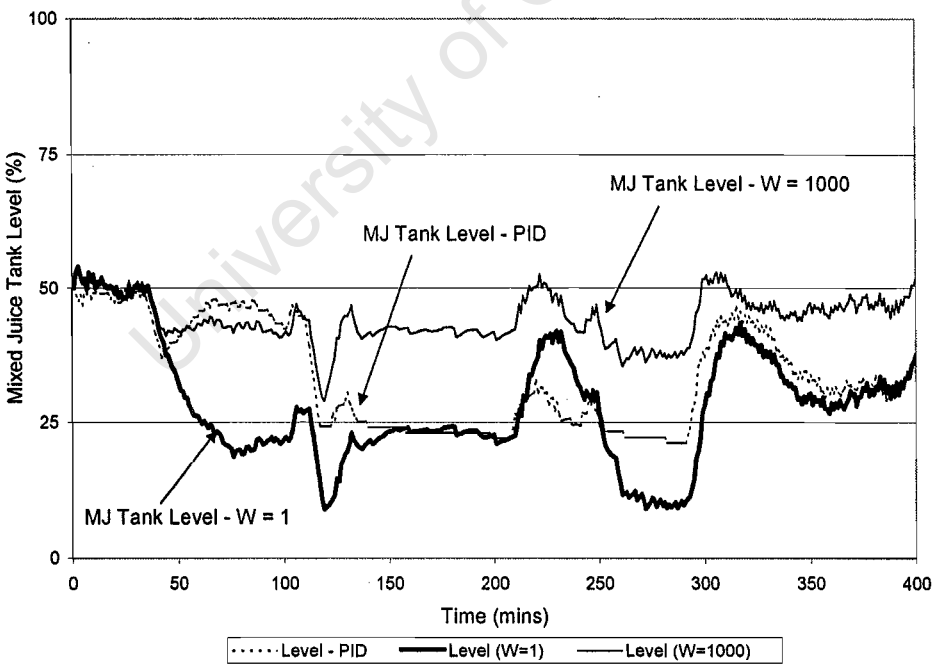

Figure 5.4 *Effects of different control responses on mixed juice tank levels under existing PID control and LQG level control at two weighting factors.*

Clearly, the smaller weighting factor ($W = 1$) results in smoother mixed juice flowrates, at the expense of larger level fluctuations. The ideal weighting factor could then be based on tests such as these, in order to correctly balance the contrasting objectives of flow filtering and level control. In this case, the high and low levels (> 80% or < 20%) were encountered at the weighting factor of 1, although not at $W = 1000$. This result, at $W = 1$, is a potentially dangerous situation as it implies that the plant could run out of buffer tank capacity within a short space of time. Conversely, the response at $W = 1000$ shows that the flowrate saturated at 0 and 100% of capacity (0 and 900 t/hr) within the trial period, and this is also an undesirable situation. A balance must therefore be found between these two extremes.

The LQG algorithm requires the operator to input steady state (expected) values for the flowrate and tank level. In these simulations, the steady state values were taken as the desired average values for these two parameters, i.e. tank level = 50%, and flowrate = 700 t/hr. While the expected tank level was easy to choose, it is not ideal to assume the expected average flowrate, as any change in mill operations, or cane availability, could greatly affect this figure. An interesting development of this algorithm was then to use a long term weighted average of past flows as the flow setpoint, or expected average flowrate. This was easily included, as outlined in Chapter 4, and the results of such a system are shown below in Figures 5.5 and 5.6. For this simulation the same two weighting factors were used, $W = 1$ and $W = 1000$, and the flow setpoint used was a moving average, based on the previous 100 minutes of inlet flowrate.

Again, the response of the existing PID control loop has been included for comparison. Figure 5.5 shows the responses of mixed juice flowrates, and Figure 5.6 shows the resulting effects on the mixed juice tank level. At the lower weighting factor, $W = 1$, the mixed juice flowrate response is slightly smoother that those in Figure 5.3, where a fixed setpoint was used. The tank level fluctuations shown in Figure 5.6 are also more damped than those in Figure 5.4, and the final levels are closer to setpoint than for the previous simulations. This can be easily explained, in that the juice flowrate setpoint is now a representative average of the most recent flowrates, and thus the system can adapt much more easily to gradual trends in incoming (draught juice) flowrate.

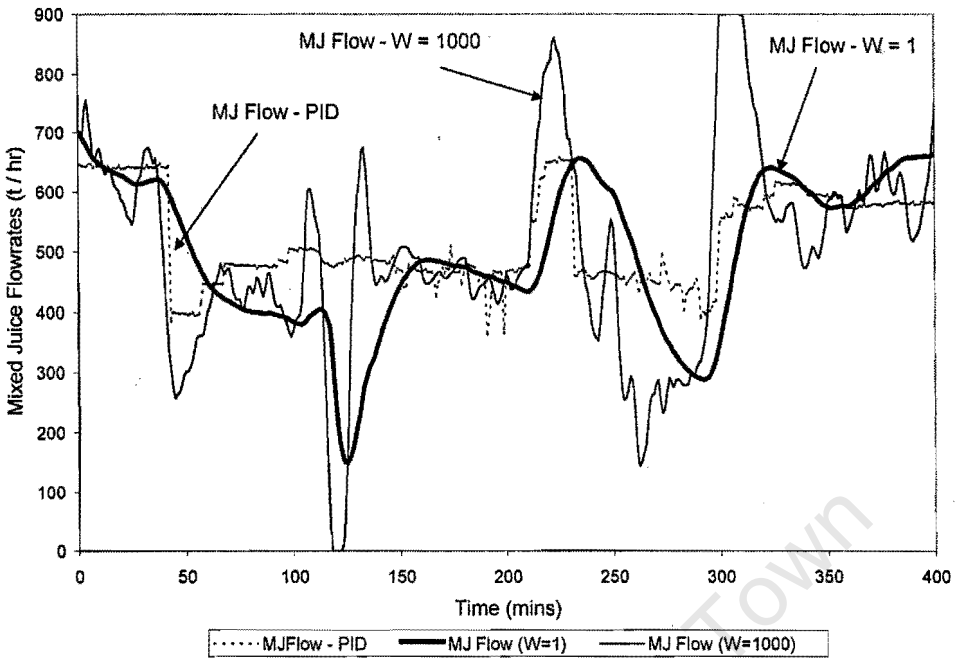

Figure 5.5 *Response of mixed juice flowrates to fluctuations in draught juice flowrate under existing PID control and LQG level control, with a moving average setpoint at two weighting factors.*

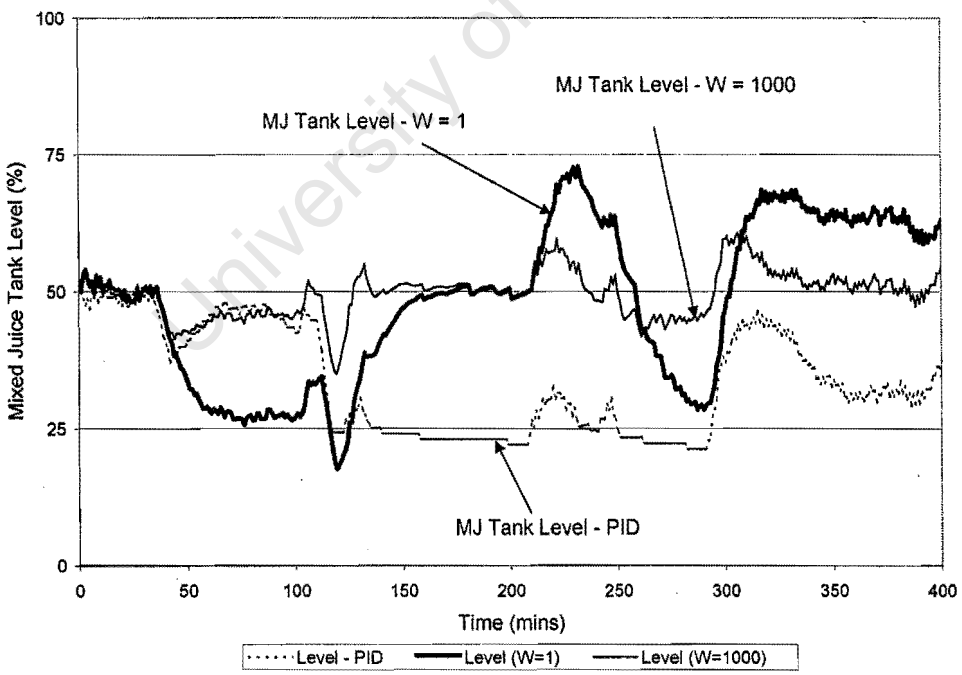

Figure 5.6 *Effects of different control responses on mixed juice tank levels under existing PID control and LQG level control, with moving average setpoint, at two weighting factors.*

However, at the higher weighting factor, $W = 1000$, the flowrate saturates for longer than with the fixed flowrate setpoint. This is a result of a rapid change in operating regime (an increase in the crushing rate) at $t = 300$ minutes, when the moving average flowrate setpoint was further away from the actual draught juice flowrate, than the fixed (expected) flowrate setpoint used for Figure 5.3. In this case it would be useful to reduce the period of the moving average.

Figures 5.7 and 5.8 below, show the responses of the MPC controller of Campo and Morari to the same set of plant disturbances. In this simulation, two prediction horizons are used, $P = 10$ and $P = 100$ minutes. Figure 5.7 shows the responses of the mixed juice flowrate to the disturbance input at the two prediction horizons. For comparison, the response of the existing control system is again included. Figure 5.8 shows the resultant effects on the mixed juice tank level under the three control alternatives (existing PID control, MPC at $P = 10$ and MPC at $P = 100$).

Figure 5.7 shows that the longer prediction horizon, $P = 100$, results in smoother flow control, although Figure 5.8 shows that this is again at the expense of larger tank level fluctuations.

Similar to the large weighting factor for the LQG controller ($W = 1000$ in Figure 5.3 above), the short prediction horizon, $P = 10$, causes the mixed juice flowrate to saturate at 0 and 100% of capacity (0 and 900 t/hr) within the trial period. The longer prediction horizon, $P = 100$, causes the level to fluctuate greatly, although this type of controller is formulated to prevent the tank from either running dry or overflowing, as these conditions are included as hard constraints.

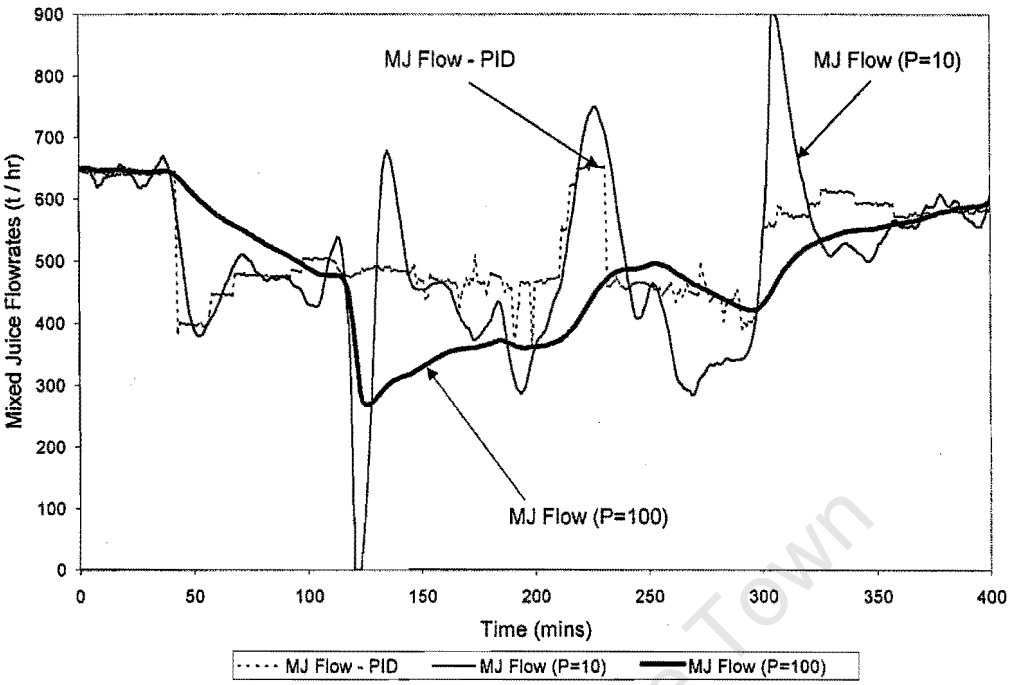

Figure 5.7 *Response of mixed juice flowrates to fluctuations in draught juice flowrate under existing PID and MPC level control, at two prediction horizons.*

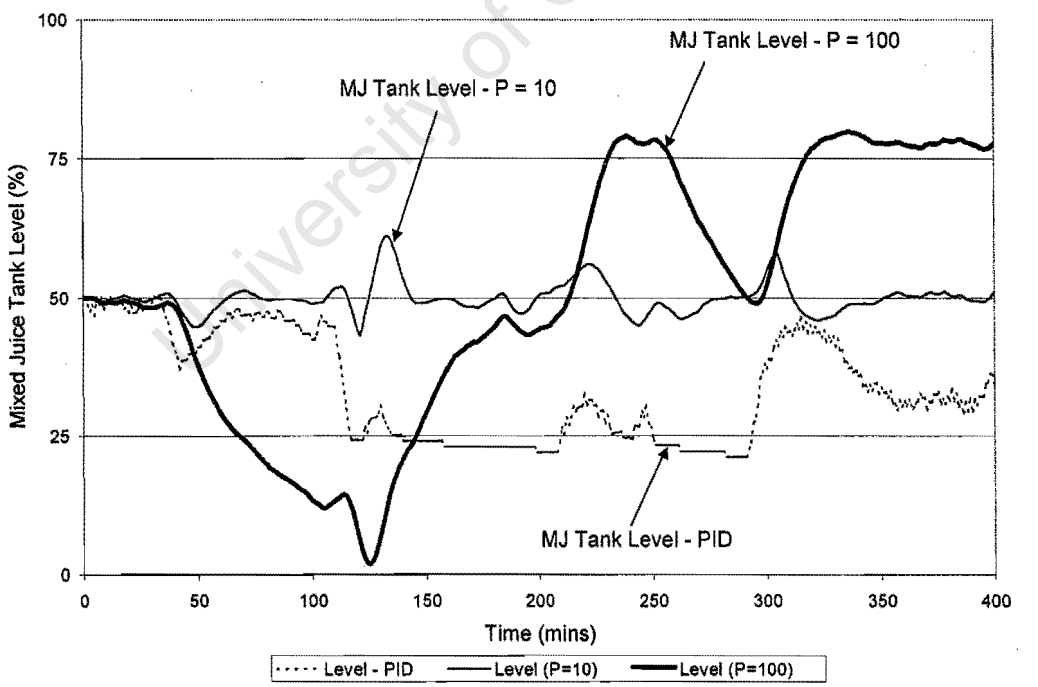

Figure 5.8 *Effects of different control responses on mixed juice tank levels under existing PID and MPC level control, at two prediction horizons.*

Table 5.3 shows a comparison of the maximum rate of change of flow for the outlet stream, when controlled by an MPC controller tuned to various prediction horizons, compared to the maximum rate of change of flow of the inlet stream, and that of the mixed juice flowrate, under the existing control system. The rate of change of flow was calculated from one minute to the next, i.e. (t / hr / min).

Table 5.3 Maximum Rate of Change for Inlet and Outlet Streams

Stream	M.R.C.O.
Inlet (draught juice) flowrate	843
Outlet (mixed juice) flowrate :	
Existing PID control	102
MPC controller, $P = 10$	91
MPC controller, $P = 20$	54
MPC controller, $P = 50$	15
MPC controller, $P = 100$	8

In this section two alternative level controllers, LQG and MPC controllers, have been examined. Both of these systems show some promise for industrial application, and both seem to give better results than the existing system. However, a lot of the improvement is due to the setup of the Triangle factory, and the fact that the mixed juice tank level is not currently a controller input, and nor is the draught juice flowrate. In fact a large part of the disturbances in mixed juice flowrates are due to the operators, who abruptly change the clear juice flowrate setpoints, which then in turn cause the clear juice tank level controller to make rapid changes in mixed juice flowrate.

It may be argued that similar responses could be obtained from a well tuned PID controller. In the case of the LQG controller, this is not strictly true, as the LQG response inevitably results in some level offset in response to a flow disturbance. To achieve a similar result a Proportional only controller would be required. The disadvantage here would be that a series of one type of disturbance, flow increases, would then accumulate total offsets, whereas with the LQG controller the offset is not accumulated, but linearly related to the total flow error. A sophisticated series of PID controllers could be substituted, which would change the tank level setpoint based on the flowrate, although these would be more difficult to tune than the

single LQG controller – a major advantage of this type of controller being that it has only one tuning parameter, W, the weighting factor.

In the case of the MPC controller, it is certainly true that a well tuned PID controller could produce similar responses. However, there are two advantages to the MPC algorithm here – first, this controller can anticipate and handle constraints on tank level and flowrate, second, this controller also only has one tuning parameter, P, the prediction horizon, and so it is easy to tune, for any given magnitude of disturbance. A final consideration for any practical implementation would be that the constrained MPC controller requires a minimization routine to be performed on line at every time step. This presents two possible problems. The software required to perform this minimization may not be available on all sugar mills, and the time taken for this minimization is exponentially related to the size of the prediction horizon, P. Thus when good flow filtering is required, i.e. P is large, the controller may require considerable processing speed in order to solve the optimization quickly.

The two systems achieve different results based on what the control system designer requires. If the factory in question requires little or no level offset, then the MPC controller would be more suitable. If the factory can accept level offset, or even if this is viewed as a sensible use of buffer capacity, by anticipating a future disturbance in the opposite direction, then the LQG controller would be more suitable.

In view of these considerations, and that of the software and hardware requirements mentioned above, it is recommended that an LQG system would be more suitable for a trial in the sugar industry.

5.2 Condensate Flowmeter and Optimal Splitting of Clear Juice Flowrate

Tests on flowmeter

The condensate flowmeter described in Chapter 4, was first tested using a condensate return line. The return line was connected to the inlet of the flowmeter, and a flexible hose was connected to the outlet, and then allowed to discharge into an empty tank. The time taken to fill the tank was then recorded, at a range of flowrates, along with recorded heights of liquid in the calibration tube.

Following these tests, the flowmeters were installed on line. There, the design proved adequate, and their operation seemed to be very consistent. Figure 5.9 shows the relationship between the flowrate readings obtained, and the calculated condensate flowrates (calculated from clear juice flowrate, SCADA signals: temperatures, pressures, and laboratory Brix readings, as shown in the Appendix)

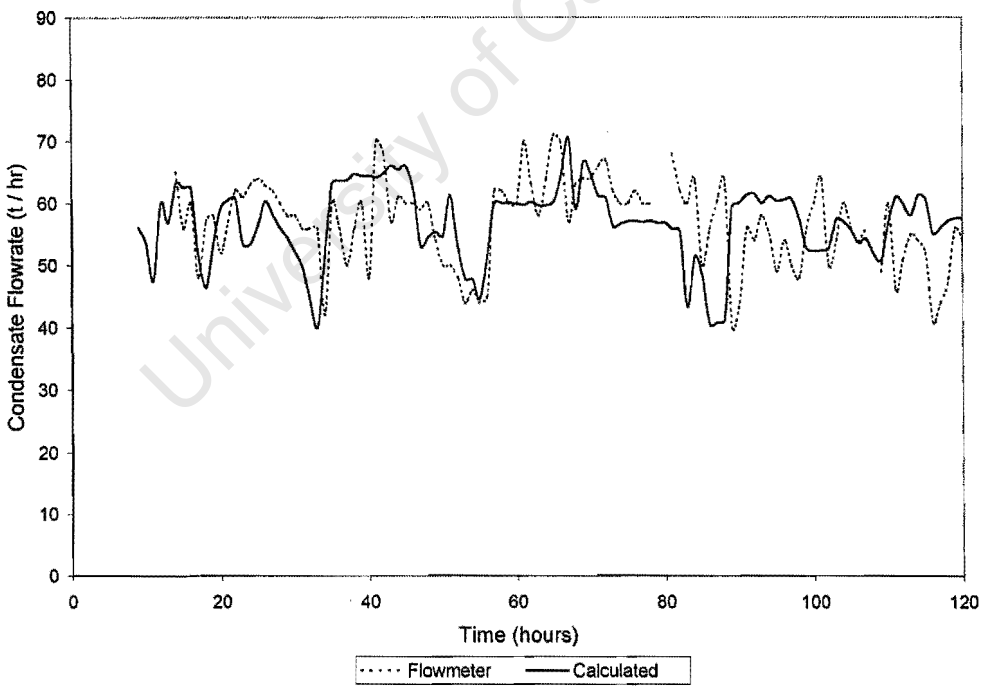

Figure 5.9 *Comparison between calculated and measured condensate flowrates on the 1C Kestner at Triangle Ltd., over a period of 120 hours in June, 2000*

Simulations were performed in order to demonstrate the value of correct flow splitting. Figure 5.10 shows the results of using a range of flow splits when the situation is such that the heat transfer coefficients (HTCs) of vessels 1A and 2A (3.15 and 2.7 kW/m^2.K respectively) are superior to their counterparts in parallel – 1B and 2B (2.85 and 2.5 kW/m^2.K respectively). In this test, the total flowrate was maintained at a fixed value, but the ratio of clear juice to the A and B sets was gradually increased. Throughout this the flowrate of juice to B and C sets was kept equal. The total tonnes of syrup delivered is used as an indication of the evaporator performance. The best performance would result in the minimum tonnes of syrup, i.e. that which best aids the downstream crystallising equipment.

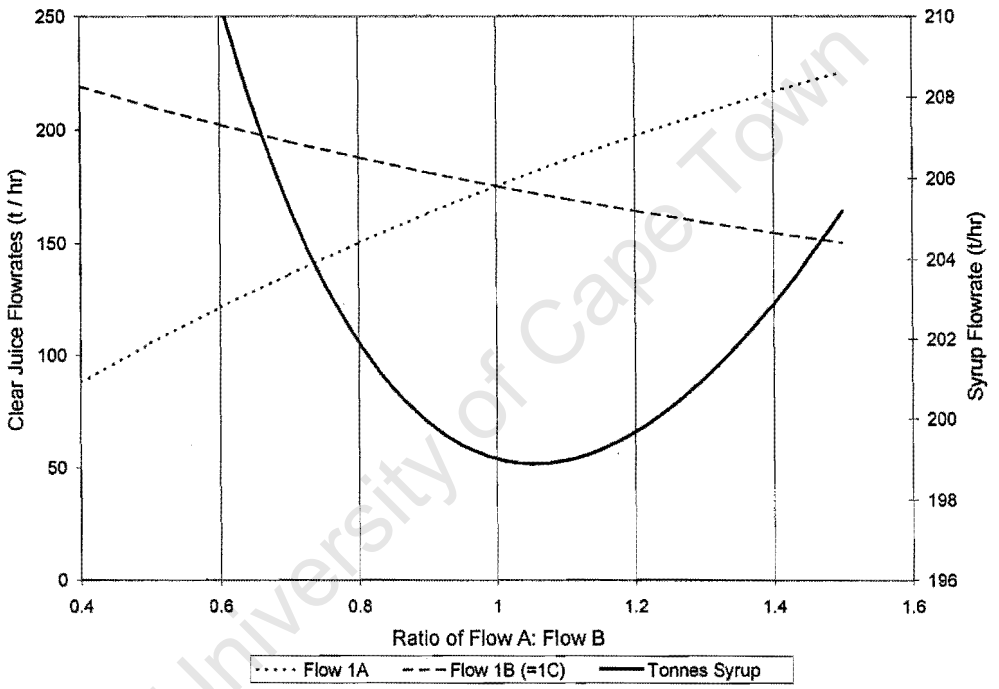

Figure 5.10 *Tonnes of syrup delivered by the evaporators at a range of flow splits for the case where HTCs for the A set were greater than those for the B set.*

Figure 5.10 shows that the optimal juice distribution is at a ratio of flow A to flow B of just greater than 1. This was expected. The cleaner A set should be able to handle a higher flowrate of juice than the fouled B set, and thus the ratio of the two flowrates should favour the A set. Similarly, if the A set was more fouled, and as a result vessels 1A and 2A had lower HTCs (2.5 and 2.3 kW/m^2.K respectively) than vessels 1B and 2B (as above), the reverse would be true, as shown below in Figure 5.11.

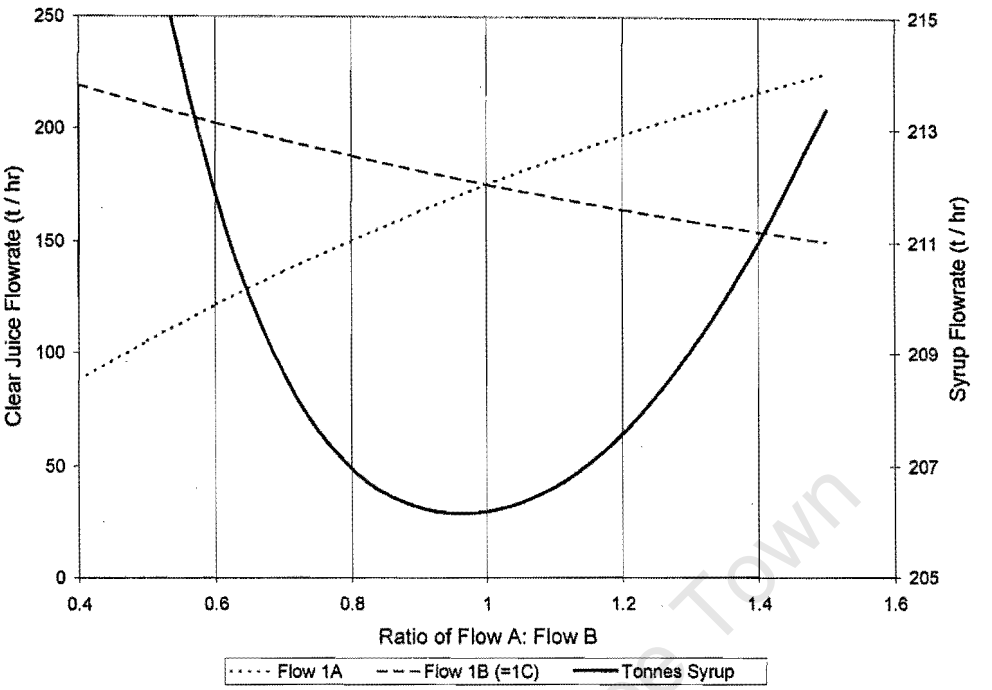

Figure 5.11 *Tonnes of syrup delivered by the evaporators at a range of flow splits for the case where HTCs for the A set were lower than those for the B set.*

Figure 5.11 shows that the optimum ratio of flow A to flow B is just less than 1, which again was expected, in that the more fouled A set, should not be able to handle as much juice as the cleaner B set.

In order to present the results for a number of different heat transfer coefficients, several simulations were run in which the HTC of a single vessel was changed, and the optimum flowrate was recorded each time. Figure 5.12 shows the optimal juice flowrate through the first vessel of the A set, 1A, as the observed HTC for either vessel 1A or 2A was varied. In each case, all other heat transfer coefficients were kept constant. For these simulations, the base case was that of equal HTCs in each of the evaporator trains, and this resulted in an optimum flowrate of 200 tph flowing through each of the first effect vessels.

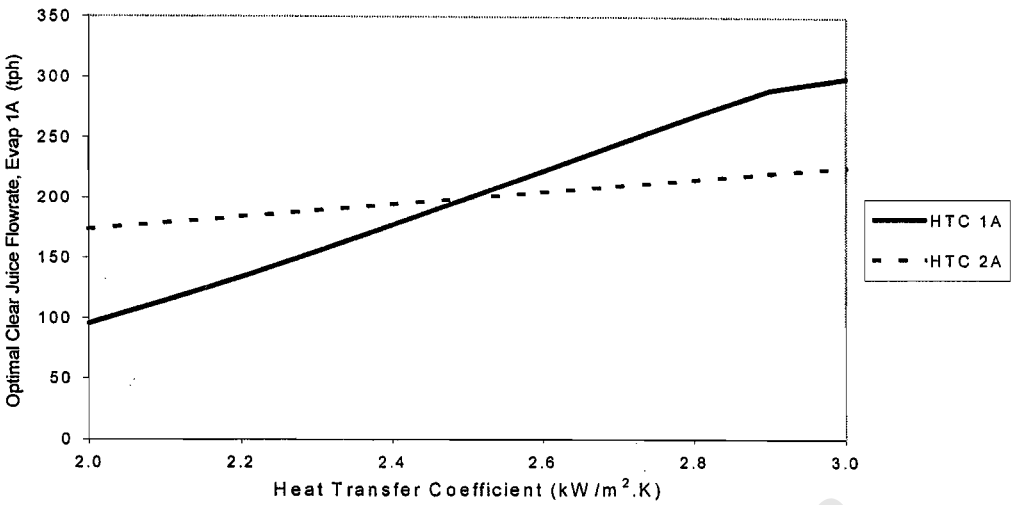

Figure 5.12 Optimal juice flowrate into vessel 1A under a range of conditions

Figure 5.12 shows that the heat transfer coefficient of the first effect is more important that that of the second effect, due to the layout of the Triangle evaporator station where there is an additional first effect vessel which feeds the two evaporator trains equally. The response of each first effect vessel was not identical. The extra first effect, 1C, was found to have a slightly different relationship between its observed heat transfer coefficient and the optimal flow distribution.

However, it is important to note that despite the fact that the HTCs were altered considerably in these simulations, the optimum ratios were not very far away from the steady state case, i.e. 1, for the situation where both lines were equally clean. While it may be useful to identify heat transfer coefficients in order to highlight extreme cases of badly fouled evaporators, it is more important that the evaporator control system maintains flexibility, than that the ratios of flowrates are maintained at the fixed optimum values. This result will be emphasised in Sections 5.3 and 5.4 where the combined controller formulation is tested using real plant data.

5.3 Brix Controller Results

The two alternative DMC formulations were coded into the Matlab simulation language, Simulink, and used to control the dynamic model of the station. In order to demonstrate the ability of the DMC controller to use both inputs, clear juice flowrate and V2 Valve position, to achieve a single output objective, i.e. to minimize the weighted sum of error from Brix setpoint on that line, and manipulated variable moves, the Brix controller of the first formulation, Alternative 1, was used with a constant clear juice flowrate setpoint. This was done by putting the upstream tank level controller into manual mode. Figure 5.13 shows the response of the Brix controller to an increase in steam pressure at time, t = 20 minutes and again at t = 60 minutes.

When the steam pressure was first increased by 10% at t = 20 minutes, this caused the juice to boil more vigorously, which would cause the syrup Brix to rise. In response the V2 valve started to close, throttling the amount of steam delivered to the third effect calandria, and bringing the syrup Brix under control. The syrup Brix gradually returned towards a setpoint of 68°Bx from t = 40 to t = 60 minutes. Then, at t = 60minutes, the exhaust steam pressure was again increased by 10%. This had a similar effect as before, in that the syrup Brix again began to rise. The V2 throttling valve was already almost fully closed, and now encountered an input constraint. Thus the controller increased the clear juice flowrate, the only remaining input variable move, in order to bring the syrup Brix back under control. A similar effect has been observed for the case where the disturbance caused a decrease in syrup Brix, e.g. a decrease in juice temperature. In this case, the V2 throttling valve was opened until it encountered a constraint (100% open) and then the clear juice flowrate was reduced, to prevent the syrup Brix from falling below its constraint of 50°Bx.

However, this was an unrealistic scenario, as such a case (with no constraints on tank level) could result in the clear juice tank either running dry, or overflowing. Having shown that the DMC Brix controller operated acceptably on its own, it was then necessary to contrast it with the alternative formulation, while considering the upstream constraints on clear juice tank level.

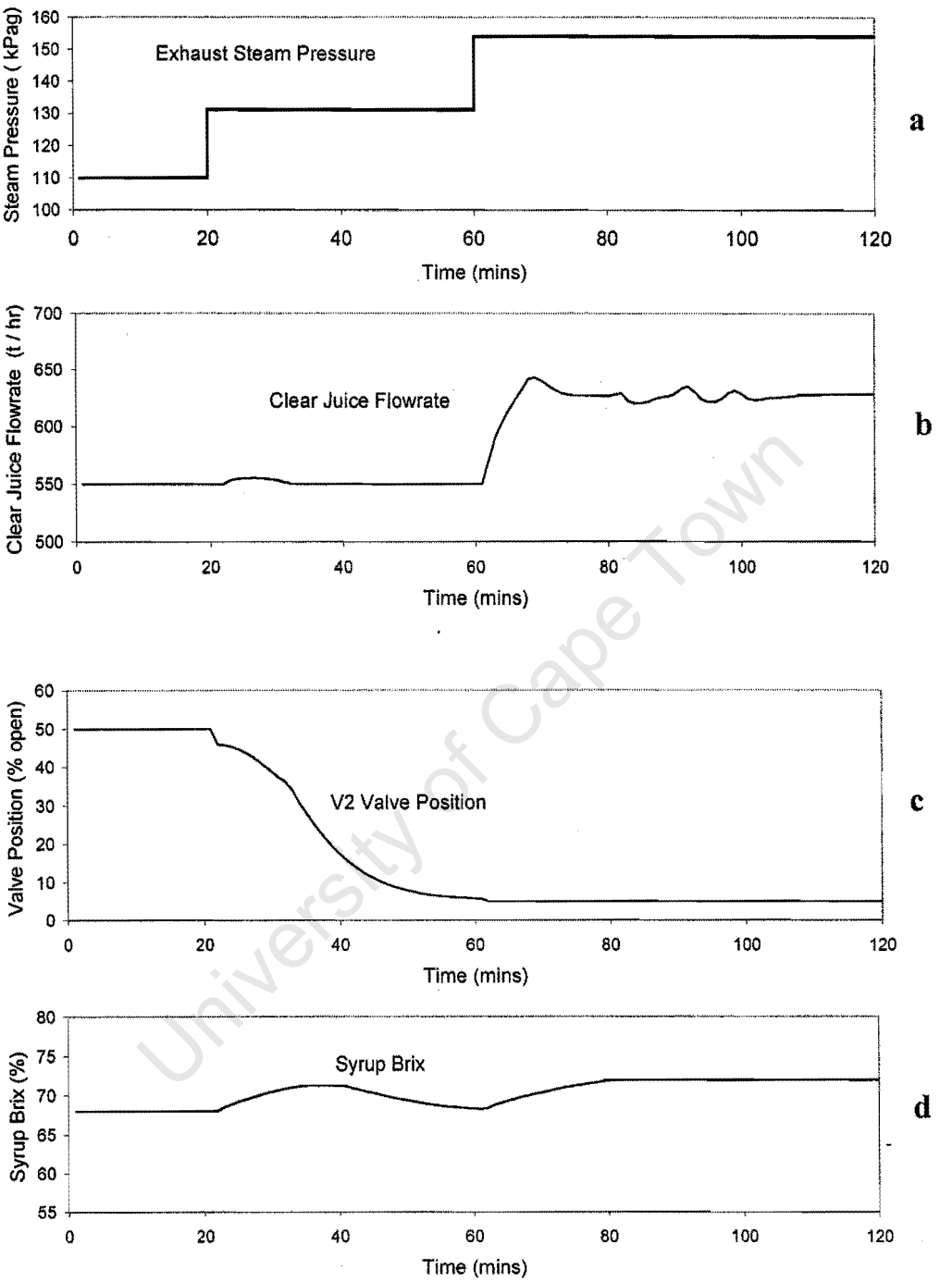

Figure 5.13 *Response of the DMC Brix controller to steps in steam pressure where (a) shows the plant disturbance, exhaust steam pressure, (b) shows the controller response, clear juice flowrate, (c) shows the controller response, V2 valve position, and (d) shows the plant output, A set syrup Brix.*

5.4 Combined Ultimate Control System

The two DMC alternatives were then compared using simple step tests. In these simulations, the combined formulation was used, i.e. each control system was required to control the clear juice tank level, as well as the operation of the evaporator station. It was also useful to compare the proposed controllers with simulations based on the existing PID control strategy.

This approach may seem biased, in that the existing control strategy is based on a feedback PID loop, whereas the two proposed DMC based controllers have an inherent feedforward capability. However, it would be difficult to devise a PID controller which would react in a feedforward manner to all of the disturbances which can be accommodated in the DMC formulations. A feedforward PID controller which reacts to fluctuations in tank level, or clear juice flowrate, would still need to be used in conjunction with a feedback element in order to react to the other disturbances. Thus the PID controller was used as a baseline from which to assess the performance of the other two systems, and to gauge the potential for improvement at Triangle.

The first set of simulations was based on a clean evaporator station, in which the heat transfer coefficients for the two trains were equal. The following graphs, Figures 5.14 and 5.15, show the responses of each control system to a step increase (20%) in the juice flowrate into the clear juice tank at time, t = 50 minutes. Figure 5.14 shows the plant inputs, i.e. the clear juice flowrates into the A train (due to the fact that the HTCs were equal, the flowrates into each first effect vessel were identical), and the V2 valve positions. Figure 5.15 shows the effects of these changes on the plant outputs, syrup Brix and clear juice tank level. The response of the syrup Brix from the B train was identical to that of the A train for each control strategy, and so only the results for the A train are presented.

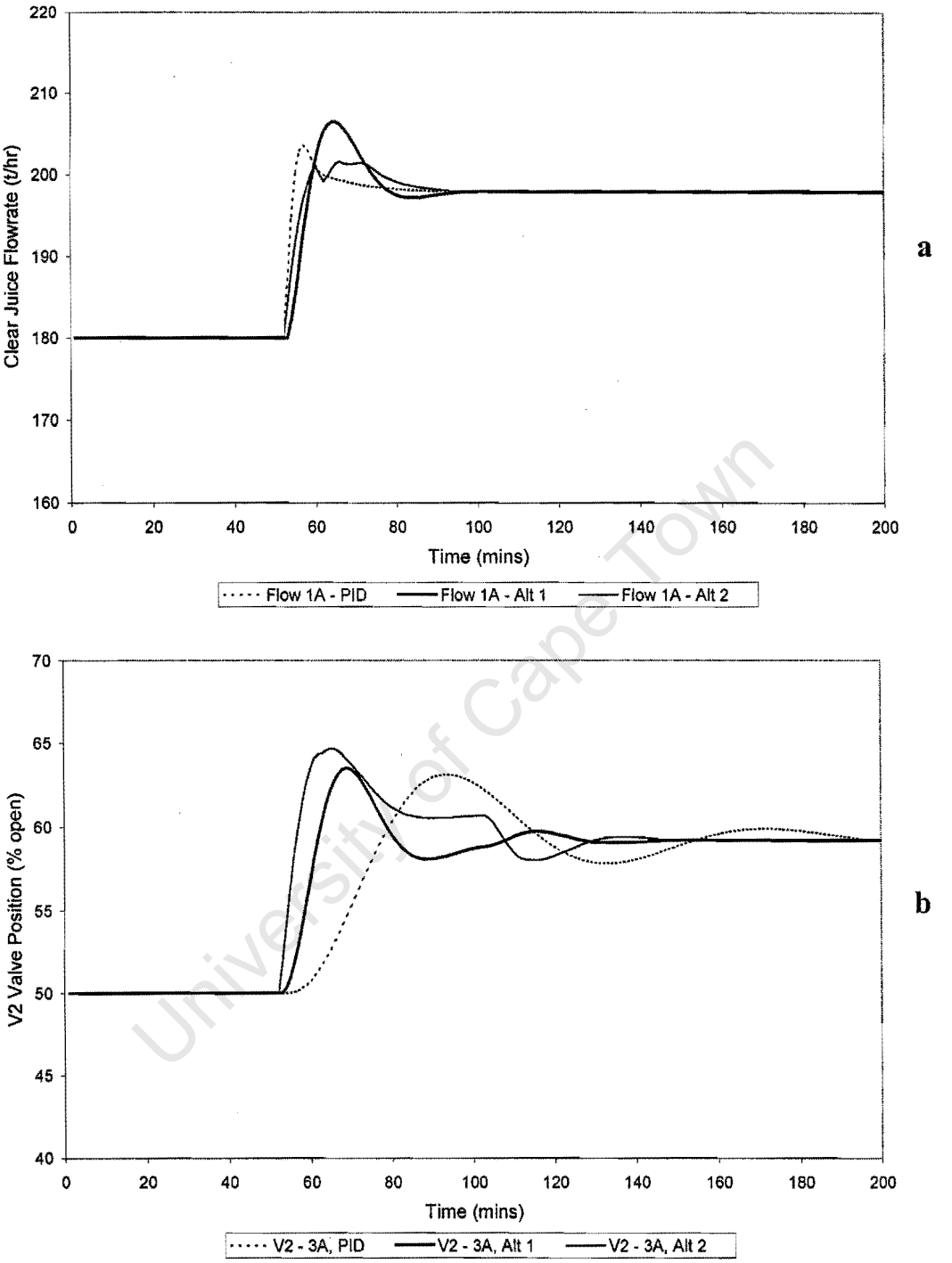

Figure 5.14 *Controller responses to a step increase in clear juice flowrate. under three control strategies, existing PID control, Alternative 1, and Alternative 2, where (a) shows the clear juice flowrates, and (b) shows the V2 valve positions. See Figure 5.15 for the plant outputs.*

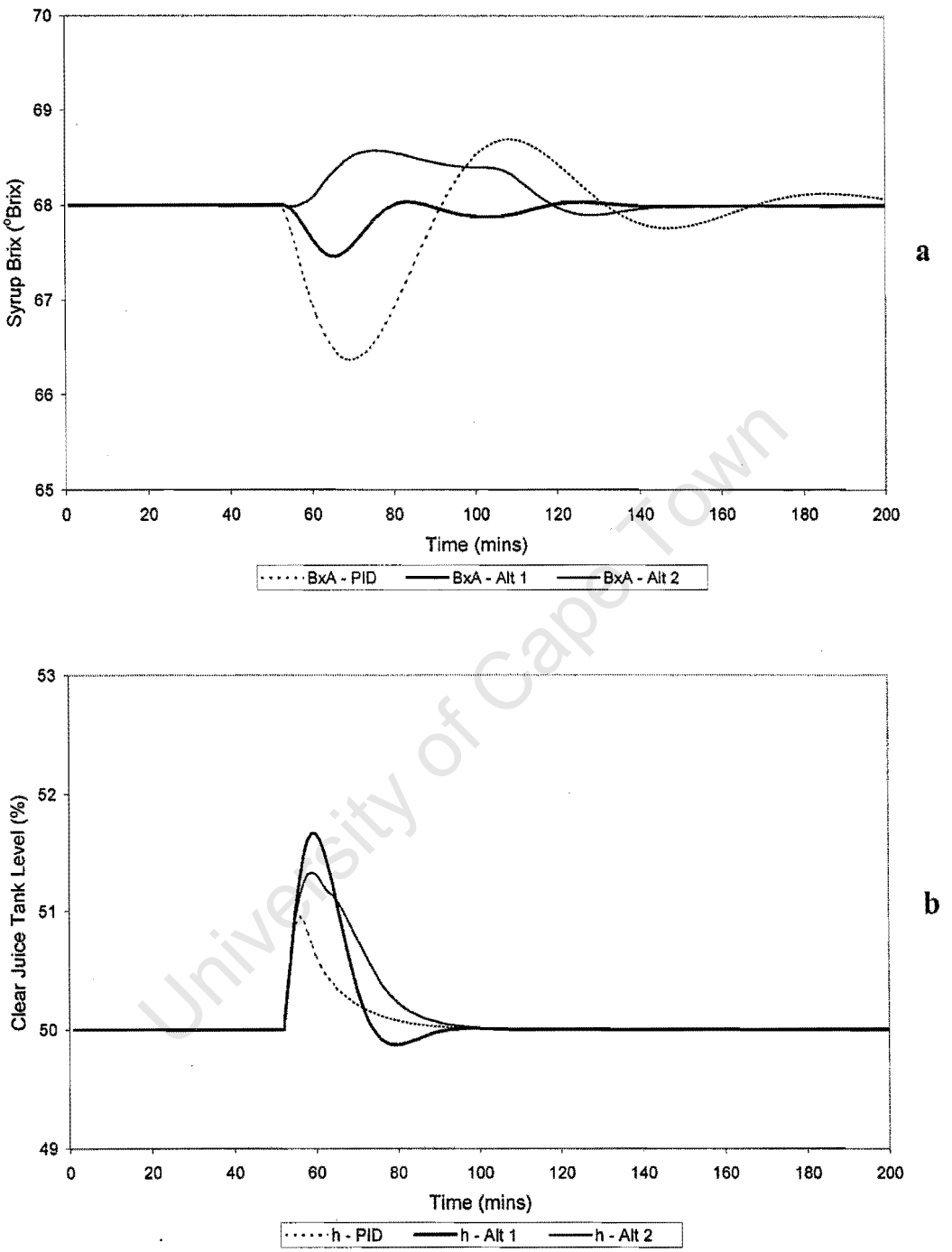

Figure 5.15 *Resultant plant outputs, after a step increase in clear juice flowrate. under three control strategies, existing PID control, Alternative 1, and Alternative 2, where (a) shows the syrup Brixes, and (b) shows the clear juice tank levels. See Figure 5.14 for the controller responses.*

Figure 5.14 shows that all three controllers responded in a similar manner to the disturbance by increasing the flowrate of clear juice through the evaporators, and then, in order to offset the resultant drop in syrup Brix, the V2 valves were all opened. The response of clear juice flowrate is very similar for Alternative 1, and the existing PID control. There is a slightly more damped response from the Alternative 2, and this is due to the combined formulation, which has the effect of modifying the changes in clear juice flowrate to meet a Brix control objective, as well as the objective of accommodating the increased flowrate.

The most significant difference however, is the response time of the throttling V2 valves. The response is far more sluggish with the PID controller, due to the long lag time in the evaporators. This PID controller must first wait for the disturbance to propagate throughout the multiple effects, and to affect the final syrup Brix, before any action is taken. The two DMC controllers however, anticipated this error, based on their internal models and were able to respond more quickly. This is borne out in Figure 5.15, where the PID controller gives the largest Brix error.

Throughout these simulations, the various tuning parameters of each controller were maintained at constant values, although an appreciation was gained that these have a significant effect on how the control systems operate. The two DMC based controllers were formulated in such a way that analogous errors were weighted equivalently in the two formulations, despite the different structures.

An important observation at this stage of the investigation was that the existing PID controller required far more conservative control parameters in simulation studies than those actually employed on the plant. Due to various instrumentation problems, the PID based Brix control loop is seldom used in automatic mode at Triangle, but when this option is chosen, typical tuning parameters are, $K_c = 0.33$, and $\tau_I = 25$ minutes. However, when the simulations were run, it was necessary to use an integral time of 100 minutes, in order to get a stable response.

The following two figures, Figures 5.16 and 5.17, show the responses of each control system to a sharp drop in steam pressure supplied to the station. This is a common scenario when one or more turbo-alternators is taken off duty. Note that the scale of the *y*-axis in plot (a) (juice flowrate) is magnified for clarity in Figure 5.16.

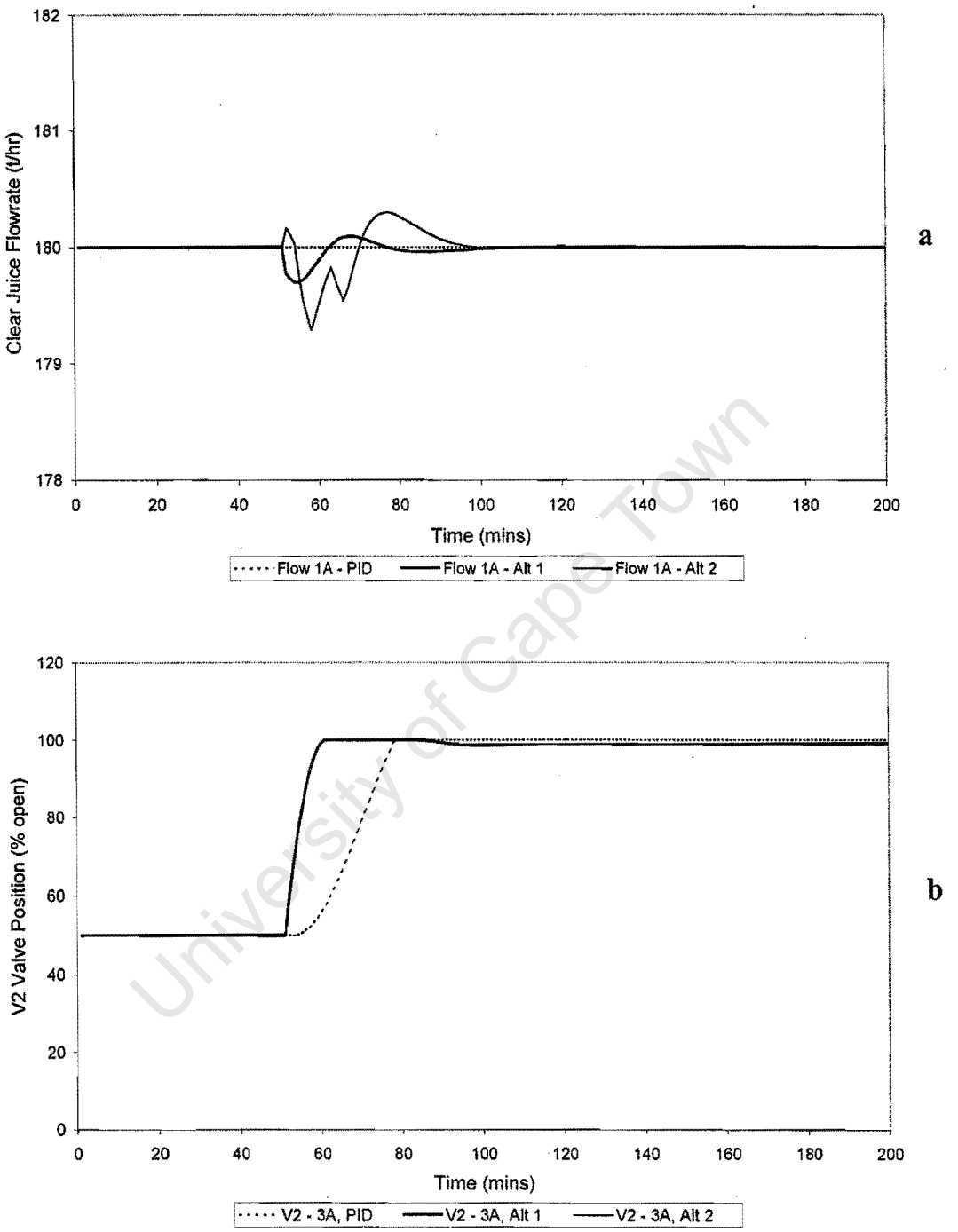

Figure 5.16 *Controller responses to a step decrease in exhaust steam pressure under three control strategies, existing PID control, Alternative 1, and Alternative 2, where (a) shows the clear juice flowrates, and (b) shows the V2 valve positions. See Figure 5.17 for the plant outputs.*

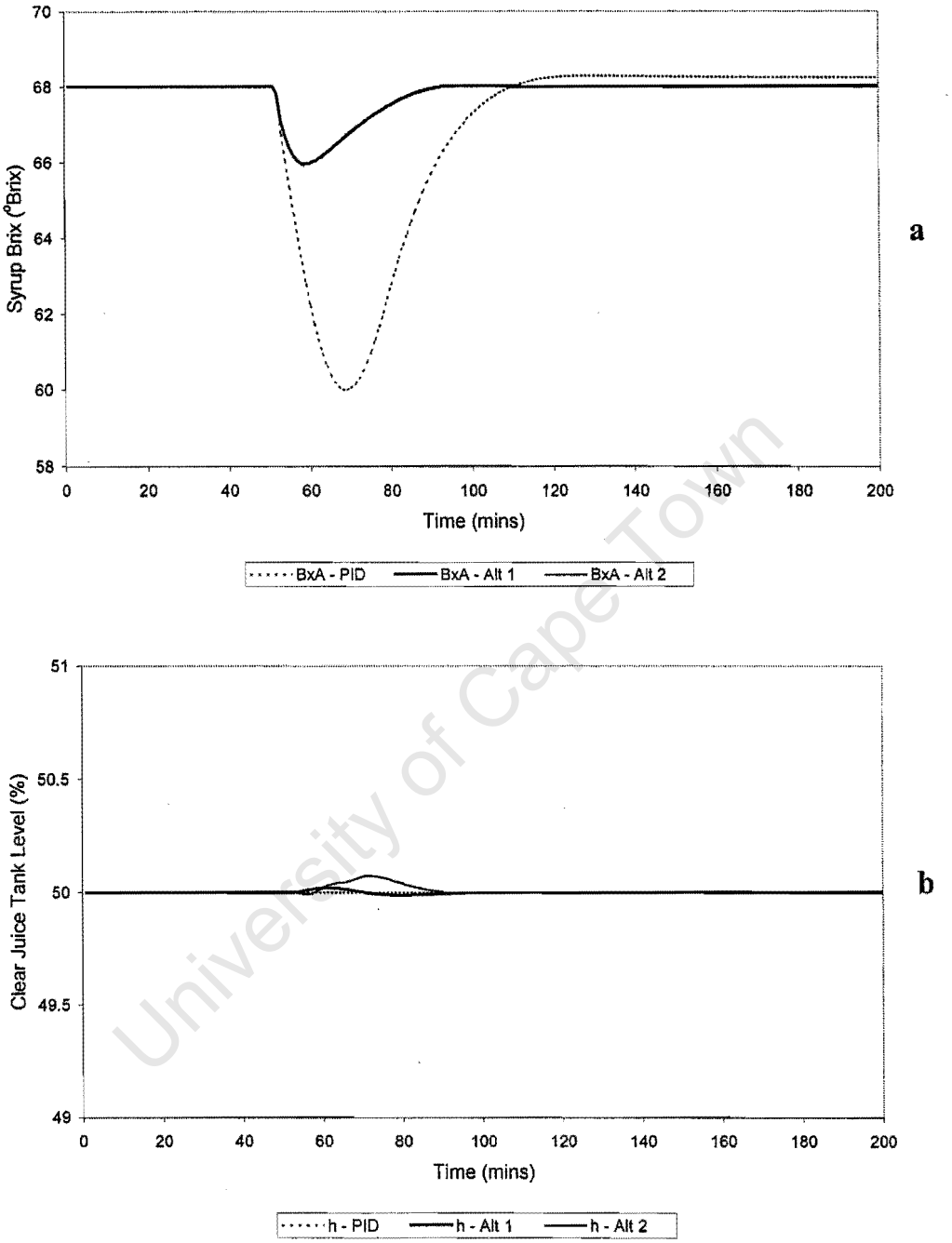

Figure 5.17 *Resultant plant outputs, after a step decrease in exhaust steam pressure under three control strategies, existing PID control, Alternative 1, and Alternative 2, where (a) shows the syrup Brixes, and (b) shows the clear juice tank levels. See Figure 5.16 for the controller responses.*

Figure 5.16 shows that only the two DMC based controllers were able to manipulate clear juice flowrate in order to alleviate the effects of the steam pressure disturbance. Due to the fact that deviations from clear juice tank level setpoint were heavily weighted in the objective functions, these manipulations of the clear juice flowrate were rather small. Apart from that, the three controllers responded in a similar manner – when the steam pressure dropped, this caused less vigorous boiling, and as the syrup Brix dropped, the V2 throttling valves were opened.

Similar to Figure 5.14 above, the PID controller was the most sluggish in response to the disturbance. Again, this was borne out in Figure 5.17, which shows the largest Brix deviation for the PID controller. The two DMC based controllers gave a very similar response. The better control performance of these two algorithms was due to their ability to anticipate the error that would be caused by the disturbance.

The next step was to try a scenario involving a series of disturbances, the last of which only affected the A train of evaporators. The disturbances which were chosen for these simulations were :

- Juice flowrate into the clear juice tank was increased by 10% at $t = 20$;
- Exhaust steam pressure supplied to the station dropped by 15% at $t = 100$;
- The final effect vacuum failed *only* for the A train (i.e. pressure in vessel 5A increased by 20%) at $t = 200$;

Figure 5.18 shows the input disturbances which were supplied to the model of the plant and the control systems. Figure 5.19 shows the responses of the separate Brix and level controllers, Alternative 1, to the disturbance, i.e. the clear juice flowrates out of the clear juice tank and into vessels 1A, 1B, and 1C, and the V2 valve positions on vessels 3A and 3B. Figure 5.20 shows similar responses for the combined formulation (Alternative 2). The responses under the existing PID control system are shown in Figure 5.21.

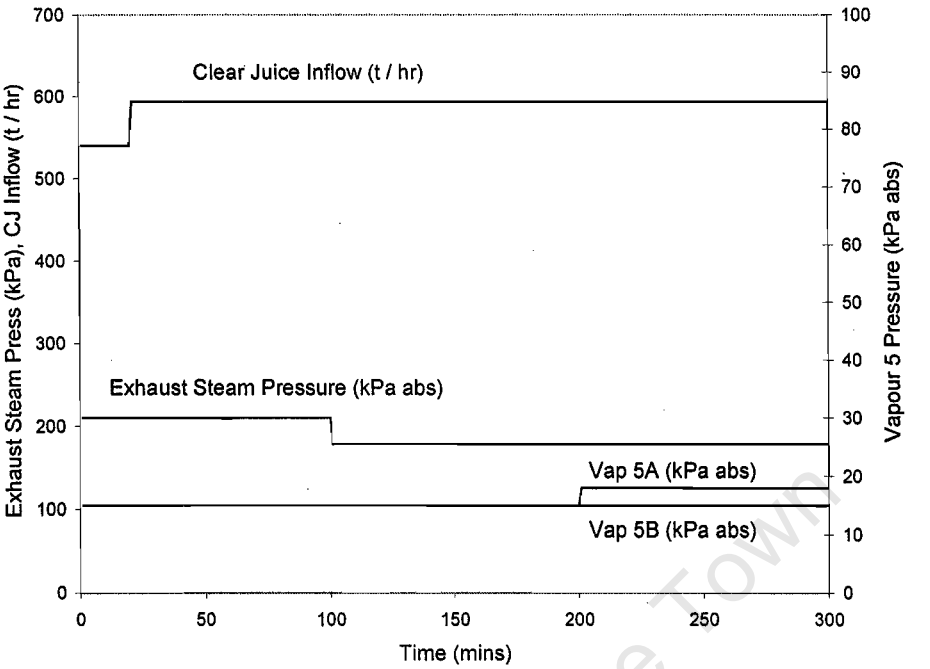

Figure 5.18 *Plant disturbances used to compare the responses of three control systems a step increase in clear juice inflow at t = 20, a step increase in exhaust steam pressure at t = 100, and a step increase in V5A pressure at t = 200. See Figures 5.19, 5.20 and 5.21 for the controller responses.*

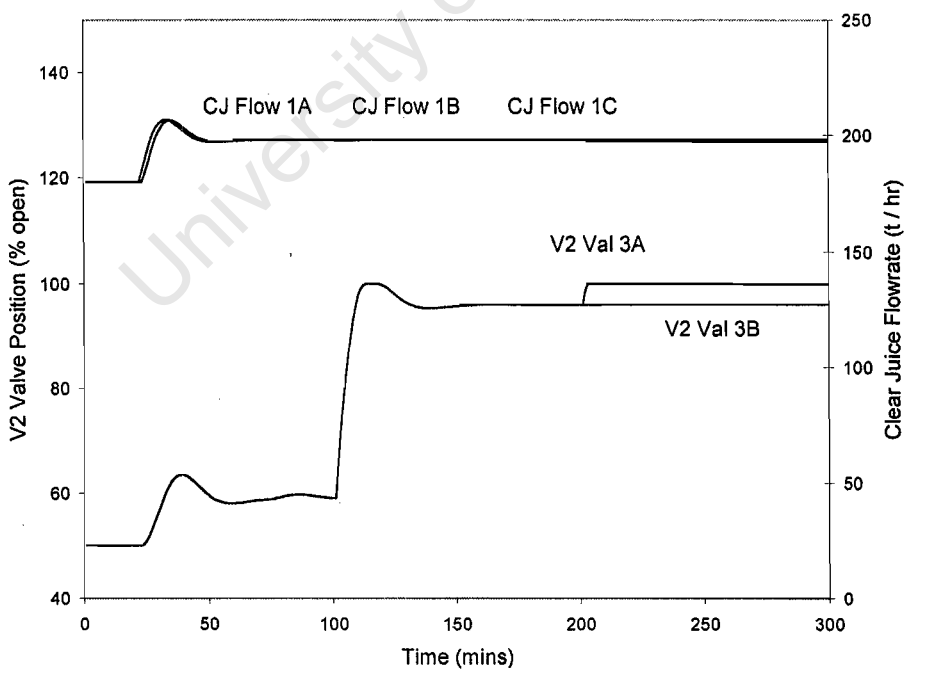

Figure 5.19 *Controller responses to a series of disturbances, using Alternative 1 See Figure 5.18 for the plant disturbances.*

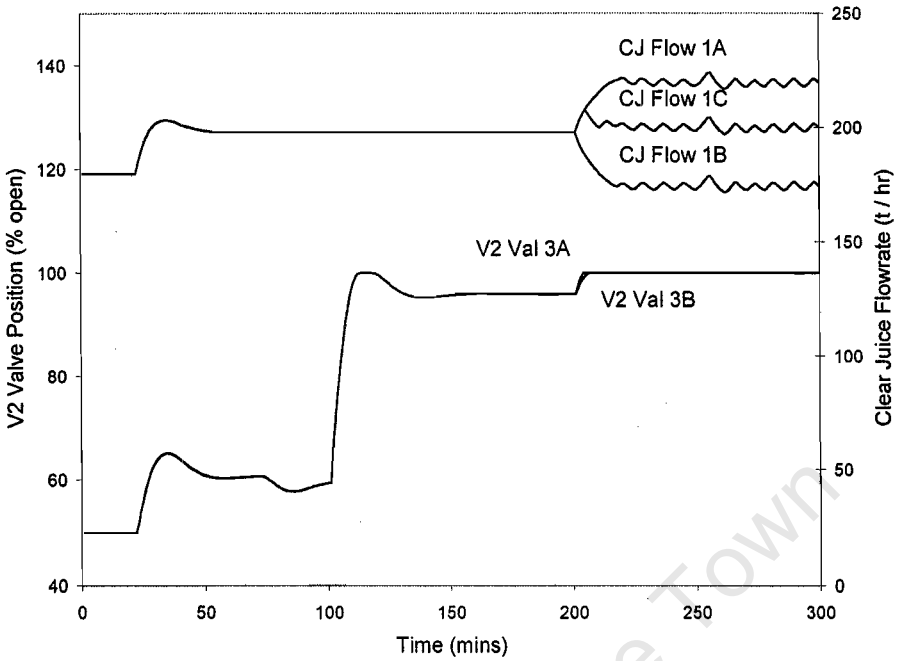

Figure 5.20 *Controller responses to a series of disturbances, using Alternative 2 See Figure 5.18 for the plant disturbances.*

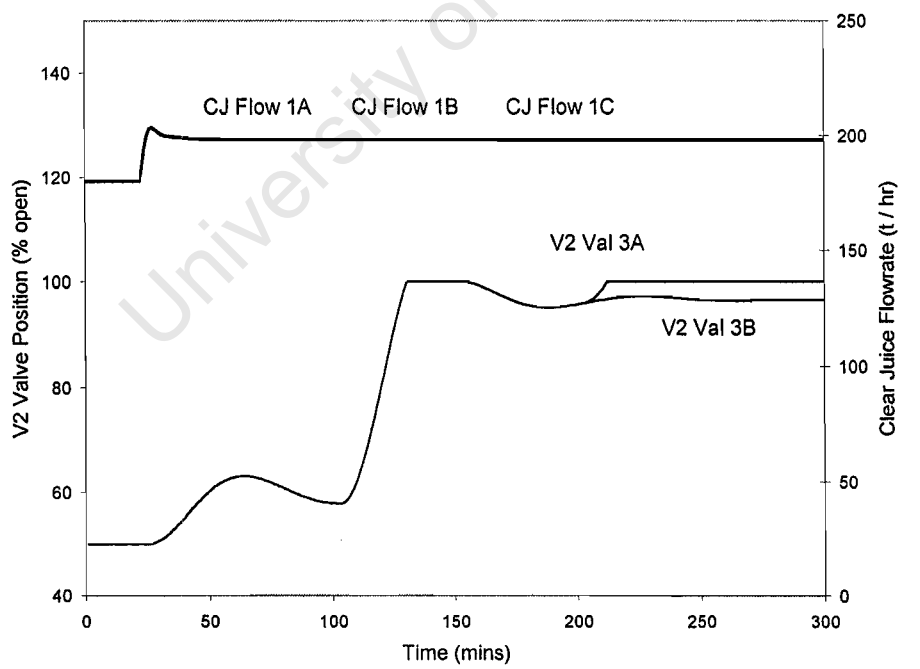

Figure 5.21 *Controller responses to a series of disturbances, for the existing PID control See Figure 5.18 for the plant disturbances.*

Dealing first with these three plots of controller response (manipulated variables), Figures 5.19, 5.20 and 5.21, all show similar behaviour. In response to the first disturbance, of an increase in clear juice supply, the clear juice flowrate was increased through the evaporators and the V2 throttling valves were both opened, so as to counteract the effects of this higher flowrate (as in Figure 5.14 above)

In response to the second disturbance, of a decrease in exhaust steam pressure, the V2 throttling valves all opened even further so as to allow a greater supply of vapour to the third effect, and thus counteract the less vigorous boiling in the first effect (as in Figure 5.16 above). Importantly, after this disturbance, none of the manipulated variables were saturated, although the V2 valves were all nearly fully open.

Finally, in response to the disturbance on the A set, Alternative 1, the separate level and Brix controllers, only reacts on the A set by further opening the V2 throttling valve. No action is taken on the B set, because this involves a separate controller which cannot sense the A syrup Brix. However Alternative 2, the combined formulation, reacts by opening the V2 throttling valves on both the A and B sets. This controller had also redistributed the total clear juice flowrate so that the A set, which was temporarily performing at a lower evaporative potential, could be favoured by a slightly lower clear juice flowrate. The B set, which was performing at a higher level, could then accommodate this change and accept the balance of the incoming clear juice flowrate. In so doing however it would be necessary to open the V2 throttling valve on the B set to allow for the increase in juice flowrate. Similar to Alternative 1, the existing PID controllers consist of separate control loops for the A and B sets, and thus the final response to a disturbance on the A set was simply to fully open the V2 throttling valve on the A set.

For the same simulation the following plot, Figure 5.22, shows the outputs, syrup Brix and clear juice tank levels, obtained under each control scheme. These plots compare Alternative 1 with PID control, and then Alternative 2 with the same existing PID control.

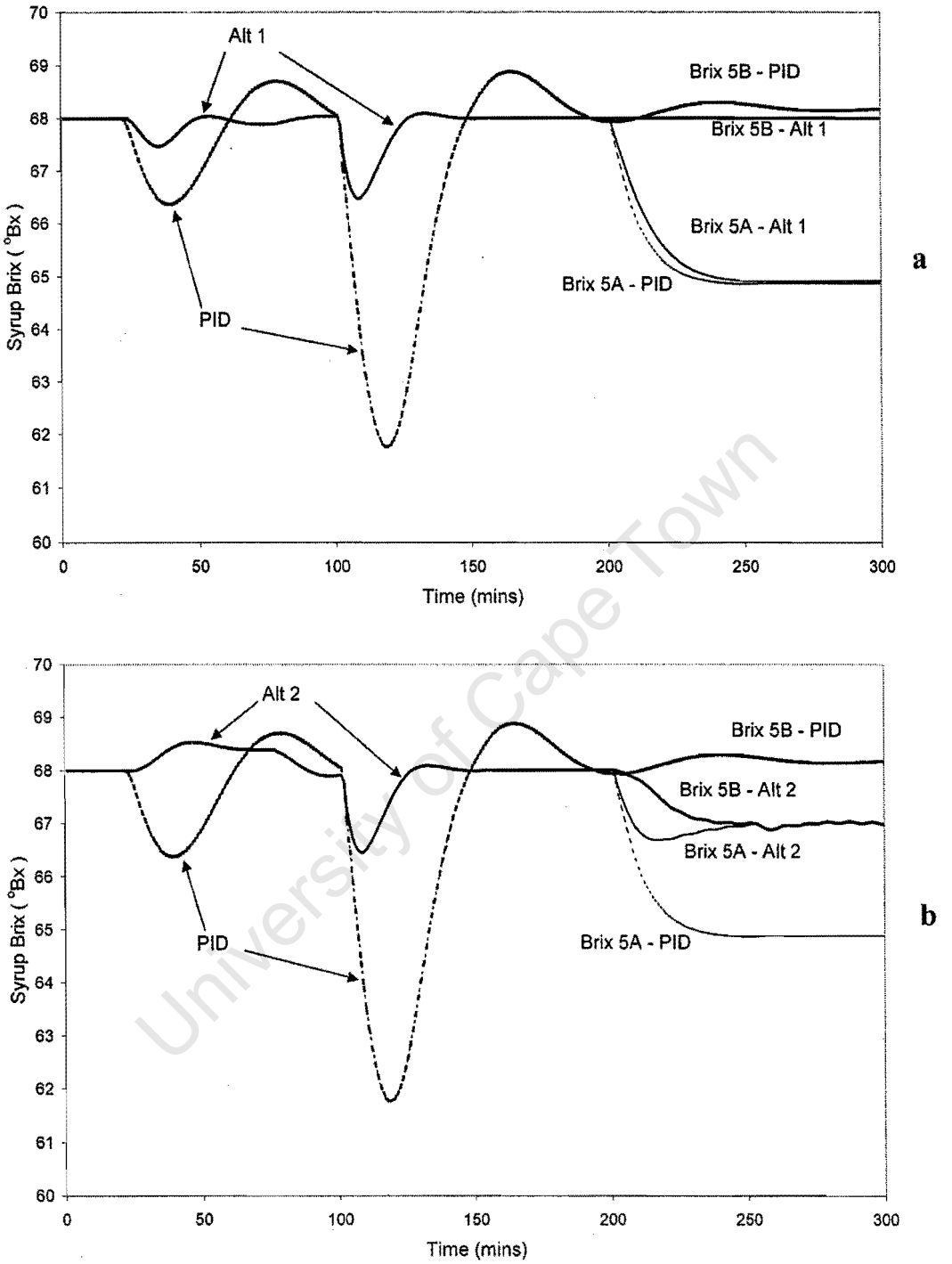

Figure 5.22 *Resultant plant outputs, under three different control strategies where (a) compares the existing PID control with and Alternative 1, and (b) compares the existing PID control with Alternative 2. See Figure 5.18 for the plant disturbances.*

Figure 5.22 shows that the average Brix delivered is closer to setpoint for Alternative 2. This is because the combined formulation was more flexible, in that it can accommodate constraints in one train by making allowances in the other train. This response also allowed the delivery of a balanced syrup Brix from the two lines. Alternative 1, however, shows a significant offset for the A syrup Brix, while the B syrup Brix is on target. Similar results were obtained with the existing PID controllers.

It is important to note that in this simulation the heat transfer coefficients were kept equal in the two trains. Thus the ratio setpoints still favoured an equal split of the clear juice between the three first effects. Although this ratio is important for the long term, it is equally important that the control system has the flexibility, as shown here, to deviate from that optimum split in the case of a disturbance which only affects one train.

Trials on actual plant data

Following this series of controlled simulations, it was decided that the most flexible framework for controlling the evaporators was the combined formulation of Alternative 2. In the next simulation, the control of the mixed juice tank level was performed by the MPC controller of Campo and Morari, as described in Chapter 4. The combined controller, Alternative 2, was used to control clear juice tank level and the evaporator station.

The following charts show the results of a simulation done using 6 hours of real plant data, collected from the the factory SCADA system. Figure 5.23 shows the disturbances which affected the plant, draught juice flowrate, exhaust steam pressure, clear juice temperature, and the final effect vacuum in each train. Figure 5.24 shows the response of the control system to these disturbances, the total mixed juice flowrate, clear juice flowrates to each first effect evaporator, and the V2 valve positions. Figure 5.25 then shows the resultant plant outputs – the syrup Brix delivered by each train, and the mixed juice and clear juice tank levels.

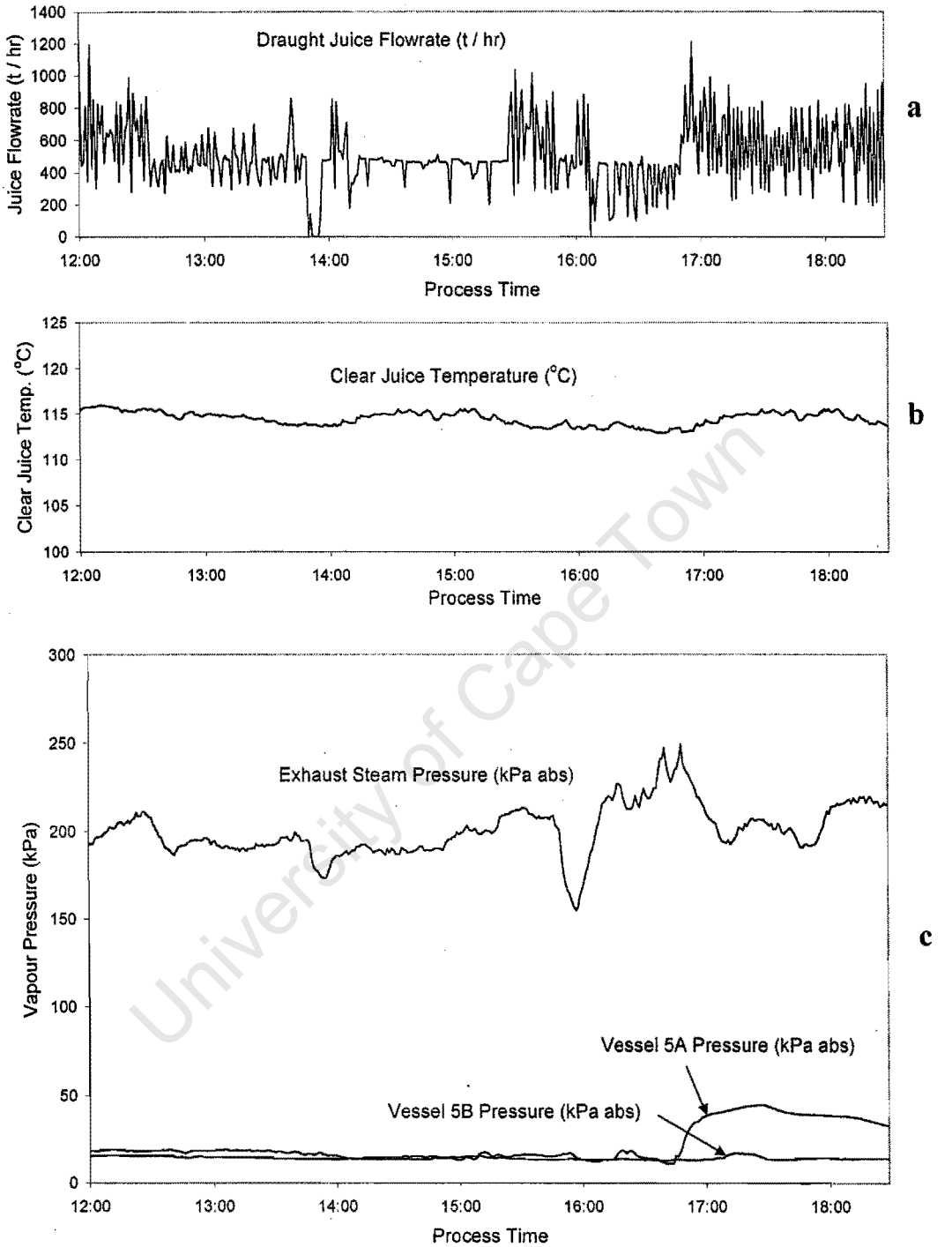

Figure 5.23 *Graphs of the data which were collected and used as inputs to the controller where (a) shows draught juice flowrate, (b) shows clear juice temperature, and (c) shows vapour pressures.*

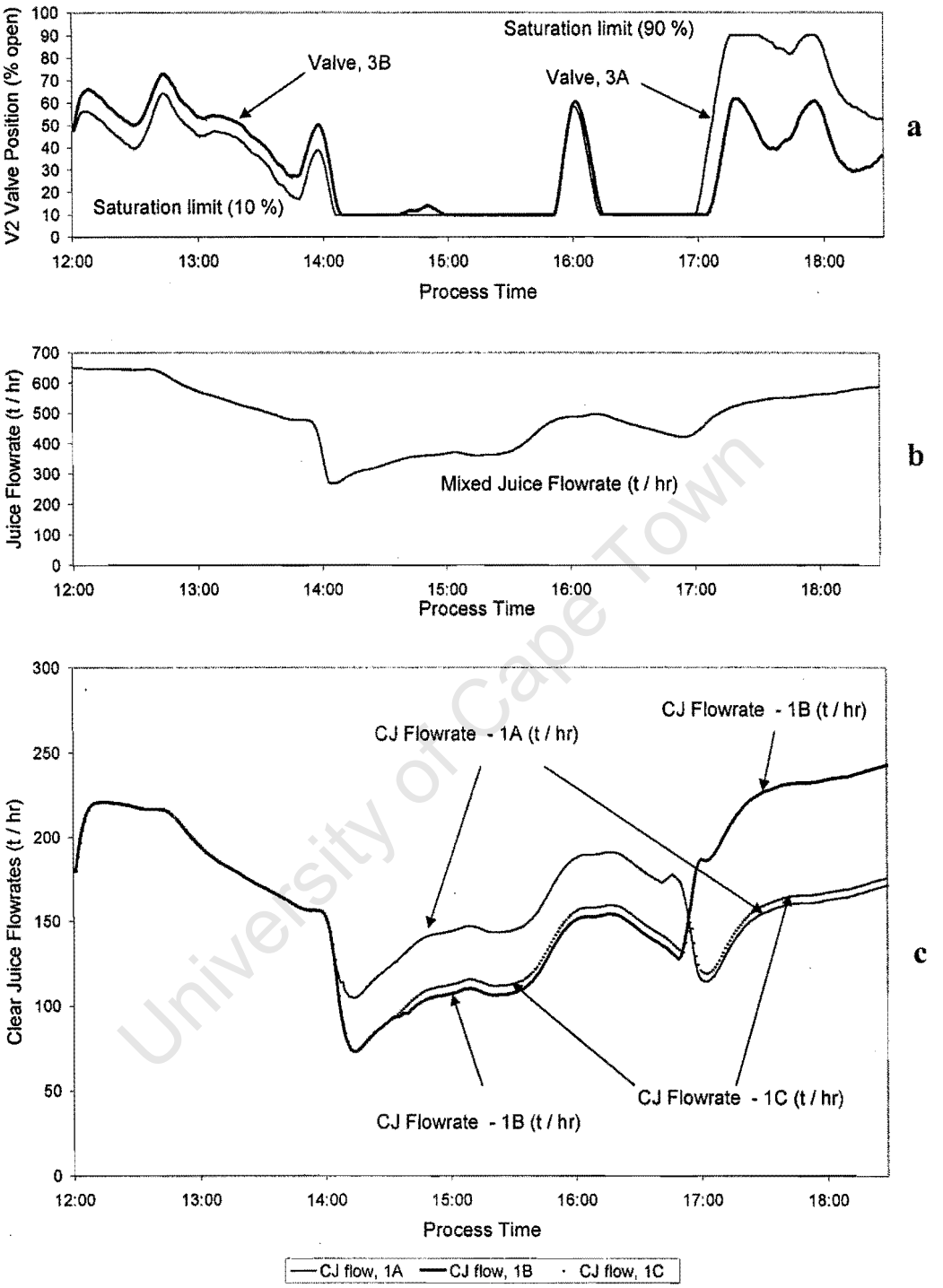

Figure 5.24 *Control system responses (manipulated variables) for real plant disturbances where (a) shows the V2 valve positions, (b) shows the mixed juice flowrate, and (c) shows the clear juice flowrates into each first effect evaporator. See Figure 5.23 for the plant inputs.*

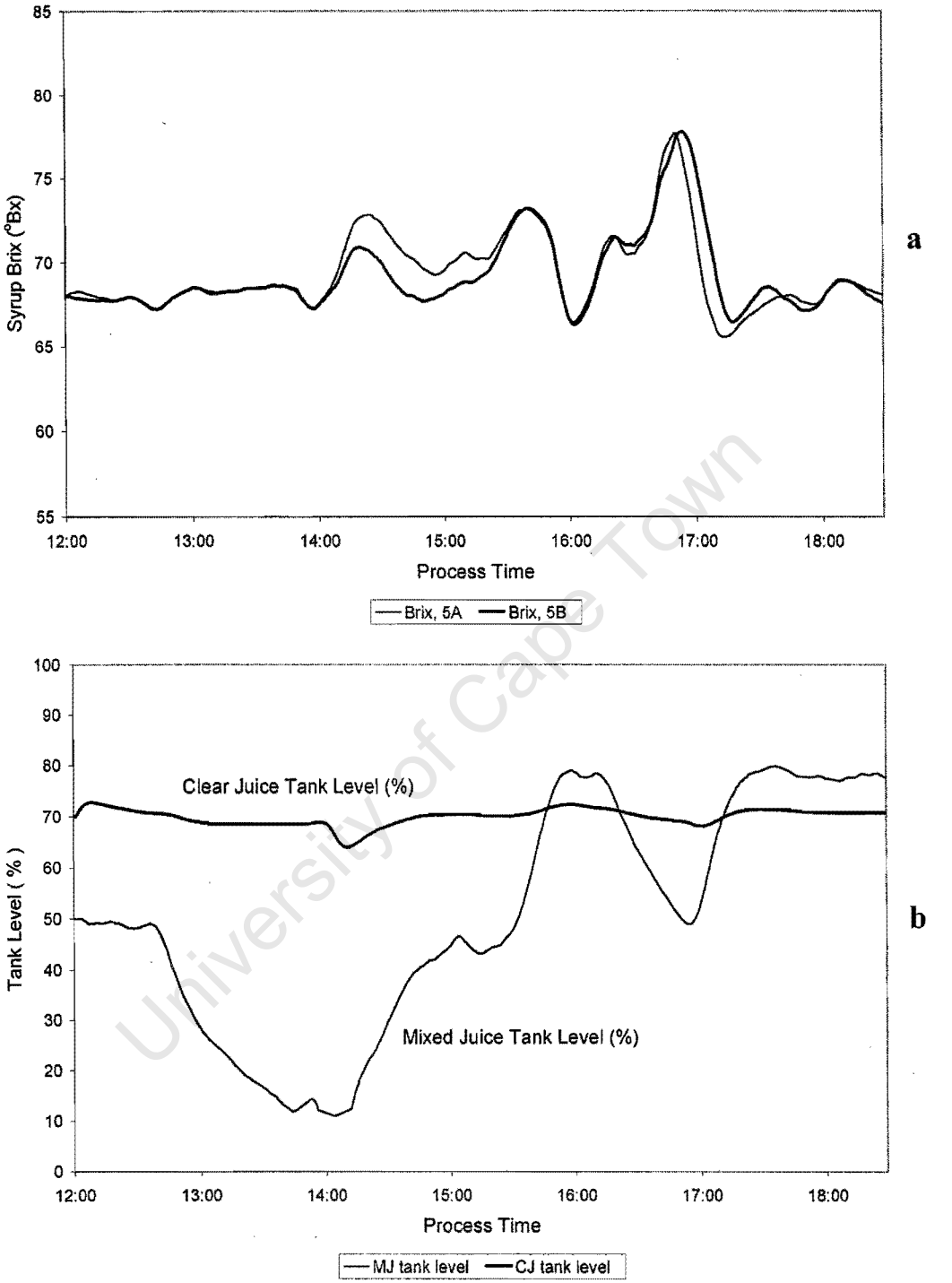

Figure 5.25 *Resultant plant outputs (process variables) under combined control system where (a) shows the syrup Brixes, and (b) shows the mixed juice and clear juice tank levels. See Figure 5.23 for the plant disturbances, and Figure 5.24 for the controller responses.*

The first point to notice is that the control system was able to deal with a very noisy input signal for the draught juice flowrate, shown in Figure 5.23. Despite the noise in this signal, the mixed juice flowrate was much smoother (Figure 5.24), and the buffer capacity of the mixed juice tank was well utilized (Figure 5.25), within safety constraints, i.e. between 10% and 90 % full. This good flow filtering allowed the clear juice tank to remain at a high level, (setpoint = 70%), which has the advantage of allowing the evaporators to carry on running in the event of a short term break in the supply of cane, which would result in sudden drop in mixed juice flowrate.

From Figure 5.24, it was observed that the clear juice flowrates in to each first effect vessel were not equal, but were varied in order to make the most of the available evaporative potential. From t = 14:00 until t = 17:00, the A set handled a greater flowrate of juice than the B set (Figure 5.24). However, from t = 17:00 until the end of the simulation at t = 18:40, the B set handled more juice than the A set.

This was brought about in response to the sudden loss of vacuum at about t = 16:50 (Figure 5.23), which reduced the evaporative potential of the A set of evaporators, and so in order to balance the load on the two sets, the controller redistributed the total clear juice flowrate so that more was handled by the B set and less by the A set. By doing this, the syrup Brixes from each train were maintained near the setpoint of 68, despite major fluctuations in the plant inputs. This also allowed the syrup Brixes from each train to follow one another closely.

This simulation has demonstrated the significance of the combined formulation, and the ability of the controller to choose flowrates which may differ from the suggested optimum ratios, depending on the state of the other inputs. This controller has also been shown to be stable, even in the face of noisy inputs, and severe plant disturbances.

Chapter 6 CONCLUSIONS

This investigation has focused on evaporator control and in particular the potential for improving control of the multiple effect evaporator station at Triangle Sugar mill in Zimbabwe. Evaporation is a key unit operation in the sugar industry and there are strong economic motivations for improved control. The most significant areas of potential benefit would be an increase in the capacity of the plant, and a reduction in the cost and time associated with evaporator cleaning.

A number of single loop PID controllers are used to control various aspects of evaporator operation at Triangle. However, due to the large number of variables and interactions, these controllers do not adequately anticipate all disturbances, and nor do they optimally handle the multiple input multiple output (MIMO) system. The theory and operation of several advanced control philosophies has been explored, including MPC, NLMPC, fuzzy logic and expert systems. Dynamic Matrix Control was chosen for the proposed control system because of its ability to anticipate and handle constraints and its ability to optimally handle the MIMO problem.

A dynamic model of the plant was developed, in order to obtain step response data and to perform simulations, which would test the controllers after they had been formulated. The model was based on mass and energy balances about each evaporator effect. Interactions between the evaporator effects were of primary importance during the setting up of the model. The response of the model was then tested by inputting actual plant data (which had been gathered by the SCADA system). The model followed the actual plant behaviour reasonably closely.

The model was used to formulate the dynamic matrix for the proposed controllers. The objective of this control system was the delivery of the maximum amount of consistently high

quality syrup, within plant constraints, and while operating the plant in as smooth a manner as possible.

One of the most significant disturbances to good evaporator control is a fluctuation in the flowrate of juice supplied to the station. Two different level controllers, an LQG controller and an MPC level controller (after Campo and Morari, 1989) were formulated and applied to a model of the buffer tanks upstream of the station. The final control layer to be investigated was that of an economic optimization layer, which was used to determine the distribution of total clear juice flowrate between the three first effect evaporators.

The objectives of Brix and level control were tackled by using two different approaches. The first of these included three separate controllers, one for level control and two independent Brix controllers (one for each evaporator train). The second algorithm was a combined formulation, where the objectives of Brix and level control were tackled simultaneously. These two controllers were then compared with the existing PID controllers in a series of simulations, using step tests and real plant data.

The two level control methods each proved to have advantages and disadvantages. The LQG controller, while simpler to implement, resulted in some offset of tank level when subjected to a flow disturbance. This offset could be minimized, however, by using a moving average setpoint, as discussed in Chapter 4. The MPC level controller, while more complex to implement, could be incorporated into the combined Brix / level controller, thereby allowing these two objectives to be tackled together. It was recommended that the LQG controller would be more readily applicable to the sugar industry, due to its relative simplicity, and the small memory requirement of this algorithm in comparison to the MPC level controller. An LQG tank level control strategy has been applied to mixed juice, clear juice, and raw syrup tanks at Triangle Ltd. This strategy allows bumpless transitions between the various modes of operation. This control system has already been commissioned, and is operating satisfactorily.

The two Brix control methods proved useful in different circumstances. The separate formulation would be a simpler system to implement on the plant and would also more easily accommodate a situation in which one train was taken off line. The combined formulation provided superior Brix control and allowed the entire evaporator station (i.e. both trains) to

react optimally to any disturbance, even when the given input disturbance affected only one train.

The distribution of clear juice to the three first effects was also investigated, and it has been shown that the incorrect distribution of this juice will result in sub-optimal Brix control, and would place an unnecessary burden on downstream equipment. In order to evaluate the condition of each evaporator, it was necessary to first find an online measure of evaporative potential. For this reason condensate flowmeters were designed and installed on the Triangle evaporator station. These flowmeters were based on a multiple orifice design which was intended to eliminate flashing and to provide a linear reading. Unfortunately, the flowmeters were not able to provide online readings, due to the unavailability of suitable instrumentation. Manual measurements were taken to validate the flowmeter design and to use these results in simulation studies.

Simulations showed that even when heat transfer coefficients were significantly worse on one train than the other, the optimal flow distribution was still close to an even split between the two trains. Further simulations on the combined control system showed that it was more important that the clear juice flowrates remained independently flexible, and were available for manipulation, than that they were fixed at an optimal ratio.

The combined control system was finally tested using a sample of real plant data, which were gathered using the SCADA system. This simulation showed again that the combined Brix / level controller was more flexible in handling disturbances, and resulted in a more consistent Brix than the existing system, while maintaining the plant within operating constraints.

This study has shown that significant benefits could be achieved with improved evaporator control. The results of this study could also be applied to similar installations elsewhere in the sugar industry, and to evaporators in other industries. The proposed control systems have been shown to provide benefits in simulation studies, what remains now is to apply this work to a practical control system.

Chapter 7 REFERENCES

Arkun, Y., and Stephanopoulos, G., (1980), *AIChE J.*, Vol. 26, pp. 975.

Bequette, W. B., (1991), "Nonlinear Control of Chemical Processes: A Review", *Ind. Eng. Chem. Res.*, Vol. 30, pp. 1391-1413.

Bhandarkar, M., and Ferron, J.R., (1988), "Transport Processes in Thin Liquid Films during High-Vacuum Distillation", *Ind. Eng. Chem. Res.*, Vol. 27, pp. 1016-1024.

Brooks, T.R., and Edwards, L.L., (1992) " A real-time, model based expert system for multiple effect evaporators", *Tappi Journal*, Vol. 75, pp. 131-135.

Campo, P.J. and Morari, M., (1989), "Model Predictive Optimal Averaging Level Control", *AIChE Journal*, Vol 35, No. 4, pp579 - 591.

Chen, C.H., and Hsiao, Y.C., (1995), "Evaluation of Control Models for Multiple-Effect Evaporator Set in a Cane Sugar Mill", *Taiwan Sugar*, Jul-Aug, 1995, pp. 24-27.

Cheng, C-M., (1989), "Linear Quadratic-Model Algorithmic Control Method: A Controller Design Method Combining the Linear Quadratic Method and the Model Algorithmic Control Algorithm", *Ind. Eng. Chem. Res.*, Vol. 28, pp. 178-186, American Chemical Society.

Clarke, D.W., (1988), "Application of Generalised predictive control to industrial processes", *IEEE Control Systems Magazine*, April 1988, pp 49-55.

Cuthrell, J.E., and Biegler, L.T., (1986), "On The Optimization of Differential-Algebraic Process Systems", to be presented at the *Annual AIChE Meeting*, Miami, FL, November 1986.

Cutler, C.R., and Ramaker, B.L., (1979), "Dynamic matrix control - a computer control algorithm", AIChE National Mtg, Houston, Texas (1979); also *Proc. Joint Aut. Control Conf.*, San Fransisco, California (1980).

DiMarco, R., Semino, D., and Brambilla, A., (1997) "From Linear to Nonlinear Model Predictive Control: Comparison of Different Algorithms", *Ind. Eng. Chem. Res.*, Vol. 36, No. 5, pp. 1708-1716.

Doyle, F.J. III, Pekny, J.F., Dave, P., and Bose, S., (1997), "Specialised Programming Methods in the Model Predictive Control of Large Scale Systems", *Computers and Chemical Engineering,* Vol. 21, Suppl., pp. S847-S852, Elsevier Science Ltd.

Efstathiou, J., (1983), "Expert systems, fuzzy logic and rule-based control explained at last", *Trans. Inst. MC*, Vol. 10, No. 4, July-September 1983, pp. 198-206.

Elhaq, S.L., Giri, F., and Unbehauen, H., (1999), "Modelling, identification and control of sugar evaporation – theoretical design and experimental evaluation.", *Control Engineering Practice,* 7, pp. 931-942.

Fisher, D.G., (1991), "Process Control: An Overview and Personal Perspective", *The Canadian Journal of Chemical Engineering*, Vol. 69, February 1991, pp. 5-26.

Forbes, J.F., and Marlin, T.E., (1996), "Design cost: A systematic approach to technology selection for model-based real time optimization systems", *Computer Chem Engng.* Vol. 20, No. 6/7, pp. 717-734.

Forbes, J.F., Marlin, T.E., and MacGregor, J.F., (1994) "Model adequacy requirements for optimizing plant operations", *Computers in Chem Engng*, Vol., 18 No. 6, pp. 497-510.

Garcia, C.E., and Morari, M., (1982), "Internal Model Control. 1. A Unifying Review and Some New Results", *Ind. Eng. Chem. Process Des. Dev.*, Vol. 21, pp. 308-323, American Chemical Society.

Garcia, C.E., and Morshedi, A.M., (1986), "Quadratic Programming Solution of Dynamic Matrix Control (QDMC)", *Chem. Eng. Commun.* Vol. 46 pp. 73-87, Gordon & Breach Scientific publ. S.A.

Garcia, C.E., Prett, D.M., and Morari, M., (1989), "Model Predictive Control: Theory and Practice-a Survey", *Automatica*, Vol. 25, No. 3, pp. 335-348, Pergammon Press, Great Britain.

Gruhle, W.-D., and Isermann, R., (1985), "Modelling and Control of a Refrigerant Evaporator", *Journal of Dynamic Systems, Measurement and Control*, December 1985, Vol. 107, pp. 235-240.

Gudmundson, C., (1972), "Heat Transfer in Industrial Black Liquor Evaporator Plants", *Svensk Papperstidning*, Nr 22, pp. 901-908.

Gupta, Y.P., (1998), "Control of Integrating Processes Using Dynamic Matrix Control", *Trans. IChemE*, Vol. 76, Part A, May 1998, Institution of Chemical Engineers.

Harris, T.J., and McLellan, P.J., (1990), "Generic Model Control - A Case Study Revisited", *The Canadian Journal of Chemical Engineering*, Vol. 68, December, 1990, pp. 1066-1071.

Heller, H., (1980), "Use weir to measure fluid flow", *Chemical Engineering*, November 17, 1980.

Henson, M.A., (1998), "Nonlinear model predictive control: current status and future directions", *Computers and Chemical Engineering*, Vol. 23, pp. 187-202, Elsevier Science Ltd.

Hoekstra, R.G., (1998), "A Computer Program for Simulating and Evaluating Multiple Effect Evaporators in the Sugar Industry.", *Proc S Afr Sug Technol Ass* (1981), vol. 55, pp. 43-50.

Holland, C.D., and Liapis, A.I., "Computer methods for solving dynamic separation problems", McGraw Hill Book Company, New York.

Hsiao, Y.C., and Chen, C.H., (1995), "Evaluation of Control Models for Multiple-Effect Evaporator Set in a Cane Sugar Mill", *Taiwan Sugar*, Jul-Aug, 1995, pp. 24-27.

Hugot, E., (1986), "*Handbook of Cane Sugar Engineering*", Third Edition, Elsevier.

Hulbert, D.G., (1995), " Multivariable control of pulp levels in flotation circuits",

Hussey, P.S., (1973), "A Digital Computer Model of a Multiple Effect Evaporator", *Proc S Afr Sug Technol Ass* (1973), vol. 47, pp. 70-76.

Hussey, P.S., (1976), "Optimal Evaporator Operation", *Proc S Afr Sug Technol Ass* (1976), vol. 50, pp. 170-175.

Khan, F.I., Gupta, S.C., and Abbasi, S.A., (1998), "Dynamic modelling and simulation of multiple effect evaporator system", *Hungarian journal of chemistry*, Vol. 26 pp173-179.

Lee, J.H., Morari, M. and Garcia, C.E. (1994), "State space interpretation of model predictive control", *Automatica,* Vol. 30, No. 4, pp. 707-717.

Lee, P.L., and Newell, R.B., (1989), "Generic Model Control - A Case Study", *The Canadian Journal of Chemical Engineering*, Vol. 67, June, 1989, pp. 478-484.

Lee, P.L., and Sullivan, G.R., (1988), "Generic Model Control (GMC)", *Comput. Chem. Engng,* Vol. 12, No. 6, pp. 573-580, Pergammon Press.

Lee, W., and Weekman, V.W., Jr., (1976), *AIChE J.*, Vol. 22, pp. 27.

Loblein, C. and Perkins, J.D., (1997), "Economic analysis of different structures on on-line process optimization systems", *Computers Chem Engng*, Vol. 22, No. 9, pp. 1257-1269.

Loblein, C. and Perkins, J.D., (1999), "Structural Design for on line process optimization : I Dynamic economics of MPC", *AIChE Journal*, May 1999 Vol 45, No 5, pp 1018-1028.

Loblein, C. and Perkins, J.D., (1999), "Structural Design for on line process optimization : II Application to a Simulated FCC", *AIChE Journal*, May 1999 Vol 45, No 5, pp 1030-1040.

Love, D.J., (1995), "Use of Buffer Tanks for Smooth Flow Control", *Personal Communication.*

Love, D.J., (1999), PhD thesis, University of Natal, Durban, *in print.*

Love, D.J., and Chilvers, R.A.H., (1986), "Tuning of Pan Feed Controls", *Proc S Afr Sug Technol Ass* (1986), vol. 60, pp. 103-111.

Lundstrom, P., Lee, J.H., Morari, M., and Skogestad, S., (1995), "Limitations of Dynamic Matrix Control", *Computers and Chemical Engineering*, Vol. 19, pp. 409-421, Elsevier Science Ltd.

Marlin, T.E., Perkins, J.D., Barton, G.W., and Brisk, M.L., (1991), "Benefits from process control: results of a joint industry university study", *J. Proc. Cont.*, Vol 1, March, pp 68-83.

McFarlane, R.C., and Bacon, D.W., (1989), "Adaptive Optimizing control of multivariable constrained chemical processes, 1 Theoretical development", *Ind Eng Chem Res*, 1989, 28, pp. 1828-1834.

Miletic I.P., and Marlin T.E., (1998), "Results diagnosis for real time process operations optimization", *Computers Chem engng* Vol 22 Suppl pp S475-S482.

Mizoguchi, A., Marlin, T.E., and Hrymak, A.N., (1991), "Operations optimization and control design for a model distillation process", *The Canadian Journal of Chemical Engineering*, Vol., December 1991, pp. 896-907.

Mohtadi, C., Shah, S.L., and Clarke, D.W., (1987), "Generalized predictive control of multivariable systems.", *System and Control Letters*, 9, 285.

Montocchio, R.G., and Scott, R.P., (1985), "Experiences in Evaporator Control at Amatikulu", *Proc S Afr Sug Technol Ass* (1985), vol. 59, pp. 99-101.

Mulholland, M., and Welman, J.C.A., (1991), "Use of a Kalman filter for observation of heat transfer coefficients in a triple effect evaporator", *Personal Communication.*

Newell, R.B., and Lee, P.L., (1989), "Applied process control: a case study", Prentice Hall, Australia

Newton, D.A., (1995), "Advanced Traction and Braking Systems", *GEC Review*, Vol. 10, No. 2, pp. 72-80.

Niemi, A, and Koistinen, R., (1972), "Dynamic Modelling of a multiple effect evaporator plant", *Papper Och Tra*, No 5., pp 297-306.

Paver, S. (1997) "Design and Construction of a Model of a Mine Refrigeration Plant as a Testbed for intelligent Control Techniques", dissertation for the degree of Master of Science in Engineering, University of the Witwatersrand.

Peacock, S. (1995), "Predicting physical properties of factory juices and syrups", *Int. Sugar Jnl.*, Vol 97, No 1162, pp. 571-577.

Peacock, S.D., (1998), "An Introduction to Neural Networks and their Application in the Sugar Industry", *Proc S Afr Sug Technol Ass* (1998), vol. 72, pp. 184-191.

Peacock, S.D., and Starzak, M., (1996), "Modelling of Climbing Film Evaporators", *Proc S Afr Sug Technol Ass* (1996), vol. 70, pp. 213-219.

Peacock, S.D., and Starzak, M., (1997), "A Simplified Model of a Climbing Film Evaporator and its Practical Application", *Proc S Afr Sug Technol Ass* (1997), vol. 71, pp. 217-225.

Perry, R.H., Green, D.W., and Maloney, J.O., (1997) "Perry's Chemical Engineer's Handbook", 7th edition, McGraw Hill Book Company, New York, 1997.

Prett, D.M. and Gillette, R.D., (1979), "Optimization and constrained multivariable control of a catalytic cracking unit.", *AIChE National Mtg*, Houston, Texas.

Qin, S.J., and Badgwell, T. A., (1997), "An Overview of Industrial Model Predictive Control Technology", *AIChE Symp. Ser.* No 316, Vol. 93, Proc., Fifth Int. Conf. on Proc. Control., Jan 7-12, 1996, pp. 232-256.

Rawlings, J.B., Meadows, E.S., and Muske, K.R. (1994), "Non linear model predictive control : a tutorial and survey." *IFAC Symposium on Advanced Control of Chemical Processes* pp. 203-214.

Radford, D.J., and Cox, M.G.S., (1986), "The Use of Electrical Properties Measured at Radio Frequencies for Pan Boiling and Brix Control", *Proc S Afr Sug Technol Ass* (1986), vol. 60, pp. 94-102.

Redelinghuys, D., and Stothert, A., (1995), "The myth-application of Fuzzy Logic", *Quantum*, June '95, pp. 16-20.

Rhodes, C., and Morari, M., (1998), "Determining the model order of nonlinear input output systems", *AIChE journal*, January 1998, Vol 44, No. 1, pp. 151-163.

Richalet, J., Rault, A., Testud, J.L. and Papon, J. (1978), "Model Predictive Heuristic Control: Applications to industrial processes", *Automatica*, Vol 14, pp. 413-428.

Ricker, N.L., and Sewell, T., (19- -), " Dynamics of Multiple Effect Evaporators: Computer Simulation and Plant Tests", *AIChE Symp. Ser.* No 232, Vol. 80, Forest Products, pp. 87-94.

Rosier, M.A., (1982), "Model to predict the precipitation of burkeite in the multiple-effect evaporator and techniques for controlling scaling", *Tappi Journal*, Vol. 80, No. 4, pp 203-209.

Rousset, F., Saincir, Y., and Daclin, M., (1989), "Automatic Process Control of Multiple Effect Evaporation. Part I: Conditions for Static and Dynamic Equilibrium", *Zukerind.*, Vol. 114, No. 4, pp. 323-328.

Rousset, F., Saincir, Y., and Daclin, M., (1989), "Automatic Process Control of Multiple Effect Evaporation. Part II: Practical Realisation and Results", *Zukerind.*, Vol. 114, No. 6, pp. 470-476.

Sugar Milling Research Institute (SMRI), (1999), "Final Annual Report", *personal communication*.

Singh, I., Riley, R., and Seiller, D., (1997), "Using Pinch Technology to Optimize Evaporator and Vapour Bleed Configuration at the Malelane Mill", *Proc S Afr Sug Technol Ass* (1997), vol. 71, pp. 207-216.

Smith, I.A., and Taylor, L.A.W., (1981), "Some Data on Heat Transfer in Multiple Effect Evaporators", *Proc S Afr Sug Technol Ass* (1981), vol. 55, pp. 51-55.

Soroush, M., (1998), "State and parameter estimations and their applications in process control", *Computers and Chemical Engineering*, Vol. 23, pp. 229-245, Elsevier Science Ltd.

Swartz, C.L.E. (1995) "An Algorithm for Hierarchical Supervisory control", *Computers in Chemeng*, Vol. 19, No. 11 pp. 1173-1180.

To, L.C., Tade, M.O., and Le Page, G.P., (1998), "Implementation of a differential geometric nonlinear controller on an industrial evaporator system", *Control Engineering Practice*, 6, pp. 1306-1319.

Tse Chi Sum, S., and Wong Sak Hoi, L., (1996), "Estimation of Sucrose Inversion in Evaporators", *Proc S Afr Sug Technol Ass* (1996), vol. 70, pp. 236-240.

Tunstel, E., Hockemeier, S., and Jamshidi, M., (1994), "Fuzzy Control of a Hovercraft Platform", *Engng. Applic. Artif. Intell.*, Vol. 7, No. 5, pp. 513-519, Elsevier Science Ltd.

Valluri, S., Soroush, M., and Nikravesh, M., (1998), "Shortest prediction horizon non linear model predictive control", *Chemical Engineering Science* vol 53 no 2 pp 273-292.

Vukov, K. (1965), "Kinetic aspects of sucrose hydrolysis" *Int Sug J*, pp. 172-175.

Walthew, D.C., and Whitelaw, R.W., (1996), "Factors Affecting the Performance of Long Tube Climbing Film Evaporators", *Proc S Afr Sug Technol Ass* (1996), vol. 70, pp. 221-224.

Wang, F.Y., and Cameron, I.T., (1994), "Control studies on a model evaporation process – constrained state driving with conventional and higher relative degree systems", *J. Proc. Cont.*, Vol 4, No 2, pp. 59-75.

White, D.C., (1998), " Online Optimization: What have we learned?", *Hydrocarbon processing*, June 1998, pp. 55-59.

Zain, O.S., and Kumar, S., (1996), "Simulation of a Multiple Effect Evaporator for Concentrating Caustic Soda Solution - Computational Aspects", *Journal of Chemical Engineering of Japan*, Vol. 29, No. 5, pp. 889-893.

Chapter 8 APPENDICES

Appendix A - Mathematical Derivations and Calculation Methods

A.1 Derivation of the LQG Level Controller

[After Love, (1999)]

The standard plant representation for LQG control is the state space model :

$$\dot{x} = Ax + Bu \tag{A.1}$$

$$y = Cx \tag{A.2}$$

and the objective function is of the form :

$$\min_u J = \int_0^\infty \left(y^T Qy + u^T Ru\right)dt \tag{A.3}$$

The solution to this problem is

$$u = Kx \tag{A.4}$$

where the gain matrix K is given by :

$$K = R^{-1}B^T P \tag{A.5}$$

and P is the solution to the Riccati equation :

$$-\left(PA + A^T P\right) - C^T QC + PBR^{-1}B^T P = 0 \tag{A.6}$$

In this case, let the states x be :

$$x = \begin{bmatrix} x_1 \\ x_2 \end{bmatrix} = \begin{bmatrix} Q_o' \\ h' \end{bmatrix} \tag{A.7}$$

where the embellishment ` denotes deviation variables.

By defining the rate of change of outlet flow as the input variable, u, the state derivatives would be given by :

$$\dot{x} = \begin{bmatrix} u \\ -\frac{1}{A_t} x_1 \end{bmatrix} \tag{A.8}$$

Thus the state space representation is given by :

$$\dot{x} = \begin{bmatrix} \dot{x}_1 \\ \dot{x}_2 \end{bmatrix} = \begin{bmatrix} 0 & 0 \\ -\frac{1}{A_t} & 0 \end{bmatrix} \cdot \begin{bmatrix} x_1 \\ x_2 \end{bmatrix} + \begin{bmatrix} 1 \\ 0 \end{bmatrix} \cdot u \tag{A.9}$$

and

$$y = \begin{bmatrix} 0 & 1 \end{bmatrix} \cdot \begin{bmatrix} x_1 \\ x_2 \end{bmatrix} \tag{A.10}$$

Now, writing matrix P in terms of its elements :

$$P = \begin{bmatrix} P_{11} & P_{12} \\ P_{21} & P_{22} \end{bmatrix} \tag{A.11}$$

the Riccati equation, equation (A.6), can be solved analytically to yield :

$$P = \begin{bmatrix} \frac{(4QR^3)^{1/4}}{\sqrt{A_t}} & -\sqrt{QR} \\ -\sqrt{QR} & (4Q^3R)^{1/4}\sqrt{A_t} \end{bmatrix} \tag{A.12}$$

which can be substituted back into equation (A.5) to calculate the gain matrix, K, with the further substitution of the weighting factor, W, where $W = Q/R$:

$$K = \left[\left(\frac{4W}{A_t^2} \right)^{1/4} \quad -\sqrt{W} \right] \tag{A.13}$$

This can then be substituted into equation (A.4) to yield the solution for the manipulated input, u, the rate of change outlet flowrate :

$$u = \frac{dQ_o}{dt} = Kx = -\left(\frac{4W}{A_t^2} \right)^{1/4} \cdot \left(Q_o - Q_{sp} \right) + \sqrt{W} \cdot \left(h - h_{sp} \right) \tag{A.14}$$

which is integrated in the control algorithm to give the process input, flowrate, Q_o.

A.2 Derivation of the MPC Level Controller

[After Campo and Morari, (1989)]

The starting point for this derivation is the mass balance around the tank :

$$A\frac{dh}{dt} = Q_i - Q_o \tag{A.15}$$

which can be approximated by the discrete state equation at time $t = k+1$:

$$h(k+1) - h(k) = -\frac{\Delta t}{A}[Q_o(k) - Q_i(k)] \tag{A.16}$$

which can be rearranged to :

$$h(k+1) = h(k) - \frac{\Delta t}{A}[Q_o(k) - Q_i(k)] \tag{A.17}$$

Now, by extension, a similar equation at time $t = k+2$:

$$h(k+2) = h(k+1) - \frac{\Delta t}{A}[Q_o(k+1) - Q_i(k+1)] \tag{A.18}$$

which by substitution yields :

$$h(k+2) = h(k) - \frac{\Delta t}{A}[Q_o(k) - Q_i(k)] - \frac{\Delta t}{A}[Q_o(k+1) - Q_i(k+1)] \tag{A.19}$$

which can in turn be simplified to :

$$h(k+2) = h(k) - \sum_{i=0}^{1}\frac{\Delta t}{A}[Q_o(k+i) - Q_i(k+i)] \tag{A.20}$$

or, more generally, for the tank height at any future time, $t = k+l+1$:

$$h(k+l+1) = h(k) - \sum_{i=0}^{l} \frac{\Delta t}{A}\left[Q_o(k+i) - Q_i(k+i)\right] \tag{A.21}$$

and by assuming that future inflows remain constant, at current estimated value :

$$h(k+l+1) = h(k) + \frac{\Delta t}{A}(l+1)Q_i(k) - \sum_{i=0}^{l} \frac{\Delta t}{A}\left[Q_o(k+i)\right] \tag{A.22}$$

Then two constraints on tank level can be formulated together :
Tank level must not leave set limits within prediction horizon.
The tank level must return to setpoint at the end of the prediction horizon.

In equation form :
for $0<l<P$:

$$h_{\min} \le h(k+l+1) \le h_{\max} \tag{A.23}$$

and

$$h(k+P) = h_{set} \tag{A.24}$$

Now by defining the height, h, to designate level error, h_{max} and h_{min} now refer to the maximum allowable deviation above and below the setpoint h_{set}. Thus the constraint for any time $t = k+l+1$ is :

$$h_{\min} \le h(k) + \frac{\Delta t}{A}(l+1)Q_i(k) - \sum_{i=0}^{l} \frac{\Delta t}{A}\left[Q_o(k+i)\right] \le h_{\max} \tag{A.25}$$

which can be rewritten in matrix form for all times $0 <l<P$.

$$1_V h_{\min} \le 1_V h(k) + \frac{\Delta t}{A} n Q_i(k) - 1_L \frac{\Delta t}{A}\left[Q_o\right] \le 1_V h_{\max} \tag{A.26}$$

where, here :

$1_V \in \Re^{P\times 1}$ a column vector of ones.

$1_L \in \Re^{P\times P}$ a lower triangular matrix on ones.

$Q_o \in \Re^{P\times 1}$ a column vector of the next P outlet flowrates

The fixed endpoint condition is incorporated by modifying the equation thus :

$$\chi \le 1_V h(k) + \frac{\Delta t}{A} n Q_i(k) - 1_L \frac{\Delta t}{A}[Q_o] \le \delta \tag{A.27}$$

where :

$$\chi \in \Re^{P\times 1} = \begin{bmatrix} 1 \\ 1 \\ \vdots \\ 1 \\ 0 \end{bmatrix} h_{\min}$$

and

$$\delta \in \Re^{P\times 1} = \begin{bmatrix} 1 \\ 1 \\ \vdots \\ 1 \\ 0 \end{bmatrix} h_{\max}$$

A useful extension of this derivation, which was used in this investigation, is for the case where the change in outlet flowrate is chosen as opposed to the actual total outlet flowrate. In that case, the constraint equation becomes :

$$\chi \le 1_V h(k) + \frac{\Delta t}{A} n Q_i(k) - H \frac{\Delta t}{A}[\Delta Q_o] - 1_L \frac{\Delta t}{A} Q_o(k) \le \delta \tag{A.28}$$

here :

$$H = \begin{bmatrix} 1 & 0 & \cdots & \cdots & 0 \\ 2 & 1 & \ddots & & \vdots \\ \vdots & 2 & \ddots & \ddots & \vdots \\ \vdots & \vdots & \ddots & 1 & 0 \\ P & \cdots & \cdots & 2 & 1 \end{bmatrix}$$

and

$\Delta Q_o \in \Re^{P\times 1}$ a column vector of the next P changes in outlet flowrates

A.3 Definition of Constraint Matrices used in DMC Formulations

[Chapter 4]

For Alternative 1, constraints were included as follows :

$$C\Delta u \leq D \tag{A.29}$$

where

$$C = \begin{bmatrix} -I & 0 \\ 0 & -I \\ I & 0 \\ 0 & I \\ 1_L & 0 \\ 0 & 1_L \\ -TR & 0 \\ 0 & -TR \\ -SA_{11} & -SA_{12} \\ -SA_{21} & -SA_{22} \\ SA_{11} & SA_{12} \\ SA_{21} & SA_{22} \end{bmatrix} \qquad D = \begin{bmatrix} -1(\Delta u_1 \min) \\ -1(\Delta u_2 \min) \\ 1(\Delta u_1 \max) \\ 1(\Delta u_2 \max) \\ 1(u_1 \max - u_1) \\ 1(u_2 \max - u_2) \\ 1(u_1 - u_1 \min) \\ 1(u_2 - u_2 \min) \\ T(y_1 - y_1 \min) \\ T(y_2 - y_2 \min) \\ T(y_1 \max - y_1) \\ T(y_2 \max - y_1) \end{bmatrix}$$

and

$$\Delta u \in \Re^{2M} = \begin{bmatrix} \Delta u_1(k+1) \\ \Delta u_1(k+2) \\ \vdots \\ \Delta u_1(k+M) \\ \Delta u_2(k+1) \\ \Delta u_2(k+2) \\ \vdots \\ \Delta u_2(k+M) \end{bmatrix}$$

$$I \in \Re^{M \times M} = \begin{bmatrix} 1 & & 0 \\ & \ddots & \\ 0 & & 1 \end{bmatrix} \quad \text{the identity matrix}$$

$$1_L \in \Re^{M\times M} = \begin{bmatrix} 1 & & 0 \\ \vdots & \ddots & \\ 1 & \cdots & 1 \end{bmatrix} \quad \text{a lower triangular matrix}$$

$$S = \begin{bmatrix} S_0 \\ S_1 \end{bmatrix}$$

where

$S_0 \in \Re^{L\times M}$ a matrix of zeros

$S_1 \in \Re^{(P-L)\times M}$ a matrix of ones

A_{ij} = step response coefficient matrices, as defined in chapter 4.

$$1 \in \Re^{M\times 1} = \begin{bmatrix} 1 \\ \vdots \\ 1 \end{bmatrix} \quad \text{a matrix of ones.}$$

$$0 \in \Re^{M\times M} = \begin{bmatrix} 0 & & 0 \\ & \ddots & \\ 0 & & 0 \end{bmatrix} \quad \text{the zero matrix}$$

$$T = \begin{bmatrix} T_0 \\ T_1 \end{bmatrix}$$

where

$T_0 \in \Re^{L\times 1}$ a column vector of zeros

$T_1 \in \Re^{(P-L)\times 1}$ a column vector of ones

For Alternative 2, constraints were included as follows :

$$C\begin{bmatrix}\mu\\ \Delta u\end{bmatrix} \leq D \tag{A.30}$$

where :

$$C = \begin{bmatrix}
-1 & -I & 0_{M\times M} & 0_{M\times M} & 0_{M\times M} & 0_{M\times M}\\
-1 & 0_{M\times M} & -I & 0_{M\times M} & 0_{M\times M} & 0_{M\times M}\\
-1 & 0_{M\times M} & 0_{M\times M} & -I & 0_{M\times M} & 0_{M\times M}\\
0 & 0_{M\times M} & 0_{M\times M} & 0_{M\times M} & -I & 0_{M\times M}\\
0 & 0_{M\times M} & 0_{M\times M} & 0_{M\times M} & 0_{M\times M} & -I\\
-1 & I & 0_{M\times M} & 0_{M\times M} & 0_{M\times M} & 0_{M\times M}\\
-1 & 0_{M\times M} & I & 0_{M\times M} & 0_{M\times M} & 0_{M\times M}\\
-1 & 0_{M\times M} & 0_{M\times M} & I & 0_{M\times M} & 0_{M\times M}\\
0 & 0_{M\times M} & 0_{M\times M} & 0_{M\times M} & I & 0_{M\times M}\\
0 & 0_{M\times M} & 0_{M\times M} & 0_{M\times M} & 0_{M\times M} & I\\
0 & 1_L & 0_{M\times M} & 0_{M\times M} & 0_{M\times M} & 0_{M\times M}\\
0 & 0_{M\times M} & 1_L & 0_{M\times M} & 0_{M\times M} & 0_{M\times M}\\
0 & 0_{M\times M} & 0_{M\times M} & 1_L & 0_{M\times M} & 0_{M\times M}\\
0 & 0_{M\times M} & 0_{M\times M} & 0_{M\times M} & 1_L & 0_{M\times M}\\
0 & 0_{M\times M} & 0_{M\times M} & 0_{M\times M} & 0_{M\times M} & 1_L\\
0 & -1_L & 0_{M\times M} & 0_{M\times M} & 0_{M\times M} & 0_{M\times M}\\
0 & 0_{M\times M} & -1_L & 0_{M\times M} & 0_{M\times M} & 0_{M\times M}\\
0 & 0_{M\times M} & 0_{M\times M} & -1_L & 0_{M\times M} & 0_{M\times M}\\
0 & 0_{M\times M} & 0_{M\times M} & 0_{M\times M} & -1_L & 0_{M\times M}\\
0 & 0_{M\times M} & 0_{M\times M} & 0_{M\times M} & 0_{M\times M} & -1_L\\
0 & -SA_{11} & -SA_{12} & -SA_{13} & -SA_{14} & -SA_{15}\\
0 & -SA_{21} & -SA_{22} & -SA_{23} & -SA_{24} & -SA_{25}\\
0 & H & H & H & 0_{M\times M} & 0_{M\times M}\\
0 & SA_{11} & SA_{12} & SA_{13} & SA_{14} & SA_{15}\\
0 & SA_{21} & SA_{22} & SA_{23} & SA_{24} & SA_{25}\\
0 & H & H & H & 0_{M\times M} & 0_{M\times M}
\end{bmatrix}
\qquad
D = \begin{bmatrix}
0\\ 0\\ 0\\
-1(\Delta u_4 \min)\\
-1(\Delta u_5 \min)\\
0\\ 0\\ 0\\
1(\Delta u_4 \max)\\
1(\Delta u_5 \max)\\
1(u_1 \max - u_1)\\
1(u_2 \max - u_2)\\
1(u_3 \max - u_3)\\
1(u_4 \max - u_4)\\
1(u_5 \max - u_5)\\
1(u_1 - u_1 \min)\\
1(u_2 - u_2 \min)\\
1(u_3 - u_3 \min)\\
1(u_4 - u_4 \min)\\
1(u_5 - u_5 \min)\\
T(y_1 - y_1 \min)\\
T(y_2 - y_2 \min)\\
F\\
T(y_1 \max - y_1)\\
T(y_2 \max - y_2)\\
G
\end{bmatrix}$$

and

$$\Delta u \in \Re^{5M} = \begin{bmatrix} \Delta u_1(k+1) \\ \Delta u_1(k+2) \\ \vdots \\ \Delta u_1(k+M) \\ \Delta u_2(k+1) \\ \Delta u_2(k+2) \\ \vdots \\ \Delta u_5(k+M) \end{bmatrix}$$

$$I \in \Re^{M \times M} = \begin{bmatrix} 1 & & 0 \\ & \ddots & \\ 0 & & 1 \end{bmatrix} \quad \text{the identity matrix}$$

$$1_L \in \Re^{M \times M} = \begin{bmatrix} 1 & & 0 \\ \vdots & \ddots & \\ 1 & \cdots & 1 \end{bmatrix} \quad \text{a lower triangular matrix}$$

$$S = \begin{bmatrix} S_0 \\ S_1 \end{bmatrix}$$

where

$S_0 \in \Re^{L \times M}$ a matrix of zeros

$S_1 \in \Re^{(P-L) \times M}$ a matrix of ones

A_{ij} = step response coefficient matrices, as defined in chapter 4.

$$1 \in \Re^{M \times 1} = \begin{bmatrix} 1 \\ \vdots \\ 1 \end{bmatrix} \quad \text{a column vector of ones.}$$

$$T = \begin{bmatrix} T_0 \\ T_1 \end{bmatrix}$$

where

$T_0 \in \Re^{L\times 1}$ a column vector of zeros

$T_1 \in \Re^{(P-L)\times 1}$ a column vector of ones

$$H = \begin{bmatrix} 1 & 0 & \cdots & \cdots & 0 \\ 2 & 1 & \ddots & & \vdots \\ \vdots & 2 & \ddots & \ddots & \vdots \\ \vdots & \vdots & \ddots & 1 & 0 \\ M & \cdots & \cdots & 2 & 1 \end{bmatrix} \left(\frac{\Delta t}{Area}\right)$$

$$0_{M\times M} \in \Re^{M\times M} = \begin{bmatrix} 0 & & 0 \\ & \ddots & \\ 0 & & 0 \end{bmatrix}$$ the zero matrix

$$0 \in \Re^{M\times 1} = \begin{bmatrix} 0 \\ \vdots \\ 0 \end{bmatrix}$$ a column vector of zeros.

$$F \in \Re^{M\times 1} = \left[-\chi + n\frac{\Delta t}{A}d(k) + 1h(k) + 1_L\frac{\Delta t}{A}(Q_o(k-1))\right], \text{ and}$$

$$G \in \Re^{M\times 1} = \left[\delta - n\frac{\Delta t}{A}d(k) - 1h(k) - 1_L\frac{\Delta t}{A}(Q_o(k-1))\right]$$

(as described in the derivation of MPC control, above, (Campo and Morari, 1989))

A.4 Design of the Condensate Flowmeter

[From Love (1999) after Heller (1980)]

The equation governing the flowrate of liquid through multiple orifices of this type is:

$$q = CA(2g)^{0.5}\left[(h-R_0)^{0.5} + (h-R_1)^{0.5} + (h-R_2)^{0.5} \ldots + (h-R_N)^{0.5}\right] \quad \text{(A.31)}$$

where q = the flowrate of condensate through the flowmeter.
C = the discharge coefficient of liquid through the orifices.
A = the cross sectional area of the orifices.
h = the height of liquid in the measurement arm.
g = acceleration due to gravity
R_i, = the height of the I^{th} hole above the level of the first set of holes R_0.

Which is solved by setting h = the height of each preceding orifice, and then solving for a linear relationship, relative to the spacing of the first two holes, which is thus defined as unity. When the liquid level in the measurement arm has risen to the level of the second hole (R_1), the flowrate of condensate will be given by equation (A.32).

Ignoring holes above R_1., and by substitution into equation (A.31):

$$q = CA(2g)^{0.5}\left[(h-R_0)^{0.5}\right] \quad \text{(A.32)}$$

For a linear relationship, we require $q = kh$, so now define :

$R_0 = 0$ as a reference for the other levels.

and

$h = R_1 = 1$ to give a convenient relative height to the other hole heights which follow.

Then, by substitution into equation (A.32) :

$$k = CA(2g)^{0.5} \quad \text{(A.33)}$$

Similarly, at the height of the third hole, (R_2):

$$q = CA(2g)^{0.5}\left[(h-R_0)^{0.5} + (h-R_1)^{0.5}\right] = kh \qquad \text{(A.34)}$$

here,

$R_0 = 0$

$R_1 = 1$ and

$h = R_2$

Now, equation (A.34) can easily be solved to give R_2 = 3.339. The same procedure is then followed to arrive at the heights of the other orifices. Usually at least 10 heights are used, in order to provide as linear a relationship as possible between liquid height flowrate.

The range of flowrates that must be measured by the flowmeter was then chosen. With this range in mind, it was necessary to choose the orifice diameter, or more specifically, the cross sectional area, in order to ensure that the range of flowrates corresponds to a wide range of liquid heights in the measurement arm. For example if the expected range of flowrates is 0 – 70 tph, an orifice diameter should be chosen so that a full measurement arm corresponds to about 80 tph of condensate.

In the case of the condensate flowmeters constructed at Triangle, the orifice diameter required to allow sufficient flowrate through the meter was too large for the orifices to be placed singly. It was decided to divide the required orifice area up into four equal orifices, which were then drilled equidistantly around the circumference of the inner pipe, at the correct height.

Calculation of the heat transfer coefficient :

The reading of condensate flowrate may then be converted to yield the heat transfer coefficient applicable to that vessel.

This was done using steady-state relationships. The inputs required for this calculation are the pressures of the heating steam, and evolved vapour, the flowrate of condensate, and the average Brix of the juice in the vessel (can be taken as a seasonal average).

At steady state, the flowrate of condensate must equal the flowrate of steam into the calandria:

$$F_{ST} = F_C \tag{A.35}$$

and the amount of heat transferred is equal to the flowrate of condensing steam multiplied by the specific latent heat of condensation :

$$Q = F_{ST} \times \Delta H_{Vap,ST} \tag{A.36}$$

where :

$\Delta H_{Vap,\,ST}$ heat of vapourisation (condensation) of the steam, is a function of the input P_{ST} (Section 3.2)

Assuming saturated steam, the temperature of the heating steam is related to the steam pressure P_{ST} (Section 3.2) :

$$T_{ST} = fn(P_{ST}) \tag{A.37}$$

and similarly the temperature of the evolved vapour is related to the vapour pressure :

$$T_{Vap} = fn(P_{Vap}) \tag{A.38}$$

The juice temperature may then be related to the vapour temperature by equation (A.39) :

$$T_{J,out} = T_{Vap} + B.P.E. \tag{A.39}$$

where :

B.P.E. (Boiling Point Elevation) is a function of Bx_{out}, $T_{J,out}$, and vessel dimensions. (Section 3.2)

Finally the heat transfer coefficient, U, may be calculated from the heat transferred, Q, and the previously calculated variables :

$$U = \frac{Q}{A\left(T_{ST} - T_{J,out}\right)} \tag{A.40}$$

Appendix B - Listing of Control Algorithm Codes

B.1 Function File for the DMC Brix / Level Controller, Alternative 2.

```
%==========================================================================
function [sys,x0,str,ts] = sfcfun3(t,x,u,flag,M)
global P ATOT;

%%First set the move, steady state, and prediction horizons.
M = M;
N = M*4;
P = N+M;

%%Then load the step response data, which is stored in workspace DMCA, in matrix, A.
load DMCA
DMA = A;

for i = 1:N
        DMAguess(i,:) = DMA(N-i+1,:);
end

%% Construct the dynamic matrix, ATOT for prediction of future outputs, and matrix BTOT, for
predicting the effect of past inputs.

for i = 1:M;
        A11(:,i) = [zeros((i-1),1);DMA(1:(N),1);ones((P-N-i+1),1).*DMA(N,1)];
        A12(:,i) = [zeros(P,1)];
        A13(:,i) = [zeros((i-1),1);(DMA(1:(N),1)./2);ones((P-N-i+1),1).*(DMA(N,1)/2)];
        A14(:,i) = [zeros((i-1),1);DMA(1:(N),2);ones((P-N-i+1),1).*DMA(N,2)];
        A15(:,i) = [zeros(P,1)];
        A16(:,i) = [zeros((i-1),1);DMA(1:(N),3);ones((P-N-i+1),1).*DMA(N,3)];
        A17(:,i) = [zeros((i-1),1);DMA(1:(N),4);ones((P-N-i+1),1).*DMA(N,4)];
        A18(:,i) = [zeros((i-1),1);DMA(1:(N),5);ones((P-N-i+1),1).*DMA(N,5)];
        A19(:,i) = [zeros((i-1),1);DMA(1:(N),6);ones((P-N-i+1),1).*DMA(N,6)];
        A110(:,i) = [zeros(P,1)];

        A21(:,i) = [zeros(P,1)];
        A22(:,i) = [zeros((i-1),1);DMA(1:(N),1);ones((P-N-i+1),1).*DMA(N,1)];
```

```
        A23(:,i) = [zeros((i-1),1);(DMA(1:(N),1)./2);ones((P-N-i+1),1).*(DMA(N,1)/2)];
        A24(:,i) = [zeros(P,1)];
        A25(:,i) = [zeros((i-1),1);DMA(1:(N),2);ones((P-N-i+1),1).*DMA(N,2)];
        A26(:,i) = [zeros((i-1),1);DMA(1:(N),3);ones((P-N-i+1),1).*DMA(N,3)];
        A27(:,i) = [zeros((i-1),1);DMA(1:(N),4);ones((P-N-i+1),1).*DMA(N,4)];
        A28(:,i) = [zeros((i-1),1);DMA(1:(N),5);ones((P-N-i+1),1).*DMA(N,5)];
        A29(:,i) = [zeros(P,1)];
        A210(:,i) = [zeros((i-1),1);DMA(1:(N),6);ones((P-N-i+1),1).*DMA(N,6)];
end

AD = [A16 A17 A18 A19 A110;
          A26 A27 A28 A29 A210];
ATOT = [A11 A12 A13 A14 A15;
          A21 A22 A23 A24 A25];

for i = 1:N;
    B11(i,:) = [ones(1,(i-1)).*DMAguess(1,1) DMAguess(1:(N-i+1),1)'];
    B12(i,:) = [zeros(1,N)];
    B13(i,:) = [ones(1,(i-1)).*(DMAguess(1,1)/2) (DMAguess(1:(N-i+1),1)./2)'];
    B14(i,:) = [ones(1,(i-1)).*DMAguess(1,2) DMAguess(1:(N-i+1),2)'];
    B15(i,:) = [zeros(1,N)];
    B16(i,:) = [ones(1,(i-1)).*DMAguess(1,3) DMAguess(1:(N-i+1),3)'];
    B17(i,:) = [ones(1,(i-1)).*DMAguess(1,4) DMAguess(1:(N-i+1),4)'];
    B18(i,:) = [ones(1,(i-1)).*DMAguess(1,5) DMAguess(1:(N-i+1),5)'];
    B19(i,:) = [ones(1,(i-1)).*DMAguess(1,6) DMAguess(1:(N-i+1),6)'];
    B110(i,:) = [zeros(1,N)];

    B21(i,:) = [zeros(1,N)];
    B22(i,:) = [ones(1,(i-1)).*DMAguess(1,1) DMAguess(1:(N-i+1),1)'];
    B23(i,:) = [ones(1,(i-1)).*(DMAguess(1,1)/2) (DMAguess(1:(N-i+1),1)./2)'];
    B24(i,:) = [zeros(1,N)];
    B25(i,:) = [ones(1,(i-1)).*DMAguess(1,2) DMAguess(1:(N-i+1),2)'];
    B26(i,:) = [ones(1,(i-1)).*DMAguess(1,3) DMAguess(1:(N-i+1),3)'];
    B27(i,:) = [ones(1,(i-1)).*DMAguess(1,4) DMAguess(1:(N-i+1),4)'];
    B28(i,:) = [ones(1,(i-1)).*DMAguess(1,5) DMAguess(1:(N-i+1),5)'];
    B29(i,:) = [zeros(1,N)];
    B210(i,:) = [ones(1,(i-1)).*DMAguess(1,6) DMAguess(1:(N-i+1),6)'];
end
```

```
B11(((N+1):P),(1:N)) = [ones((P-N),N).*DMAguess(1,1)];
B12(((N+1):P),(1:N)) = [zeros((P-N),N)];
B13(((N+1):P),(1:N)) = [ones((P-N),N).*(DMAguess(1,3)/2)];
B14(((N+1):P),(1:N)) = [ones((P-N),N).*DMAguess(1,2)];
B15(((N+1):P),(1:N)) = [zeros((P-N),N)];
B16(((N+1):P),(1:N)) = [ones((P-N),N).*DMAguess(1,3)];
B17(((N+1):P),(1:N)) = [ones((P-N),N).*DMAguess(1,4)];
B18(((N+1):P),(1:N)) = [ones((P-N),N).*DMAguess(1,5)];
B19(((N+1):P),(1:N)) = [ones((P-N),N).*DMAguess(1,6)];
B110(((N+1):P),(1:N)) = [zeros((P-N),N)];

B21(((N+1):P),(1:N)) = [zeros((P-N),N)];
B22(((N+1):P),(1:N)) = [ones((P-N),N).*DMAguess(1,1)];
B23(((N+1):P),(1:N)) = [ones((P-N),N).*(DMAguess(1,3)/2)];
B24(((N+1):P),(1:N)) = [zeros((P-N),N)];
B25(((N+1):P),(1:N)) = [ones((P-N),N).*DMAguess(1,2)];
B26(((N+1):P),(1:N)) = [ones((P-N),N).*DMAguess(1,3)];
B27(((N+1):P),(1:N)) = [ones((P-N),N).*DMAguess(1,4)];
B28(((N+1):P),(1:N)) = [ones((P-N),N).*DMAguess(1,5)];
B29(((N+1):P),(1:N)) = [zeros((P-N),N)];
B210(((N+1):P),(1:N)) = [ones((P-N),N).*DMAguess(1,6)];

BTOT = [B11 B12 B13 B14 B15 B16 B17 B18 B19 B110;
        [[B21 B22 B23 B24 B25 B26 B27 B28 B29 B210]]];

switch flag,

% Initialization %
case 0,
  [sys,x0,str,ts]=mdlInitializeSizes(M,N,P);

% Derivatives %
case 1,
  sys=mdlDerivatives(t,x,u);

% Update %
case 2,
  sys=mdlUpdate(t,x,u,M,N,P,AD,BTOT)
```

```
% Outputs %
case 3,
   sys=mdlOutputs(t,x,u,M,N,P);

% GetTimeOfNextVarHit %
case 4,
   sys=mdlGetTimeOfNextVarHit(t,x,u);

% Terminate %
case 9,
   sys=mdlTerminate(t,x,u);

% Unexpected flags %
otherwise
   error(['Unhandled flag = ',num2str(flag)]);
end

% end sfuntmpl

%=============================================================================
% mdlInitializeSizes
% Return the sizes, initial conditions, and sample times for the S-function.
%=============================================================================
function [sys,x0,str,ts]=mdlInitializeSizes(M,N,P)

sizes = simsizes;
sizes.NumContStates  = 0;
sizes.NumDiscStates  = (10*N+9);%720; 6*moves+2 total inputs + 2 states(brix,flow);
sizes.NumOutputs     = 14;
sizes.NumInputs      = 14;
sizes.DirFeedthrough = 1;
sizes.NumSampleTimes = 1;   % at least one sample time is needed

sys = simsizes(sizes);

% initialize the initial conditions
x0  = [zeros((10*N),1);180;180;180;50;50;68;68;50;0];
%%Number of input move parameters: Flow,V2Val,T,Bx,PS,P5;
```

```
% str is always an empty matrix
str = [];

% initialize the array of sample times
ts  = [1 0];

% end mdlInitializeSizes

%=============================================================================
% mdlDerivatives
% Return the derivatives for the continuous states.
%=============================================================================
function sys=mdlDerivatives(t,x,u)

sys = [];

% end mdlDerivatives

%=============================================================================
% mdlUpdate
% Handle discrete state updates, sample time hits, and major time step
% requirements.
%=============================================================================
function sys=mdlUpdate(t,x,u,M,N,P,AD,BTOT)

global Ydev ATOT ratioBC FL;

Yset = [(ones(P,1).*u(9))' (ones(P,1).*u(10))'];
Disturb = [u(1) zeros(1,(M-1)) u(2) zeros(1,(M-1)) u(3) zeros(1,(M-1))
                                u(4) zeros(1,(M-1))  u(5)  zeros(1,(M-1))];
Ypast = BTOT * [x(1:(10*N))];
dev = [[ones(1,P).*u(6) ones(1,P).*u(7)]' - [ones(1,P).*Ypast(1) ones(1,P).*Ypast(P+1)]'];
Be = Ypast + dev + AD * [Disturb]';  %%2*Pby1
Ydev = Yset - Be;  %%2*Pby1

%% Now using the MRCO approach of Campo and Morari (1989) to control the level.
hset = u(11);
```

```
x(10*N+8) = u(8);
T = (1/60);
Area = 38.4845*(6.83/100);
h = x(10*N+8) - hset;
qopast = x(10*N+1)+x(10*N+2)+x(10*N+3);

dfut = (Area/T)*(h - x(10*N+9) + (T/Area)*(x(10*N+1)+x(10*N+2)+x(10*N+3)));
%%this is now %*(m/%)*(m^2)/(mins)*(60mins/h) = tph

qomin = 0;
qomax = 300;
hmin = hset - 100;  % NB - important that we are dealing with height deviation here;
hmax = 100 - hset;

FLA = x(10*N+1);
FLB = x(10*N+2);
FLC = x(10*N+3);
FL = [FLA FLB FLC];
FLav = (FLA+FLB+FLC)/3;

guess = (2*(dfut-qopast)/(M+1)+2*(Area/(T*M*(M+1))*(h)))/3;
guess = [guess*FLA/FLav guess*FLB/FLav guess*FLC/FLav];

muqo0 = [abs(max(guess));ones(M,1)*guess(1);ones(M,1)*guess(2);ones(M,1)*guess(3)];
dU0 = [muqo0;zeros(2*M,1)];  %%Starting guess;  %%2M+1by1

Umin = [0 0 0 0 0];
Umax = [300 300 300 100 100];

DUmin = [zeros(3*M,1);ones(2*M,1).*(-20)];  %%%%2*M+1by1
DUmax = [zeros(3*M,1);ones(2*M,1).*20];

Ymin = [ones(2*P,1).*40;ones(P,1).*0];%% 55 to 72
Ymax = [ones(2*P,1).*80;ones(P,1).*300];

n = [1:1:M]';
een = ones(M,1);
H = tril(ones(M,M)).*(T/Area);
```

```
for i = 1:M;
        HJesu(:,i) = [zeros((i-1),1);(1:1:(M-i+1))'];
end;

HJesu = HJesu.*(T/Area);
alph = een.*qomin;
bet = een.*qomax;
gamm = [ones((M-1),1);0].*hmin;
delt = [ones((M-1),1);0].*hmax;

AA = [zeros(10*M,1) [(tril(ones(M,M)).*(1)) zeros(M,M) zeros(M,M) zeros(M,M);
        zeros(M,M) (tril(ones(M,M)).*(1)) zeros(M,M) zeros(M,M) zeros(M,M);
        zeros(M,M) zeros(M,M) (tril(ones(M,M)).*(1)) zeros(M,M) zeros(M,M);
        zeros(M,M) zeros(M,M) zeros(M,M) (tril(ones(M,M)).*(1)) zeros(M,M);
        zeros(M,M) zeros(M,M) zeros(M,M) zeros(M,M) (tril(ones(M,M)).*(1));
        (tril(ones(M,M)).*(-1)) zeros(M,M) zeros(M,M) zeros(M,M) zeros(M,M);
        zeros(M,M) (tril(ones(M,M)).*(-1)) zeros(M,M) zeros(M,M) zeros(M,M);
        zeros(M,M) zeros(M,M) (tril(ones(M,M)).*(-1)) zeros(M,M) zeros(M,M);
        zeros(M,M) zeros(M,M) zeros(M,M) (tril(ones(M,M)).*(-1)) zeros(M,M);
        zeros(M,M) zeros(M,M) zeros(M,M) zeros(M,M) (tril(ones(M,M)).*(-1))]];

ba = [(Umax(1)-x(10*N+1))*ones(M,1);
        (Umax(2)-x(10*N+2))*ones(M,1);
        (Umax(3)-x(10*N+3))*ones(M,1);
        (Umax(4)-x(10*N+4))*ones(M,1);
        (Umax(5)-x(10*N+5))*ones(M,1);
        (x(10*N+1) - Umin(1))*ones(M,1);
        (x(10*N+2) - Umin(2))*ones(M,1);
        (x(10*N+3) - Umin(3))*ones(M,1);
        (x(10*N+4) - Umin(4))*ones(M,1);
        (x(10*N+5) - Umin(5))*ones(M,1)];

AB = [[ones(3*M,1).*(-1);zeros(2*M,1)] [eye(5*M).*(-1)];
        [ones(3*M,1).*(-1);zeros(2*M,1)] [eye(5*M)]];
bb = [DUmin.*(-1);
        DUmax];
```

```
L=ceil(M/2);
Lp = P-L;

AC = [zeros(6*P,1) [[zeros(L,M*5);ones(Lp,M*5);zeros(L,M*5);ones(Lp,M*5);ones(P,M*5)].*...
        [(ATOT*(-1));[HJesu*(-1) HJesu*(-1) HJesu*(-1) zeros(M,M) zeros(M,M);zeros(N,M*5)]];
        [zeros(L,M*5);ones(Lp,M*5);zeros(L,M*5);ones(Lp,M*5);ones(P,M*5)].*...
        [[(ATOT)];[HJesu HJesu HJesu zeros(M,M) zeros(M,M);zeros(N,M*5)]]];
bc = [zeros(L,1);
        (Be(L+1:P)-Ymin(L+1:P));
        zeros(L,1);
        (Be(L+P+1:2*P)-Ymin(L+P+1:2*P));
        (delt - n.*(T/Area*dfut) - een.*h + H*(een*qopast));
        zeros(N,1);
        zeros(L,1);
        (Ymax(L+1:P)-Be(L+1:P));
        zeros(L,1);
        (Ymax(P+L+1:2*P)-Be(L+P+1:2*P));
        (gamm.*(-1) + n.*(T/Area*dfut) + een.*h - H*(een*qopast));
        zeros(N,1)];

ratioB = u(13)/u(12);
ratioC = u(14)/u(12);
ratioBC = [ratioB ratioC];

A = [AA;
     AB;
     AC;
    (-1) zeros(1,5*M)];

b = [ba;
     bb;
     bc;
     0];
B = b;

Aeq = [];
Beq = [];
lb = [];
```

```
ub = [];
nlcon = [];
options = optimset('fmincon');
options = optimset(options,'TolFun',1e-3,'TolX',1e-3,'TolCon',1e-3);%%'Display','iter');

dU = fmincon('DMCfun3',dU0,A,b,Aeq,Beq,lb,ub,nlcon,options);

xold = [x(1) x(N+1) x(2*N+1) x(3*N+1) x(4*N+1) x(5*N+1) x(6*N+1) x(7*N+1)
                x(8*N+1) x(9*N+1)];

x(1:(10*N-1)) = x(2:(10*N));
x(N) = dU(2);
x(2*N) = dU(M+2);
x(3*N) = dU(2*M+2);
x(4*N) = dU(3*M+2);
x(5*N) = dU(4*M+2);

x(6*N) = u(1);
x(7*N) = u(2);
x(8*N) = u(3);
x(9*N) = u(4);
x(10*N) = u(5);

x(10*N+1) = x(10*N+1) + dU(2);   %%TOTAL MOVE (Flow)
x(10*N+2) = x(10*N+2) + dU(M+2);
x(10*N+3) = x(10*N+3) + dU(2*M+2);
x(10*N+4) = x(10*N+4) + dU(3*M+2);
x(10*N+5) = x(10*N+5) + dU(4*M+2);

x(10*N+6) = (BTOT(1,:) * x(1:(10*N))) + dev(1)
                + xold * [BTOT(1,1) BTOT(1,(N+1)) BTOT(1,(2*N+1)) BTOT(1,(3*N+1))
                BTOT(1,(4*N+1)) BTOT(1,(5*N+1)) BTOT(1,(6*N+1)) BTOT(1,(7*N+1))
                BTOT(1,(8*N+1)) BTOT(1,(9*N+1))]';              %(NewState(Bx))

x(10*N+7) = (BTOT((P+1),:) * x(1:(10*N))) + dev(P+1) ...
        + xold * [BTOT((P+1),1) BTOT((P+1),(N+1)) BTOT((P+1),(2*N+1)) BTOT((P+1),(3*N+1))
        BTOT((P+1),(4*N+1))  BTOT((P+1),(5*N+1))  BTOT((P+1),(6*N+1))  BTOT((P+1),(7*N+1))
        BTOT((P+1),(8*N+1)) BTOT((P+1),(9*N+1))  ]';              %(NewState(Flow))
```

```
x(10*N+9) = h;

sys = [x];
% end mdlUpdate

%=============================================================================
% mdlOutputs
% Return the block outputs.
%=============================================================================
function sys=mdlOutputs(t,x,u,M,N,P);

sys = [x(N) x(2*N) x(3*N) x(4*N) x(5*N) x(10*N+1) x(10*N+2) x(10*N+3) x(10*N+4)
       x(10*N+5) x(10*N+6) x(10*N+7) x(10*N+8) x(10*N+9)];
% end mdlOutputs
%=============================================================================
% mdlGetTimeOfNextVarHit
% Return the time of the next hit for this block.  Note that the result is
% absolute time.  Note that this function is only used when you specify a
% variable discrete-time sample time [-2 0] in the sample time array in
% mdlInitializeSizes.
%=============================================================================
function sys=mdlGetTimeOfNextVarHit(t,x,u)

sampleTime = 1;
sys = t + sampleTime;

% end mdlGetTimeOfNextVarHit
%=============================================================================
% mdlTerminate
% Perform any end of simulation tasks.
%=============================================================================
function sys=mdlTerminate(t,x,u)

sys = [];
% end mdlTerminate
```

This file was used for the minimization :

```
function f = DMCfun3(dU)
global P ATOT Ydev ratioBC FL;

M = (size(dU,1) - 1)/5;

Q = [(eye(2*P).*3)];
R = [(eye(2*M).*1)];
S = [(eye(2).*(M*5))];
c = [M*25;zeros(3*M,1)];

f = (Ydev - (ATOT * dU(2:5*M+1)))' * Q * ...
    (Ydev - (ATOT * dU(2:5*M+1))) + ...
    [dU(3*M+2:5*M+1)]' * R * [dU(3*M+2:5*M+1)] + ...
    c' * dU(1:3*M+1);
```

B.2 Function File for the MPC Tank Level Controller

[Based on the MRCO approach of Campo and Morari (1989)]

```
%=============================================================================
function [sys,x0,str,ts] = sfcFlow1(t,x,u,flag,PFLOW)
% The following outlines the general structure of an S-function.
switch flag,
P = PFLOW;
% Initialization %
case 0,
  [sys,x0,str,ts]=mdlInitializeSizes(PFLOW);

% Derivatives %
case 1,
  sys=mdlDerivatives(t,x,u);

% Update %
case 2,
  sys=mdlUpdate(t,x,u,PFLOW);

% Outputs %
case 3,
  sys=mdlOutputs(t,x,u);

% GetTimeOfNextVarHit %
case 4,
  sys=mdlGetTimeOfNextVarHit(t,x,u);

% Terminate %
case 9,
  sys=mdlTerminate(t,x,u);

% Unexpected flags %
otherwise
  error(['Unhandled flag = ',num2str(flag)]);
end
% end sfuntmpl
```

```
%=============================================================================
% mdlInitializeSizes
% Return the sizes, initial conditions, and sample times for the S-function.
%=============================================================================
function [sys,x0,str,ts]=mdlInitializeSizes(PFLOW);
sizes = simsizes;
sizes.NumContStates  = 0;
sizes.NumDiscStates  = 7;  %hmodel. mu. qo, dhtmin1
sizes.NumOutputs     = 7;
sizes.NumInputs      = 3;
sizes.DirFeedthrough = 1;
sizes.NumSampleTimes = 1;   % at least one sample time is needed

sys = simsizes(sizes);

% initialize the initial conditions
x0  = [540 0 540 540 50 540 0];
%Total Fluid in (tph*mins),   %height dev.   %muqo(2) = qo decided,   %qopast;
%Actual tank height,   %Previous x(1) = Total Fluid in;

% str is always an empty matrix
str = [];

% initialize the array of sample times
ts  = [1 0];

% end mdlInitializeSizes

%=============================================================================
% mdlDerivatives
% Return the derivatives for the continuous states.
%=============================================================================
function sys=mdlDerivatives(t,x,u)
sys = [];

% end mdlDerivatives
```

```
%=============================================================================
% mdlUpdate
% Handle discrete state updates, sample time hits, and major time step
% requirements.
%=============================================================================
function sys=mdlUpdate(t,x,u,PFLOW);  %,ATOT,dUconst,Yset)

P = PFLOW;
hset = u(3);
x(5) = u(2);

T = (1/60);
Area = 38.4845*(6.83/100);
h = x(5) - hset;
qopast = x(6); %used to be u(3);

dfut = (Area/T)*(h - x(7) + (T/Area)*x(6));
%%this is now %*(m/%)*(m^2)/(mins)*(60mins/h) = tph

R0  = zeros(P,P);
R1 = eye(P,P);
R2((2:P),(1:(P-1))) = eye((P-1),(P-1)).*(-1);
R2(:,P) = zeros(P,1);
R = R0 + R1 + R2;

e1 = [1;zeros((P-1),1)];
n = [1:1:P]';
een = ones(P,1);
H = tril(ones(P,P)).*(T/Area);

qomin = 0;
qomax = 900;
hmin = hset - 100;% NB important that we are dealing with height deviation here;
hmax = 100 - hset;
alph = een.*qomin;
bet = een.*qomax;
gamm = [ones((P-1),1);0].*hmin;
delt = [ones((P-1),1);0].*hmax;
```

```
Amat = [(een*(-1)) R;...
        (een*(-1)) (R*(-1));...
        zeros(P,1) eye(P,P);...
        zeros(P,1) H;...
        zeros(P,1) (H*(-1))];

beeeta = [(e1*qopast - R*alph);...
        (e1*((-1)*qopast) + R*alph);...
        (bet - alph);...
        (gamm*(-1) + n*(T/Area*dfut) + een*h - H*alph);...
        (delt - n*(T/Area*dfut) - een*h + H*alph)];

global AT b;

AT = [Amat;
        (eye(P+1).*(-1))];
b = [beeeta;
        zeros((P+1),1)];
B = b;
options = optimset('fmincon');
guess = 2*(dfut-qopast)/(P+1)+2*(Area/(T*P*(P+1))*(h));
muqo0 = [(abs(guess));(n*guess)+qopast];
%Starting guess;[zeros(P+1,1)];

muqo = fmincon('DMCFLOW1',muqo0,AT,b,Aeq,Beq,lb,ub,nlcon,options);

x(7) = h;
x(6)= muqo(2);
x(1) = muqo(1)
x(2) = muqo(2);
x(3) = dfut;
x(4) = muqo(P+1);

sys = [x];
% end mdlUpdate
```

```
%=============================================================================
% mdlOutputs
% Return the block outputs.
%=============================================================================
function sys=mdlOutputs(t,x,u);

sys = [x];
% end mdlOutputs

%=============================================================================
% mdlGetTimeOfNextVarHit
% Return the time of the next hit for this block.  Note that the result is
% absolute time.  Note that this function is only used when you specify a
% variable discrete-time sample time [-2 0] in the sample time array in
% mdlInitializeSizes.
%=============================================================================
function sys=mdlGetTimeOfNextVarHit(t,x,u)

sampleTime = 1;    %  Example, set the next hit to be one second later.
sys = t + sampleTime;

% end mdlGetTimeOfNextVarHit

%=============================================================================
% mdlTerminate
% Perform any end of simulation tasks.
%=============================================================================
function sys=mdlTerminate(t,x,u)

sys = [];           % end mdlTerminate

%%Where the minimization was included as :
function f = DMCFLOW1(muqo)
P = size(muqo,1) - 1;
c = [1;zeros(P,1)];
f = c' * muqo;
```

B.3 Function File for the Steady State Optimizer

```
%=============================================================================
function [fl] = FLOPT(u);
global FLSET flO Vout;

%%%HTCs(1:5) = u(1:5);
FLSET = u(6);
FLA = u(7);
FLC = u(8);
FLB = u(9);
flO = [FLA FLC FLB];

A = 3150;
DT = [121.7 121.7 121.7 114.5 114.5]
        - [116.3 116.3 116.3 111.5 111.5];
DHVap = [2220.9 2220.9 2220.9 2234.1 2234.1];

Vout(1:5) = u(1:5)' .* A .* DT(1:5) ./ DHVap(1:5);
fl = flO;
options(13) = 1;
options(14) = 100;
fl = constr('SSOPT',fl,options);


%%Where the optimization was as follows :
%=============================================================================
function [f,g] = SSOPT(fl);
global FLSET flO Vout;

Bxin = 12.32;

A = Vout;
B = fl;
C = flO;
FLmin = ones(3,1) .* 0;
FLmax = ones(3,1) .* 300;
```

```
f = (100 - (  (fl(1)*Bxin/(fl(1)-
        Vout(1)*(fl(1)^0.8/flO(1)^0.8)) ...
        *(fl(1) - Vout(1)*(fl(1)^0.8/flO(1)^0.8) ) ...
        +(fl(2)*Bxin/(fl(2)-Vout(2)*(fl(2)^0.8/flO(2)^0.8)) ) ...
        *(fl(2) - Vout(2)*(fl(2)^0.8/flO(2)^0.8) )/2 )) ...
        /( fl(1) - Vout(1)*(fl(1)^0.8/flO(1)^0.8) ...
        +(fl(2) - Vout(2)*(fl(2)^0.8/flO(2)^0.8))/2 ...
        -Vout(4) * ((fl(1)+fl(2)/2)^0.8/((flO(1)+flO(2)/2)^0.8)))) ...
        *( fl(1) - Vout(1)*(fl(1)^0.8/flO(1)^0.8) ...
        +(fl(2) - Vout(2)*(fl(2)^0.8/flO(2)^0.8))/2 ...
        - Vout(4) * ((fl(1)+fl(2)/2)^0.8/((flO(1)+flO(2)/2)^0.8)))...
        +(100 - ( fl(3)*Bxin/(fl(3)-Vout(3)*(fl(3)^0.8/flO(3)^0.8))...
        *(fl(3) - Vout(3)*(fl(3)^0.8/flO(3)^0.8) ) ...
        +(fl(2)*Bxin/(fl(2)-Vout(2)*(fl(2)^0.8/flO(2)^0.8)) ) ...
        *(fl(2) - Vout(2)*(fl(2)^0.8/flO(2)^0.8) )/2 ) ...
        /(fl(3) - Vout(3)*(fl(3)^0.8/flO(3)^0.8) ...
        +(fl(2) - Vout(2)*(fl(2)^0.8/flO(2)^0.8))/2 ...
        -Vout(5) * ((fl(3)+fl(2)/2)^0.8/((flO(3)+flO(2)/2)^0.8)))) ...
        *(  fl(3) - Vout(3)*(fl(3)^0.8/flO(3)^0.8) ...
        +(fl(2) - Vout(2)*(fl(2)^0.8/flO(2)^0.8))/2 ...
        -Vout(5) * ((fl(3)+fl(2)/2)^0.8/((flO(3)+flO(2)/2)^0.8)));

g(1) = sum(fl(1:3)) - FLSET;
g(2:4) = FLmin - fl(1:3)';
g(5:7) = fl(1:3)' - FLmax;
```